ORIGINAL COPY
OF
FINAL REPORT

JPL - Contract #951463

Herbert C. Roters Assoc., Inc. April 18, 1969


JET PROPULSION LABORATORY
CALIFORNIA INSTITUTE OF TECHNOLOGY
PASADENA, CALIFORNIA

ORIGINAL COPY
OF
FINAL REPORT

J P L - Contract #951463

Herbert C. Roters Assoc., Inc. April 18, 1969

RE-ORDER NO. 69-91

# Final Report

for

# Brushless DC Motor

(1 April 1966 - 18 April 1969)

Contract No. 951463

Prepared by

Herbert C. Roters Associates, Inc.
45 North Mall
Plainview, N. Y. 11803

APPROVAL:

This work was performed for the Jet Propulsion Laboratory, California Institute of Technology, sponsored by the National Aeronautics and Space Administration under Contract NAS7-100.

Helmar O. Jensen
Cognizant Engineer

Marg. E. Auppeerle
Contract Administrator

Herbert C Roters
Company Officer

for

Jet Propulsion Laboratory
Pasadena, California

## NOTICE

This report was prepared as an account of Government-sponsored work. Neither the United States, nor the National Aeronautics and Space Administration (NASA), nor any person acting on behalf of NASA:

a. Makes warranty or representation, expressed or implied, with respect to the accuracy, completeness, or usefulness of the information contained in this report, or that the use of any information, apparatus, method, or process disclosed in this report may not infringe privately-owned rights; or

b. Assumes any liabilities with respect to the use of, or for damages resulting from the use of any information, apparatus, method, process disclosed in this report.

As used above, "person acting on behalf of NASA" includes any employee or contractor of NASA, or employee of such contractor, to the extent that such employees or contractor of NASA, or employee of such contractor prepares, disseminates, or provides access to, any information pursuant to his employment with such contractor.

Requests for copies of this report should be referred to:

National Aeronautics and Space Administration
Office of Scientific and Technical Information
Washington 25, D. C.

Attention: AFSS-A

## SUMMARY

This report refers to a small dc brushless motor with logic controlled semiconductor commutation power supply to provide reversibility and to include a speed control system. The objective of the work is to explore the possibility of building such a motor in a 3/4" diameter x 1-1/4" length body. The work done covers the design development and testing of an engineering model including environmental tests. Performance tests were conducted for motor operation in continual run and in a stepping mode with pulsed inputs.

The running performance of the motor agreed quite well with the calculated performance, producing maximum efficiencies in the region of 55% for the motor input only. The logic control power supply works and provides equally good performance in either direction. Operation of the motor by 1 millisecond pulses of voltage is not satisfactory because the mechanical steps resulting are erratic and dependent upon the starting position of the motor rotor. The motor speed control has not worked satisfactorily because of instability when the loop system is closed. It is believed possible with further analysis to find some method of system gain control to achieve stability in the speed-control system. Tests of the motor in the environmental conditions specified for shock and vibration were successfully passed. There is some indication of a lack of stability in the sensor output which is believed to be the result of construction of the sensors using separate parts encapsulated with an Epon resin. In general, it has been demonstrated that it is feasible to build a dc brushless motor in a size 0.750" diameter x 1.312" long and having the equivalent of a six bar commutator, and that control of motor direction of rotation can be obtained by a single reversing signal to the logic control of the commutation power supply.

## REPORT OUTLINE

## DC BRUSHLESS MOTOR

## DRAWINGS

## DRAWINGS continued

B-2966 - Assembly Unit #159 S/N 1

A-2967 - Ring - Crown Terminal

A-2968 - Terminal Pin

A-2972 - Speed Control Circuit (Final)

A-2972 Supp - Parts List for Speed Control Circuit

A-3008 - Spring Preload

## GRAPHS

M-2275 - Performance Characteristics Brushless DC Motor Design #2

M-2276 - Performance Characteristics Brushless DC Motor Design #1

M-2283 - Performance Characteristics Brushless DC Motor, Calculated Design #3

M-2348 - Variation of Voltage Output from One-Shot Multivibrators of Speed Control Circuit A-2761 B Versus Signal Frequency

M-2391 - Motor Characteristics Unit #159 DC Brushless Motor and Logic Controlled Commutation Power Supply 17 Volts

M-2392 - Motor Characteristics Unit #159 DC Brushless Motor and Logic Controlled Commutation Power Supply 23 Volts

M-2404 - Motor Characteristics Unit #159 DC Brushless Motor and Logic Controlled Commutation Power Supply 10 Volts

M-2405 - Motor Characteristics Unit #159 DC Brushless Motor and Logic Controlled Commutation Power Supply 25 Volts

M-2406 - No Load Motor Characteristics Unit #159 DC Brushless Motor and Logic Controlled Commutation Power Supply

## GRAPHS continued



## PHOTOGRAPHS

## 1. CONTRACT SCOPE

1.1 General. The contract covers the development of a small Brushless DC Motor and a breadboard electronic circuit with the general intent of obtaining minimum torque pulsations. A system of speed control by an external frequency controlled signal was to be provided. The performance of the system in a pulsed input stepping mode was to be evaluated.

1.2 Performance Requirements in Specifications. The important performance requirements of JPL Spec GMY-50464-DSN are repeated here for completeness, comprising sections 3.3, 3.4 and 3.5.

3.3.1 General. The Brushless DC Motor does not utilize a commutator or brushes. Commutating shall be accomplished by a switching circuit, controlled by a shaft positioning sensor.

3.3.2 Motor size. The outside diameter of the motor shall be 0.75 inch. The length, exclusive of the shaft, shall not exceed 1.25 inches.

3.3.3 Mounting flange. The motor shall have a mounting flange, which will extend above the outside diameter specified in 3.3.2. The mounting flange shall conform to JPL Drawing A 129847.

3.3.4 Motor speed. At continuous operation, motor speed shall be 4500 rpm at 10 V with no external load.

3.3.5 Efficiency. Efficiency shall be maximized within the constraints of the other specifications.

3.3.6 Speed control. Motor speed shall be controlled by an external frequency of rectangular waveform. The speed control shall be effective within the speed range between 200 and 8000 rpm. The external frequency of 2400 cps shall result in a motor speed of 4500 rpm with speed variations of not more than 1.0 percent.

3.3.7 Torque output. At continuous operation from 10 V, the motor shall be capable of developing a maximum torque of 40 gcm on the motor shaft for a minimum period of 1.0 second.

3.3.8 Stepping rate. On application of a low frequency, square wave, ac-voltage, the motor shall be capable of stepping at a rate of at least 500 increments per second. Within the constraints of the other specifications, the maximum stepping rate shall be minimized. It is expected to be considerably higher than 500 increments per second.

3.3.9 Shaft displacement. In the stepping mode, the angle of rotation for each step shall depend only on the voltage applied to the motor. With constant voltage pulses, this angle shall not vary by more than 5 percent, dependent on the shaft position. This shall require a very uniform stator winding. Slot effects shall have to be minimized or the slots may be eliminated by fixing the winding on the stator bore.

3.3.10 Bearings. Minimum radial play ball bearings shall be used. The bearings shall not be preloaded and shall be heavily

lubricated with GE Versilube F50.

3.3.11 Runout. Runout of the motor shaft shall not exceed 0.0003 inch total indicator readout (tir).

3.3.12 Reliability. Throughout the design work, emphasis shall be placed on achieving the highest reliability and longest life.

3.4 Radio-interference suppression (external and internal). The motor design shall incorporate features to minimize external or internal interference with electrical or electronic equipment in accordance with the requirements of JPL Specification 30236.

3.5 Environmental requirements. The motor shall operate within the electrical design requirements of this specification following the environmental tests listed in paragraphs 4.3.1, 4.3.2, 4.3.3.1, 4.3.3.3, of JPL Specification 30250 B.

1.3 Performance Requirements in Statement of Work. The work program for the contract contains the following performance and test requirements as stated by Article I. Statement of Work, Items 1, 2 and 3 as follows:

(1) Design one (1) each engineering model of a brushless D. C. motor, in accordance with the requirements of JPL Design Specification No. GMY-50464, entitled, "Design Specification, Telecommunications Development, Spacecraft Equipment, Brushless DC Motor," dated 8 June 1965.

The design of the brushless D. C. motor shall be subject to the

following:

(i) Shaft and Shaft Extension. A firm diameter chosen for the shaft and the extension is 0.1232" with an extension of 3/8" beyond the face of the motor.

(ii) Bearings. The bearings shall be selected and lubricated so to achieve minimal friction combined with long lifetime.

In the performance of the design effort of the brushless D. C. motor, the Contractor shall fully inform JPL of its progress and JPL shall direct the effort toward a design most congruous with the overall performance requirements of spacecraft application described in JPL Design Specification GMY-50464-DSN.

(2) Develop and fabricate an engineering model of the brushless D. C. motor and a breadboard circuit capable of demonstrating conclusions of the design developed under paragraph (a)(1) set forth herein.

This work shall include the following:

(i) Make detailed drawings that are necessary for fabricating the brushless D. C. motor.

(ii) Punch sufficient laminations for eight (8) motors.

(3) Test and evaluate the brushless D. C. motor. The tests and

evaluations shall be directed toward determining feasibility of the brushless D. C. motor design for subsequent use in spacecraft application described in JPL Specification No. GMY-50464-DSN, and shall include, but not necessarily be limited to the following:

(i) The following motor characteristics shall be measured without employing the speed control circuit:

(A) Motor speed, motor current, and overall efficiency versus D. C. voltage at 0, 10, 20 gcm external torque applied to the motor shaft.

(B) Motor speed, overall efficiency, motor current and output power versus shaft torque at 10V, 25V, and 40V.

(ii) The following motor characteristics shall be measured by employing the speed control circuit:

(A) Pull out torque versus D. C. voltage at the stabilized motor speeds of 2000 RPM, 4500 RPM, and 8000 RPM.

(B) Determine required time to reach the stabilized speed of 4500 RPM versus D. C. voltage without external load.

(C) Overall efficiency of the system at the stabilized

speed of 4500 RPM versus D. C. voltage at 10 gcm and 20 gcm external load.

(D) Motor speed versus time during acceleration to a stabilized speed of 4500 RPM at no external load.

(iii) The following stepping characteristics shall be measured without employing the speed control circuit:

(A) Maximum and minimum shaft displacement depending on the rotor position on application of one rectangular voltage pulse of 50V, and a duration of 1 millisecond.

(B) Waveform of the current on application of a pulse of 50V during 1 millisecond.

A Technical Direction Memorandum #1 requested that the electronics package be built as a separate unit and need operate only in a room environment with a cable connection to the motor at least six feet long.

1.4 Proposal Outline. A brief outline of our proposal is presented in the following sections.

1.4.1 Motor and Sensor. The original proposal for the motor design was based on a two pole, ten slot motor stator using ten-point commutation, which is equivalent to ten commutator bars

per pair of poles in an ordinary type of motor. The motor size and outline were to be made to agree with the specified specification outlines. The sensor unit was proposed to be an electromagnetic type as used in other dc brushless motors built by us except that modifications would be needed to fit within the desired motor outlines.

1.4.2 Speed Control. The motor speed was to be controlled in a manner shown in the diagramatic sketch of A-2667. The square-wave signal control frequency is fed in on the left side of the circuit diagram and actuates a one-shot multivibrator. The output of the multivibrator is a pulse having constant amplitude and constant width. A low-pass filter smooths this signal into a dc signal whose amplitude varies directly with the frequency of the multivibrator output signal. This dc signal output is fed into one side of a differential amplifier. In a similar manner, the motor speed signal is derived from the voltage drop across one of the motor commutating transistors. This signal is fed in on the right side of the circuit diagram through a one-shot mulitvibrator and a low-pass filter to form a dc signal proportional to motor speed which is applied to the differential amplifier. The pulse width of the signal B' can be adjusted with respect to signal A' so that a motor speed of 4500 rpm, corresponding to 75 Hz, will be equal to that of signal A' corresponding to 2400 Hz. Thus the pulse width of the signal B' will be

32 times as wide as signal A'. The two low-pass filters will have the same amplitude of dc signal and the net input to the differential amplifier will be zero, with zero output to the variable voltage absorption circuit. If the two speeds are not in the balance of 32 to 1, the higher frequency signal will have the higher amplitude of dc from its low-pass filter. The differential amplifier is to be arranged so that when the motor speed is higher than required, a voltage drop will result in the variable voltage absorption circuit. This will decrease the voltage on the motor and slow it down until the balance point is reached at the governed speed setting. The sensitivity of control can be varied by adjusting the gain of the differential amplifier.

1.4.3 Stepping Mode. The characteristics of the dc brushless motor in a stepping mode are difficult to predict. The ability of such a motor is dependent upon having a low mechanical moment of inertia and a low electrical inductance. Because of the nature of the design which of itself makes the motor mechanically small, the moment of inertia of the rotor will be correspondingly small. Since the stator winding will be confined to a small volume its electrical inertia or inductance will also be small. Consequently, the machine theoretically will have a high stepping rate because of its small size. For producing uniformity of steps regardless of geometrical position, it is certainly desirable to have as many commutation

points as possible to insure this uniformity. It therefore appeared very desirable that a minimum of ten-commutation points be chosen.

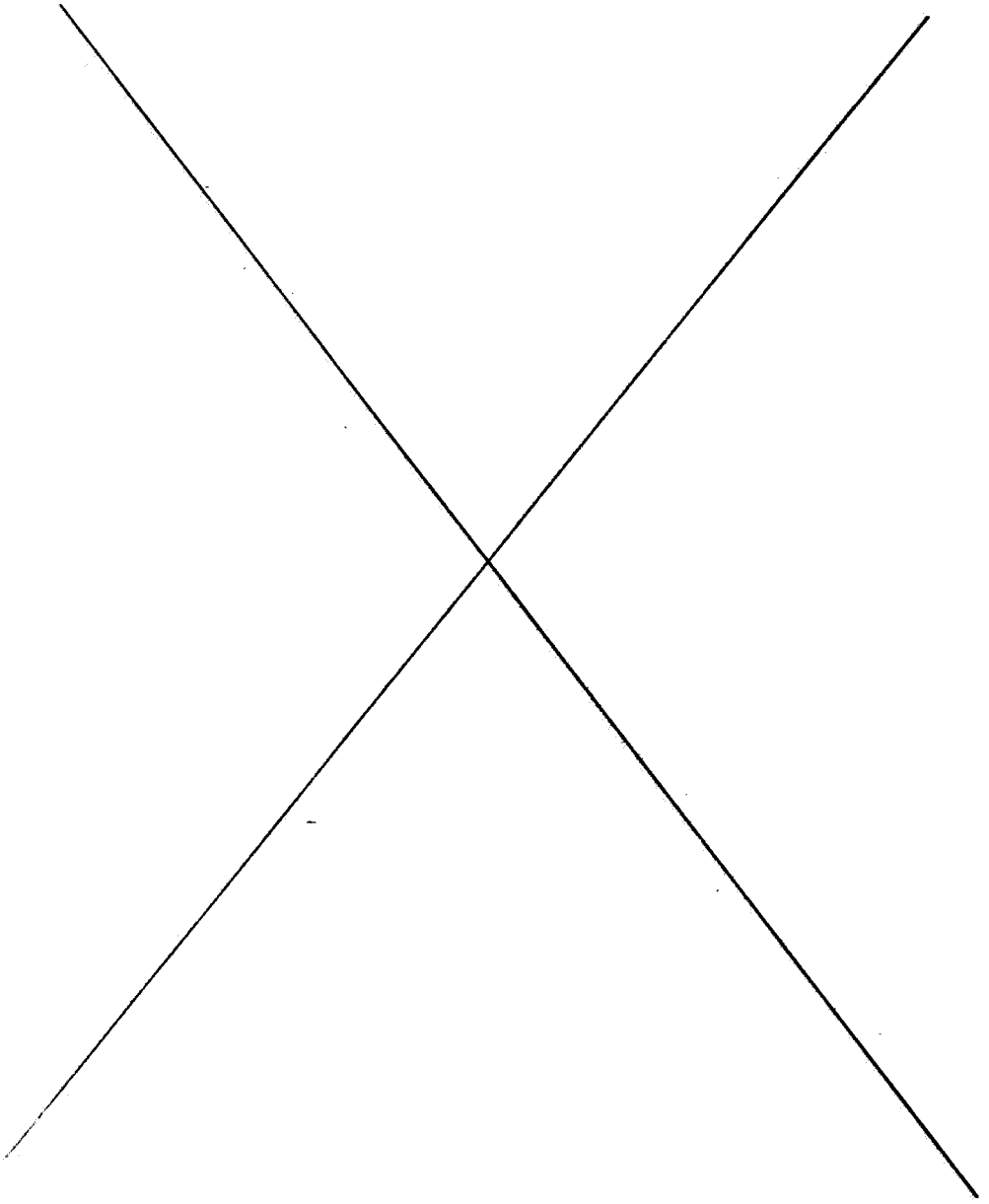

## 2. MOTOR AND SENSOR

2.1 General. For the main body of this report, the final motor and sensor will be discussed. Appendix I contains data on additional designs made prior to the final choice. Although it was possible to build a motor in the 1.25" length allowed, enough improvement in performance was obtained by increasing the length to 1.312" to obtain approval for this greater length for the final motor. Where the motor body size is quoted, this includes the sensor unit which is mounted in the motor case. After initial consideration of an 11 slot stator, it was finally decided to make the stator with 12 slots permits the choice of a ring or star winding with a minimum amount of coils such as six (6) full pitched coils, which can be connected in either ring or star manner. It was decided not to use the star type of winding because the dissipation of the stored energy in the armature coils during commutation could result in added losses and possible commutation problems. In order to keep the size of the motor stator to a minimum, the yoke rings which form the return path of the stator flux at the outer periphery were made from ferro-cobalt material which was checked for magnetic properties after being hydrogen annealed. Low silicon content steel is used for the armature lamination. The details for the lamination and punch are shown on drawings B-2751 and A-2752. The ID of the armature laminations B-2751, is 0.313". After final assembly of the stator when it is encapsulated in the case, this ID is bored out to 0.3425"

leaving a nominal thickness of 0.003" between the ID and the bottom of the slots. Although some of the magnetic flux is shunted off by this bridge ring, any tendency towards slot lock effect is reduced by avoiding the sharp permeance changes caused by open slots. The final winding choice was 12 coils, each 82 turns per coil #38 HF wire, full pitch, 2 coil sides per slot and connected in a ring winding with 12 leads coming off from the coil junction points. The resistance across the diameter of this ring winding measured 36.0Ω at room temperature. Alnico IX material was chosen for the rotor magnet because this material has a very high coercive intensity and energy product. The magnet is enclosed in a 303 stainless steel housing with a wall thickness of 0.010". An actual physical air gap of 0.005" exists between the stainless steel rotor cover and the ID of the finished stator. This gives a 0.015" effective magnetic air gap. The overall length of the stator stack and of the Alnico rotor is 0.372", with an overall motor length of 1.312".

This motor design can easily be modified to obtain more or less torque by changing the length of the stator stack and of the Alnico rotor. The overall motor length will change correspondingly. This is shown on the generalized motor drawing B-2757.. X may be any value between 0.3" and 1.00".

2.2 Motor Construction. The final motor assembly is shown on drawing B-2966.. This drawing shows the motor and sensor unit in cross-section, with the motor case enclosing this sensor housing at the end opposite the shaft extension.

2.2.1 Stator. The motor stator consists of 26 laminations B-2751.

These laminations are sprayed on one side with an epoxy adhesive and stacked in a suitable fixture with guide pins to align the slots and then baked under heat and pressure to obtain a self supporting stator stack. The OD of this stator stack is then turned to give a size to size to 0.0003" loose fit under the yoke ring lamination A-2752 which is assembled on it after the winding is in place. The stator winding consists of 12 coils each 82 turns #38 HF wire. Each coil is inserted in the stator to have a full pitch (slot 1 to slot 7) and form a lap winding. Each coil will have one side in the lower part of a slot and one side in an upper part of another slot 180° away from the first slot. The winding thus looks symmetrical when viewed from the end and does not have any bulges such as may be produced when coils are wound unsymmetrically with one coil having both its sides in the upper halves of the slots which the coil occupies. Each of the coils is connected to its following one (finish 1 - start 2) with a lead connected to the junction. This makes 12 leads in all, which in an ordinary motor would be connected to a 12 bar commutator. Approximately 36 yoke rings A-2752 are then assembled on the OD of the stator. In order to reduce the winding overhang to a minimum, the winding pressing fixture A-2812 is assembled on the winding so that the overhang is retained between two cylinders of metal while a third cylinder is pressed down on the winding between the other two cylinders in order to compact the winding. This is necessary in

order to hold the overall length to the required minimum. Slots are provided in the pressing cylinder for the twelve leads to emerge from the winding overhang. The winding is impregnated with a suitable electrical varnish and baked. During the baking cycle, the winding overhang is held under a very light pressure so that it will not expand. The OD of the yoke rings is then finished concentric to the stator tunnel just enough to clean off the excess varnish and lightly touch the metal surface, so the assembly will fit in the case with a slide fit. It is important to maintain concentricity during this and following finishing operations so that the final bridge ring will be uniform. The stator is assembled in the motor case and the leads brought out through the appropriate grommet exit hole. The stator assembly is then encapsulated in this case with a suitable epoxy encapsulating resin. During the encapsulation baking cycle a teflon plug must be pushed into the open end of the case so that the encapsulated stator length will not exceed its specified value. After the encapsulating resin has hardened, the stator tunnel is finished to its final size of 0.343" nominal. At the same setting, the front bearing tube is also finished to fit the SR2-5PPK25 bearings. The fit should be a very light thumb press fit in the bearing tube section.

2.2.2 Rotor. The rotor assembly is described in A-2821. The Alnico IX rotor could not be purchased in the form of a cylinder magnetized across its diameter. It was necessary to take a larger slug of

material 1" in diameter and 1" in length with its magnetic axis along the 1" length. A flat was cut from it so that the magnetic axis of the flat was perpendicular to the 0.372" length. A round cylinder was cut from this slab using a copper cylindrical lap and abrasive grinding powders. The cylindrical lap was rotated while being intermittently pressed down against the magnet slab with a mixture of oil and abrasive powders puddled on the work surface. This gradually cut a circular groove through the slab and left the desired cylindrical magnet in the center of the lap but with an oversized diameter. The magnet cylinder was then finished to size on its OD after first cementing two soft steel cylindrical faces on the ends of the magnet and putting centers in these soft faces for mounting in the grinder. It is necessary to maintain pressure on the centers and grind extremely slowly as the cement joint and the Alnico IX itself are quite weak. This is fortunate because a strong bond would probably break the Alnico when trying to release the pole faces after the grinding operation. The two 303 stainless steel halves of the shaft shown on A-2821 are then pressed over the cylindrical magnet with loctite Type A adhesive. The relief holes shown permit the excess adhesive to escape from under the flat faces of the ends of the cylindrical magnet. The 303 stainless steel shaft parts were left oversized to they could be finished after the final assembly on the Alnico IX magnet and thus assure concentricity and straightness for the

final rotor assembly. When the rotor is finished to its final size the 303 stainless shell will be 0.010" radial thickness over the magnet and 0.010" smaller in diameter than the stator tunnel, therefore giving a radial magnetic gap of 0.015" with a physical gap of 0.005". When the rotor is assembled in its stator, the axial clearance is held to the order of 0.001", but with no preload. SR2-5PPK25 bearings lubricated with the F-50 Versilube oil are used. The axial end play is held to a workable minimum because the axial air gap in the sensor unit must be kept at a reasonably close value in order to maintain the electrical performance characteristics. The remaining assembly procedures on the motor will be treated in the section on the sensor.

2.3 Sensor Construction. The basic stationary elements of the sensor are an oscillator coil mounted on a ferrite core piece, twelve pickup coils and twelve ferrite poles on which the coils are mounted and the enclosing case. The rotating element is a ferrite armature mounted in a cupped aluminum piece which in turn is mounted on the shaft. The ferrite armature forms the magnetic path for the flux of the oscillator coil as it passes through the center section of the ferrite core piece across the axial air gap to the ferrite armature and thence out to the arm of the armature. The magnetic flux then crosses the axial gap from the armature arm to the stationary ferrite pole pieces and down the pole piece to the ferrite core section. As the flux passes down each

of the poles it produces a voltage in the coil on that pole. Each coil in turn will produce a higher voltage during the interval when it is covered by the rotating armature which occurs once per revolution of the shaft.

2.3.1 Oscillator Coil. The bobbin of the oscillator coil is shown on A-2801. The OD is deliberately made large so that holes in the flange can be provided to position the ferrite poles. The coil winding consists of 73 turns #35 HF wire with a resistance of 1.93Ω, or 2.56Ω with 15" of #32 lead wire. This coil only occupies the space below the twelve ferrite poles and the leads come out to the exterior between the pole pieces. In the left hand flange, which is relatively thick, there are twelve counterbored holes surrounding the holes for the poles. These counterbored holes receive the sensor pole bobbins. The thick walled flange of the oscillator coil bobbin also serves to give a good mounting surface for the crown terminal ring A-2967. This part is used as the connection point for all the leads of the sensor coils and forms the common connection. The heavy flange also permits the mounting of twelve terminal pins A-2968, to which the remaining wire from each sensor coil is connected.

2.3.2 Ferrite Sensor Core. The ferrite core of the sensor is designed to be made from a standard ferrite piece CF 202 #F975. Some grinding is required as shown by the detail A-2763. Special tooling to

form ferrite parts is quite expensive so the design was based on trying to use standard available parts with the minimum of grinding.

2.3.3 Ferrite Sensor Pole. The ferrite sensor pole A-2778 has also been designed to use a standard part with the minimum amount of rework. In this case, the part is available in longer lengths which must be cut off to the size shown. This can be done by careful grinding for larger parts or by sanding with emery discs or belt sanders.

2.3.4 Ferrite Sensor Armature. The ferrite sensor armature is shown on A-2843 and has been designed so that it can be made from a standard cup core by grinding. It was found later that the lobe shape arm can be formed from a part with a complete flanged end by using an emery disc to grind away the unused flange portion. This is of value from an experimental standpoint as it permits a differently shaped lobe to be formed relatively easily. Because of the weakness of the material, it cannot be mounted directly on the shaft but must be cemented into a sensor armature hub A-2779. Due to the dissymmetry caused by the ferrite lobe, the assembly would be quite unbalanced. This was compensated partially by cementing a thinner brass duplicate of the ferrite lobe shape on the opposite side of the hub. This accomplished only a gross correction and the assembly was finally statically balanced. This was done by mounting the assembled hub on a 0.005" loose shaft and vibrating the shaft axially. The vibration greatly minimized the static friction and

the hub part would rotate to bring its heavy side down. Excess cement and some of the aluminum hub were ground off to lighten the heavy side until no further action was observed. The limit of detection was the equivalent of a piece of 0.005" adhesive tape 3/16" square. No dynamic balancing was done.

2.3.5 Sensor Pole Coil. The sensor coil consists of 90 turns of #41 HF wire wound on the sensor bobbin A-2777. No leads were attached as the design is aimed toward the elimination of stranded wire leads attached directly to the coils. A preliminary design was tried with stranded lead wires attached to the coils and found to be impracticable . The leads could not be tied down to the coil bobbins without making such a large lump that it was impossible to fit the coils in. After some attempts using stranded lead wires the method was abandoned in favor of the system described in the following sections.

2.3.6 Sensor Case. The housing which encloses the stationary sensor assembly is shown on A-2814. This sensor case fits into the motor housing by spreading the end of the motor housing sufficiently for the sensor housing to pass under the tapered section at the end of the motor housing. The motor housing will not spread sufficiently with only the lead slot and it is necessary to cut three 0.015" wide slots 5/16" long at 90° intervals so the end can be spread open to admit the sensor housing. In order to insure a locking action, a 3/16" ring

0.012" thick is pressed over the motor housing which clamps the sensor housing securely.

2.3.7 Sensor Assembly. The sensor assembly procedure involves the two main steps of assembling the parts and soldering leads to the terminal pins. The first step is mounting the crown terminal ring on the wound oscillator coil, and then placing this on the ferrite sensor core. The twelve ferrite poles are pushed into position and the twelve sensor coils pushed over the ferrite poles. The twelve terminal pins are also pushed into their holes in the bobbin but not completely because the pins are heated when the leads are soldered on and if they are not fully seated, the nylon bobbin is heated less. The sensor coils are wound so that the start and finish leads are easily discerned and the winding direction is kept the same. Each sensor coil has one coil end soldered to the crown terminal ring and the other end soldered to a terminal pin. Due to the fact that the electrical load on the sensor coils is a half-wave rectifier, the best method of connecting the coils is to have adjacent coils connected in opposite polarity. This means that coil #1 has its start connected to the common crown terminal ring, coil #2 has its finish connected to the common crown terminal ring, and so on. This connection avoids the possibility of three adjacent coils with the same polarity connection producing a dc component of current and magnetic flux in the sensor. After completing this lead soldering

the terminal pins are pushed into the bobbin and the leads arranged visually so there is no shorting. The external leads for the sensor coils are then soldered to the opposite ends of the terminal pins with the common lead soldered to the tab of the crown terminal ring. Considerable care must be taken with heating to prevent the unsoldering of the coil lead on each terminal pin when the external lead is attached. A heat sink on the coil end of the pin helps in this operation.

2.3.8 Sensor Encapsulation. The sensor encapsulation is done with the encapsulation fixture A-2813. There is no great need for concentricity of the various parts of the assembly because the axial air gap makes the axial dimensions of greater importance. In the fixture there is a central teflon plug which forms the clearance hole in the center of the assembly and also blocks off the center hole in the ferrite core piece. A piece of 0.007" teflon sheet blocks the open end of the assembly. The teflon sheet is backed up by a sheet of rubber and this in turn by an aluminum block which presses the parts together. Any clamp can be used and this is not shown. The rubber allows for the varying height of the sensor poles and presses these poles down against the flange of the ferrite core piece so that the air gap at the joint is a minimum. Also the pressure of the rubber against the sensor pole makes an indentation which results in a fillet of plastic material around the sensor pole. This is helpful in supporting the ferrite poles

for the final operation where the face is lightly ground until the pole heights are even. Epon 828 resin (Shell Chemical) is used for encapsulation because it is quite fluid when warmed. Even so, it was found very difficult to eliminate pockets when the material was poured into the pouring slot at the top. (A similar unit was made for another JPL job and the entire fixture was immersed in the Epon resin and a vacuum pumped to extract the air from the assembly. This worked much better as regards elimination of voids.) After encapsulation, the unit is cleaned up and then baked in the fixture at 110°C for a minimum of 4 hours. The ends of the ferrite poles are lightly ground to give a 0.004" - 0.007" smaller air gap than the core axial gap. The final assembled axial gaps are 0.004" - 0.006" for the sensor poles and 0.011" for the center gap between the armature and the ferrite core.

## 3. ELECTRONIC COMMUTATOR

3.1 General. The electronic commutator consists of the shaft position sensor, logic circuits and the power switches. Its purpose is to connect all 12 motor coils alternately and at the right time with the right polarity to the dc power supply. A "Direction of Rotation" command signal $R_{in}$ is given to the commutator. If $R_{in}$ is at +5 V, the motor shall run in a clockwise direction if viewed from the shaft side and if $R_{in}$ is at 0 V, the motor shall run counterclockwise. The description of the electronic commutator in this section applies to the present condition of the unit and after the numerous changes made in the system

during the experimental phase. A summary of the experimental changes will be found in Appendix II.

The battery voltage supply is separated into two sections, a +5 V section and a -19 V section. The +5 V is required for the logic circuits and the -19 V is the balance necessary to form a total of 24 V, the usual supply voltage.

3.2 Shaft position sensor electronics.

3.2.1 Oscillator. The oscillator coil of the shaft position sensor is excited with a sinusoidal current of high frequency. The oscillator is shown on detail A-2839. It is constructed as a separate unit on its own circuit board and produces a good sinusoidal waveform with no detectable dc component. The sensor unit needs a true ac excitation with as small a dc component as possible to avoid such difficulties as magnetic saturation of the ferrite parts in the sensor or distortion of the signal output from the sensor. If dc were applied to the sensor primary coil, as the sensor armature moves across a coil pole there would be a positive voltage signal as it entered the pole and a negative voltage as it left the pole. This would be of relatively small magnitude and probably not usually troublesome. However, since an ac output oscillator is easily made it is preferable to avoid these possible difficulties. The sensor primary (exciting) coil is the "L" in the circuit and it forms a tank circuit with the tuning capacitor "C". The circuit as finally used requires 20.8 volts battery with an input of 5.1 mA or 106 mW. The oscillator

frequency is approximately 105 kHz. This frequency is not at all critical because the sensor is essentially a transformer where a voltage in the primary (exciting) coil is transformed into a voltage in the individual sensor coils and this transformation ratio is not dependent upon the frequency directly.

3.2.2 Signal Conditioner. As shown on schematic A-2866, the 12 individual coils of the sensor are connected to a common ground, and the other 12 leads going to the commutation circuits. The high frequency voltages from these 12 leads are modulated with the shaft position information. Demodulation is accomplished by rectification and filtering of each of the 12 sensor output signals. The resulting signal is a dc voltage whose amplitude is determined by the sensor rotating armature position. Schematic A-2780A Rev. B shows on the left side the demodulators for two of the 12 sensor outputs. These signals are subsequently amplified and squared by an SN17910 operational amplifier in series with SG220 integrated circuit. The SG220 is a Quad 2-Input NAND/NOR Gate made by Sylvania used here as an inverter.

3.2.2.1 Sensor Signal. Signals from two sensor coils are shown on the accompanying oscillograms, with the coils connected to the demodulator circuit. These were taken at 4500 rpm no-load and show the envelope of the high frequency signal. The oscillator voltage was made the minimum so that there was no signs of transistor cut off when viewing the dc battery supply current. Note there is a minimum signal

of approximately 0.6 V p-p through a large part of a revolution of the motor for the orange sensor.

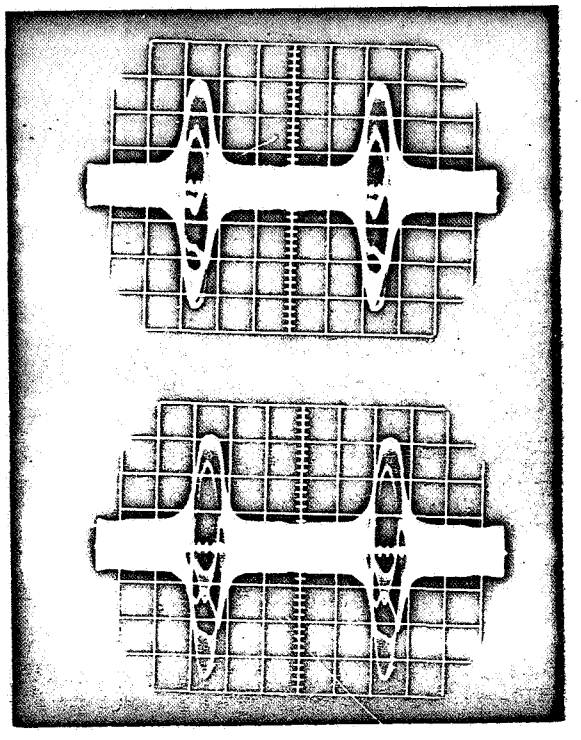

AC Coil Output Voltage
Sweep: 5 ms/cm x 2
Vert: 0.5 V/cm
4500 rpm No Load

Upper: Orange Sensor
(Lowest Output Sensor)

Lower: Violet Sensor
(Highest Output Sensor)
Coils connected to rectifier circuit.

The orange sensor had the lowest output. The violet sensor (highest) had corresponding values of 0.7 V p-p. The upper lobe shows the positive polarity part of the signal which is rectified by the half wave rectifier, with a peak of 1.45 V for the orange sensor and 1.51 V for the violet sensor. The lower lobe, the negative cycle is for the non-rectifying part of the cycle due to the rectifier being half-wave. The peak voltage of the envelope are 1.7 and 1.9 V respectively.

3.2.2.2 Demodulation of Sensor Signal. The sensor signal voltage of 3.2.2.1 is fed to a half wave rectifier such as $CR_1$ on A-2780A and

to a simple filter circuit of a 0.1 $\mu$F capacitor and a 10 K$\Omega$ resistor, whose output becomes a signal input to the SN 17910. The demodulated signals are shown below for the same conditions as the sensor coil voltages of 3.2.2.1

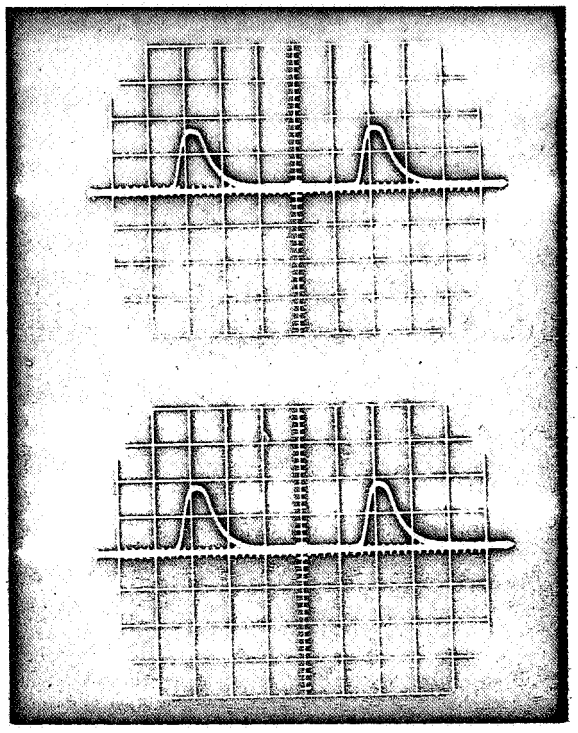

DC Output To 17910 Base
Sweep: 5 ms/cm x 2
Vert: 0.5 V/cm
4500 rpm No Load

Upper: Orange Sensor

Lower: Violet Sensor

The peak values are approximately 0.8 - 0.9 V dc. Because the diode has a roughly constant conduction voltage drop of 0.6 V, the minimum ac sensor signal does not pass through the rectifier circuit and become a dc voltage. The signal is not a square wave shape, particularly the trailing edge which shows a trail off typical of a C-R circuit. The "on" time is therefore slightly dependent upon the voltage level.

3.2.2.3 Amplification of Sensor Signal. The SN 17910 unit receives the demodulated signals as described in 3.2.2.2 and inverts and squares these off while amplifying them as regards to voltage. The SN 17910 turns on between a signal level of 0.6 V to just start and 0.72 V to be fully conducting. At a level of 0.7 V, the "on" time for the signal would be about 8.5 to 10.5% of the full cycle. The output of the SN 17910 unit is shown below. The normal output with zero signal is substantially 5 V and with sufficient signal to actuate the unit, the output is approximately zero volts. Thus the signal is inverted while being voltage amplified. Note that the "on" time for the signal is approximately 8 to 11% of the total time which is roughly the same as estimated from the demodulated sensor signal of 3.2.2.2.

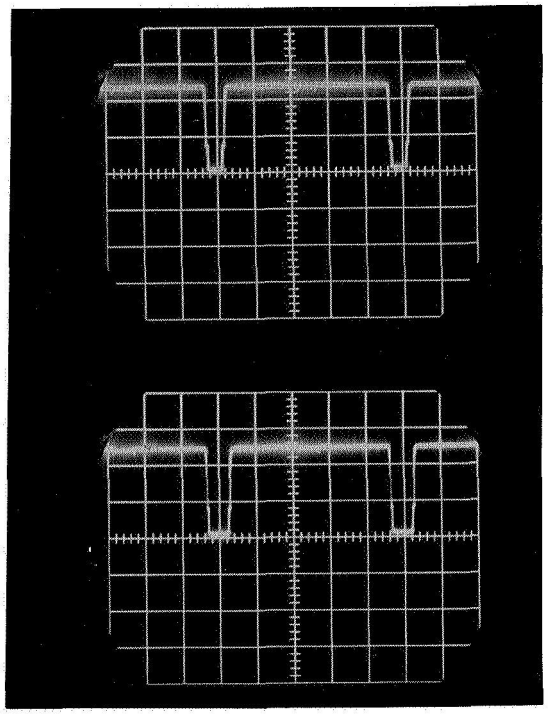

DC Output from 17910
Sweep: 5 ms/cm x 2
Vert: 2 V/cm
4500 rpm No Load

Upper: Orange Sensor

Lower: Violet Sensor

The inverted sensor signal is fed into the SG220 to be inverted again and to be compatible with the logic circuit. The SN 17910 and the SG220 together form a non-inverting amplifier and signal conditioner. One of the SG220 is also being used to invert the "direction of rotation" command $R_{in}$ and to increase the fan-out of $R_{in}$ so it can drive all gates of the logic circuit. It shall be noted that the amplifiers are only needed because of the low power of the shaft position sensor outputs. If it had been possible to build a somewhat larger sensor structure, the demodulated sensor signals could drive the logic circuits without amplification.

3.3 Power Switches. As shown on schematic A-2866 the 12 motor coils are connected to form a ring winding with 12 junction point connections. These 12 junction point connections receive current from the dc power supply by means of six power switches. A pair of opposite junction points are simultaneously connected to the dc power supply, while all other junction points are "open". The current then divides up into the two symmetrical branches of the winding.

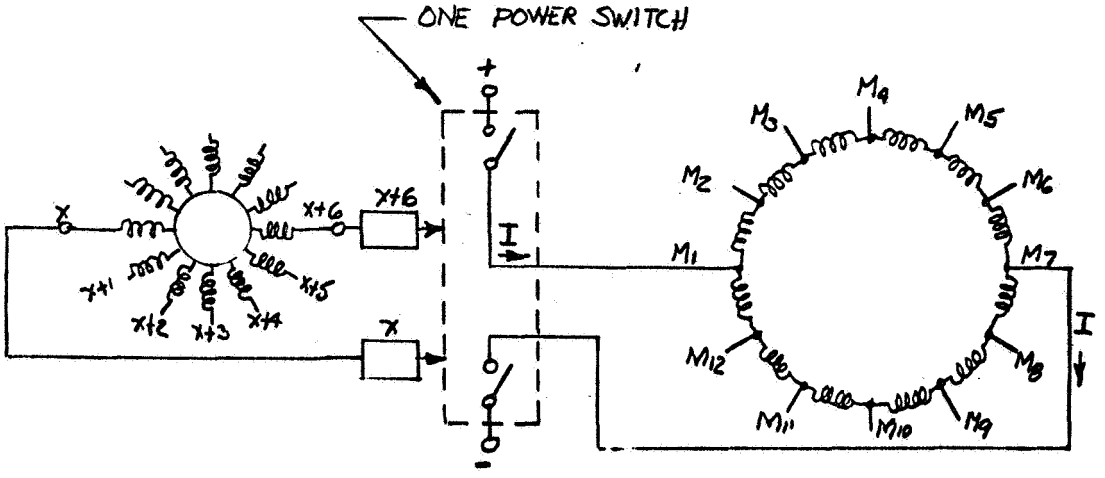

This is analogous to the conventional dc motor, the only difference being the electronic switching instead of the mechanical switching.

Only one out of the six pairs of junction points needs to be connected to the power supply at a time. Timing is controlled by the six pairs of sensor signals. Therefore, the commutating circuits consist of six identical groups working completely independent of each other. One such group is shown in schematic A-2780A. These groups become activated one after the other as the rotor rotates. The sensor, which is in the "on"-state, determines which group is activated.

Each power switch has to supply current to opposite junction points of the ring winding in both directions. The circuit is shown on the right side of detail A-2780A. It is a bridge circuit, consisting of the power transistors $Q_3$ through $Q_6$ and the base drivers $Q_1$ and $Q_2$. If base driver $Q_1$ is in the "on" condition, current will be allowed to flow from the positive terminal of the power supply through transistor $Q_3$, the motor ring winding, and transistor $Q_6$ to the negative terminal of the power supply. If base driver $Q_2$ is on, current will flow in the opposite direction through the ring winding, causing the motor to run in the opposite direction. This is similar to the reversal of polarity applied to the brushes of a conventional dc motor causing it to reverse rotation. Both base drivers $Q_1$ and $Q_2$ are never allowed to be on simultaneously.

Reverse polarity diodes $CR_3$ through $CR_6$ have been placed across

the collector-emitter of the power transistors $Q_3$ through $Q_6$. These diodes prevent voltage spikes on the collectors of the power transistors during the switching off of the inductive motor current by providing a secondary pass over which these motor currents can flow until their energy is exhausted.

Theoretically, only one out of the six power switches needs to operate at a time. However, this cannot be accomplished precisely because the power switch operates as long as one of the two associated sensor outputs is sufficiently high. The "on"-time of the sensor outputs cannot be controlled very precisely. In order to avoid any shaft position at which no current is flowing, the "on"-time of the sensor outputs is made long enough to provide considerable overlap between succeeding sensor signals. The consequence is that alternately one and two power switches are feeding current into the ring winding. This results in temporary shorting of individual motor coils. But since these coils are passing through the neutral zone of the rotor field at that time, no harmful effects occur. This is also in analogy to the conventional dc motor.

3.4 Logic Circuit. This circuit generates the proper waveforms to control the power switches. Only the reversible motor needs a logic circuit. The unidirectional motor would use the amplified sensor signals directly to actuate the power switches. The logic circuit of each group

has four inputs: the sensor signals X and (X+6) and the "Direction of Rotation" command $R_{in}$ as well as its complement $\overline{R_{in}}$. The logic circuit of each group has two outputs $Q_1$ and $Q_2$ which control one power switch.

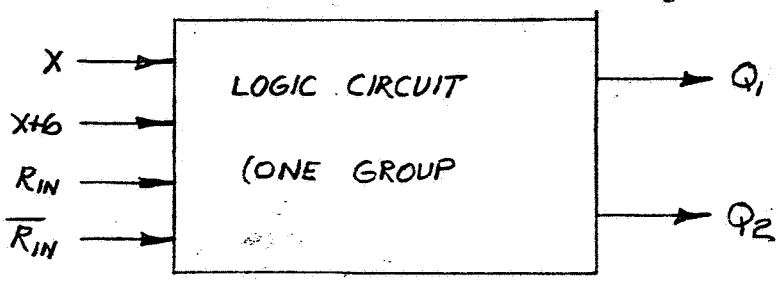


If $Q_1$ is low, current shall flow into junction point $M_1$ and out of point $M_2$ . If $Q_2$ is low, current shall flow backwards. The truth table for this logic is:

| X | X+6 | $R_{in}$ | $Q_1$ | $Q_2$ |
|---|---|---|---|---|
| 0 | 0 | 0 | 1 | 1 |
| 1 | 0 | 0 | 1 | 0 |
| 0 | 1 | 0 | 0 | 1 |
| 1 | 1 | 0 | - | - |
| 0 | 0 | 1 | 1 | 1 |
| 1 | 0 | 1 | 0 | 1 |
| 0 | 1 | 1 | 1 | 0 |
| 1 | 1 | 1 | - | - |

Taking advantage of the fact that X and (X+ 6) are never "on" simultaneously, the simplest Boolean equations are:

$$Q_1 = \overline{X \cdot R_{in} + (X+6) \cdot \overline{R_{in}}}$$

$$Q_2 = \overline{X \cdot \overline{R_{in}} + (X+6)\ R_{in}}$$

The hardware consists of a Sylvania SG220 Quad 2-Input NAND/NOR Gate integrated circuit. Each contains four logic circuits which each have the logic pattern shown below.

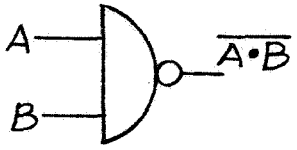


| A | B | $\overline{A \cdot B}$ |
|---|---|---|
| 0 | 0 | 1 |
| 1 | 0 | 1 |
| 0 | 1 | 1 |
| 1 | 1 | 0 |

This means that the output signal will always be unity unless both input signals are unity. If both input signals are unity then the output signal is zero. The unity signal corresponds to roughly 3.5 to 4 V and the zero signal to approximately 0.25 V. If the outputs of 2 NAND Gates are tied together, the circuit will perform the function expressed in each of the Boolean equations above. Fig. 1 shows in tabular form how the logic sequence occurs for a pair of sensors "X" and "X + 6" which are separated by 180° on the motor. To help in the descriptive designation, each of the four NAND Gates comprising an SG 220 unit is designated by its output terminal as a subscript with a number indicating whether it is the first or second SG 220 unit. Thus the first four NAND Gates of number one SG 220 will be designated as $1_C$, $1_G$, $1_K$ and $1_N$. The actual terminals are designated as $A_1$, $B_1$ or $A_2$, $B_2$ depending upon whether they are the first or second AG unit.

Referring to Fig. 1, it can be seen that each of the four NAND Gates

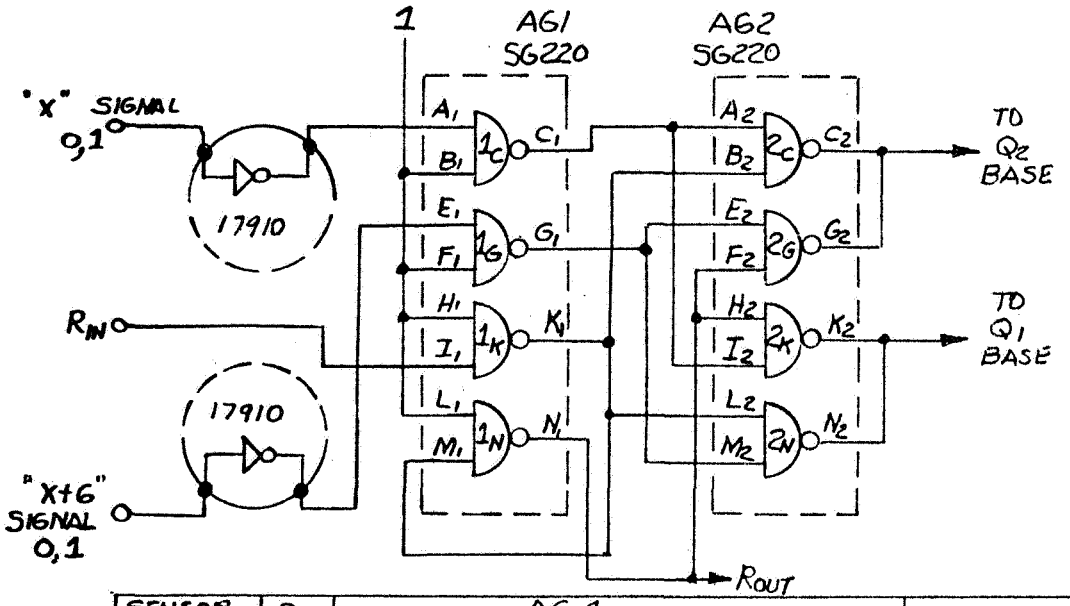


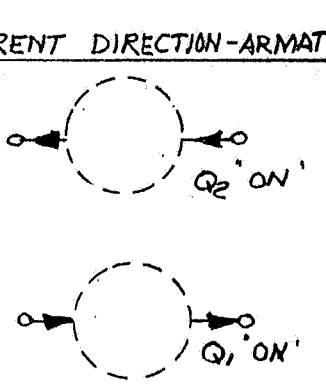


| SENSOR "X" | SENSOR "X+6" | $R_{IN}$ | AG 1 $1_C$ $A_1$ | $B_1$ | $C_1$ | $1_G$ $E_1$ | $F_1$ | $G_1$ | $1_K$ $H_1$ | $I_1$ | $K_1$ | $1_N$ $L_1$ | $M_1$ | $N_1$ | AG 2 $2_C$ $A_2$ | $B_2$ | $C_2$ | $2_G$ $E_2$ | $F_2$ | $G_2$ | $2_K$ $H_2$ | $I_2$ | $K_2$ | $2_N$ $L_2$ | $M_2$ | $N_2$ | "ON" TRANSISTOR |
|---|---|---|---|---|---|---|---|---|---|---|---|---|---|---|---|---|---|---|---|---|---|---|---|---|---|---|---|
| 1 | 0 | 1 | 0 | 1 | 1 | 1 | 1 | 0 | 1 | 1 | 0 | 1 | 0 | 1 | 1 | 0 | 1 | 0 | 1 | 1 | 1 | 1 | 0 | 0 | 0 | 1• | $Q_1$ |
| 1 | 0 | 0 | 0 | | 1 | 1 | | 0 | | 0 | 1 | | 1 | 0 | 1 | 1 | 0 | 0 | 0 | 1• | 0 | 1 | 1 | 1 | 0 | 1 | $Q_2$ |
| 0 | 1 | 1 | 1 | | 0 | 0 | | 1 | | 1 | 0 | | 0 | 1 | 0 | 0 | 1• | 1 | 1 | 0 | 1 | 0 | 1 | 0 | 1 | 1 | $Q_2$ |
| 0 | 1 | 0 | 1 | | 0 | 0 | | 1 | | 0 | 1 | | 1 | 0 | 0 | 1 | 1 | 1 | 0 | 1 | 0 | 0 | 1• | 1 | 1 | 0 | $Q_1$ |
| 0 | 0 | 1 | 1 | | 0 | 1 | | 0 | | 1 | 0 | | 0 | 1 | 0 | 0 | 1 | 0 | 1 | 1 | 1 | 0 | 1 | 0 | 0 | 1 | NONE |
| 0 | 0 | 0 | 1 | | 0 | 1 | | 0 | | 0 | 1 | | 1 | 0 | 0 | 1 | 1 | 0 | 0 | 1 | 0 | 0 | 1 | 1 | 0 | 1 | NONE |
| | | | | | | | | | | | | | | | | | | | | | | | | | | | |
| | | | | | | | | | | | | | | | | | | | | | | | | | | | |

1• BECOME 0 BECAUSE COMMON POINT IS 0

FIG 1

LOGIC OPERATION - ONE PAIR OF SENSORS

of integrated circuit AG1 has one of its inputs maintained at unity because they are connected to the +5 V line. The unit $1_C$ inverts the signal from the 17910 which has already inverted the signal from the "X" sensor so that in effect the output terminal $C_1$ is always the same logic state as the "X" signal. The same procedure follows for terminal $G_1$ with respect to the "X + 6" signal. $K_1$ will always be the inverse of $R_{in}$ and $N_1$ will be the same as $R_{in}$. The output of $N_1$, is used to drive the remaining five commutation logic circuits. This procedure is necessary because it was requested that $R_{in}$ signal input be kept to the lowest possible power requirement. The table in Fig. 1 under AG 1 shows all the possible combinations for the inputs of "X", "X + 6" and $R_{in}$. The first two rows show the signal "X" is on and the "X + 6" is off, $R_{in}$ may be forward or reverse as shown. The next two rows show "X + 6" being on and "X" being off, again with $R_{in}$ being forward or reverse. The final two rows show the conditions where "X" and "X + 6" are both off, with $R_{in}$ being forward or reverse. For these last two conditions, one or two of the other five commutation circuits will be activated. The condition that "X" and "X + 6" are both unity does not occur in actuality and therefore is not included in the logic table.

All of the inputs of Integrated Circuit AG 2 may fluctuate from zero to unity. As was stated in the previous section, it can be seen that the inputs $A_2$ and $I_2$ follow exactly the logic of the "X" signal and $E_2$ and $M_2$ follow the logic of the "X + 6" signal. Referring to the top line of the table

so as to demonstrate the sequence of the logic operation, the "X" signal is "on" and thus at unity, the "X + 6" signal is off and therefore zero and the $R_{in}$ signal is at unity. $A_2$ and $I_2$ follow the "X" signal and are therefore unity. $E_2$ and $M_2$ follow the "X + 6" signal and are therefore zero. $B_2$ and $L_2$ are the inverse of $R_{in}$ and therefore zero. $F_2$ and $H_2$ are the same as $R_{in}$ and therefore unity. The only one of the four NAND Gates having two unity inputs and therefore a zero output is $2_K$. Referring to the circuit A-2780A, when $K_2$ goes to zero the base of $Q_1$ transistor conducts current and turns on the transistors $Q_1$, $Q_3$, and $Q_6$. This allows current to flow to the right as shown in the armature current direction sketch on Fig. 1 or as seen on circuit A-2780A. It should be noted that when $K_2$ is zero, the unity output of $N_2$ is pulled down to zero. The second line of the table has similar conditions of "X" being on and "X + 6" being off but with a reversing signal $R_{in}$ now being zero. If the logic sequence is followed through in the same manner it will be found that the "on" transistor is now $Q_2$ which also turns on $Q_4$ and $Q_5$ (see A-2780A). This means that the current in the armature goes from right to left and therefore the direction of motor rotation will be reversed. A similar sequence of events will be found in lines 3 and 4 but with a condition that "X + 6" is on and "X" is off. The current direction in the armature is reversed from the first two lines for the same direction of rotation. This is a requirement because the rotor has turned one-half a revolution from its first position when "X" was on and the armature current must

reverse in order to maintain torque in the same direction as before. The last two lines merely show that when "X" and "X + 6" are off, there is no current flowing into the armature from the circuit being considered. At this time, one or two of the remaining five commutation circuits will be conducting current to the armature winding. As mentioned before, the logic and commutation schematic of Fig. 1 and A-2780A is repeated a total of six times or six circuits control a total of twelve armature winding input points. The arrangement of these six circuits on one board is shown on A-2888, which also shows the various input terminals to each circuit.

4. TACHOMETER CIRCUIT. The shaft position sensor delivers one positive voltage pulse at each of 12 output lines for every shaft revolution. Any one of the 12 sensor signals can therefore be considered a tachometer signal and could be used for speed control.

The pulses on the 12 sensor output lines appear one after the other as the shaft rotates due to the equal spacing of the sensor coils inside the motor. If these pulses would be sufficiently short to not overlap, the 12 sensor signals could be logically added to provide a string of 12 pulses per shaft revolution. This would provide the sensor with the capability of a tachometer having a resolution of 12 pulses per shaft revolution.

The pulse isolation amplifier has been designed to generate a narrow trigger pulse on the leading edge of every shaft position sensor

output pulse. Twelve pulse isolation amplifiers, as shown on A-2865, are connected to the 12 outputs of the logic circuit. The outputs of all isolation amplifiers are tied together and form the tachometer output. A narrow voltage pulse appears on this line whenever the motor shaft has rotated by 30 degs.

5. SPEED CONTROL CIRCUIT. The specifications call for a control frequency of 2400 Hz to result in a motor speed of 4500 rpm. Because twelve pulses per motor revolution are now available, the motor produces a tachometer frequency of 900 Hz at 4500 rpm. A comparison of the frequencies is tabulated below.

| Motor Speed | Control Frequency | Tachometer Frequency |
|---|---|---|
| rpm | Hz | Hz |
| 8000 | 4260 | 1600 |
| 4500 | 2400 | 900 |
| 2000 | 1065 | 400 |
| 200 | 106.5 | 40 |

The speed control circuit generates a DC voltage proportional to the control frequency and another DC voltage proportional to the tachometer frequency with the same proportionality factor. The two DC voltages are compared by a differential amplifier, which controls a motor current regulator see A-2667. The circuits are adjusted so that at a control frequency of 2400 Hz and a motor speed of 4,500 rpm the error signal

of the differential amplifier is zero. This will cause the regulator to supply the motor with just enough current to maintain this speed. Whenever the speed deviates from 4,500 rpm, a positive or negative error signal will be generated by the differential amplifier causing the regulator to supply the motor with more or less current.

The speed control circuit is shown on A-2972. The tachometer signal from the twelve pulse isolation circuits are fed into the right hand side of the speed control circuit A-2972. The first section is a one-shot multivibrator. This takes each signal pulse input and generates a constant width pulse output to a simple filter circuit $R_1C_1$. The output of the filter circuit becomes a signal to terminal 3 of the differential amplifier SN724L. The zener diode $CR_5$ holds pin 2 at some potential higher than the -19 V input. The zener $CR_5$ has an 11.8 V total in this unit. On the left hand side of the circuit A-2972, a similar one-shot multivibrator and filter circuit operates on the control frequency in the same manner. The only difference in the two multivibrator circuits is the value of the capacitors $C_5$ and $C_6$ which must be chosen to give the proper pulse width for each section so that a balance is reached in the differential amplifier. The output of the differential amplifier appears on pin 6 and first passes through a zener diode $CR_3$ of 5.6 V. This zener diode insures that the base of $Q_2$ transistor will always be negative with respect to the zero volts input to the collector of $Q_2$. $Q_2$ and $Q_4$ are an emitter follower

configuration where $Q_4$ is a larger transistor which actually regulates the motor current. The values for all the parts are shown on the "Parts List for Speed Control Circuit" A-2972 Supp.

5.1 Speed Control Circuit Operation. Assume that the motor has been running at some present speed in a stable manner and then has slowed down due to some mechanical load increase. Due to the slower speed, the tachometer frequency is lower and integrates to a lower dc signal applied to pin 3 of the operational amplifier SN 724. The unbalance between pin 1 and 3 signals results in a higher voltage at pin 6 which results in a higher base current to $Q_2$ and greater base current on $Q_4$ with a resultant higher collector-emitter current. This applies more current to the motor which then speeds up. As the motor once more approaches the desired control speed, the signal at pins 1 and 3 of SN 724L approach toward balance and the voltage on pin 6 falls. In so doing, the base drive currents of $Q_2$ and $Q_4$ decrease and the collector-emitter current of $Q_4$, which is also the motor current decreases, until equilibrium is once more established. If the opposite unbalance occurs, with the motor speed rising beyond the desired controlled speed, an opposite sequence of events occurs.

6. MOTOR PERFORMANCE

6.1 General. For this section of the report, the motor performance will be discussed for the motor as it now exists at the end of the

development work. Where necessary, the commutator performance is discussed at the same time because the components are so intimately connected that it is difficult to quote performance of the motor without simultaneously considering the commutator. Three modes of operation are discussed; operation as a motor with constant voltage or constant torque, operation as a speed-controlled motor and operation as a stepper motor with pulsed electrical inputs.

6.2 Motor Performance at Constant Load. Section (3, i, A) of the JPL Work Statement requires a test of the motor unit at zero, 10 and 20 g-cm shaft external torque applied to the motor shaft. These tests were made and the results are summarized on curve sheets M-2406, M-2407 and M-2408. The data are plotted against the total voltage input to the commutator as the axis of abscissa. Since the voltage shown is the actual battery voltage to the commutator, the motor power inputs shown include the loss in the power switches which mainly is the drop across each collector-emitter of the output transistors. The efficiencies shown are for the actual shaft output torque and also include this loss in the power switches. The power required for the logic circuit, sensor oscillator and the bases of the final output transistors is not included as part of this power input to the motor. The actual shaft efficiencies reach a peak of 50 to 55% which is reasonable considering the small size of the motor.

6.2.1 Comparison of Design and Test Performance. At the time of making the design, the motor c aracteristics were computed at a constant speed of 4500 rpm for variable loads and plotted on curve M-2283. This curve shows the electromagnetic torque output of the motor but does not include the iron loss which would add an estimated 6.5 mA of current input to the values shown for the motor. In order to make a comparison of the computed and actual performance, the computed curve data of M-2283 are replotted on curve sheet M-2453. An actual test was never made of the motor under precisely the same condition as called for by the design computations. However, using curves M-2391, M-2404, M-2406, M-2407 and M-2408 and making the proper allowances, a comparison can be made. The torques measured for these latter curves is shaft output torque, and an adjustment is necessary to change these to electromagnetic torques. From M-2406, a curve of no-load output at variable speed, at 4500 rpm the power input is 0.19 W with a current of 26 mA. Copper loss in the motor is $0.026^2 \times 36.0 = 24.4$ mW, where 36Ω is the resistance of the armature. Therefore the total of core losses, windage and friction loss, spurious and miscellaneous is 190 minus 24 or 166 mW. This power can be converted into an equivalent torque as follows:

$$T_{oz\text{-}in} = \frac{\text{watts}}{\text{rpm} \times 0.0\,0074} = \frac{0.166}{4500 \times 0.00074} = 0.050 \text{ oz-in}$$

If the computed design value of 0.0109 oz-in for iron loss is subtracted from 0.050 oz-in, the remainder 0.039 oz-in is a maximum possible windage and friction at 4500 rpm, neglecting spurious and other losses. This is not unreasonable. Values at 4500 rpm are taken from the curves M-2391 etc, and plotted on M-2453 with two adjustments in values. The estimated windage and friction torque of 0.039 oz-in is added to the shaft torque to give a total electromagnetic output torque. In order to allow for the omitted iron loss, 6.5 mA of current is subtracted from the measured value of current and plotted on M-2453. A similar procedure is followed for the remaining curves. An examination of these data show that the tested performance is considerably better than the computed performance. The principal reason for this improvement is that the computed performance makes an allowance for the loss in the power switches, this being stated as a 2 V total constant drop across the collector-emitter of the two transistors in series with the motor armature. This voltage drop actually is much smaller than anticipated and therefore the tested efficiency is considerably higher. It is concluded that the design performance has been achieved and even slightly surpassed.

6.3 Motor Performance at Various Voltages and Ambient Temperatures.

6.3.1 Motor Characteristics at 10 and 25 Volts. The motor charac-

teristics were measured at 10 and 25 V input as required by Section (3, i, B) of the JPL Work Statement. The 40 V point was omitted by verbal permission because it was relatively less important and there could be some problem with the transistors at this level of input. The motor characteristics measured are shown on curve M-2404 for 10 V input to the commutator and M-2405 for 25 V input to the commutator. Because 5 V is always necessary for the logic portion of the power supply, the input of 10 V is split up as 5 V + 5 V, and the 25 V is split up into 5V + 20 V. M-2404 shows a peak efficiency of 49.5% occurring at a shaft output torque of 9.5 g-cm. Curve M-2405 for 25 V input shows a peak efficiency of 55.5% occurring at 21 g-cm output shaft torque. These data were taken at room temperature before the unit was sent for vibration and environmental testing. For the 25 V input level, the data was not continued on down to the stall point but stopped at an output torque of approximately 50 g-cm which is 125% of the nominal maximum load of 40 g-cm considered useful for the motor.

6.3.2 Motor Characteristics at -10°C, +75°C and Room Temperature. Before sending the motor out for environmental testing, (vibration, shock, etc.) it was also tested at the ambient temperature extreme limits of -10°C and +75°C followed by a room temperature test. The three tests were conducted at a constant input of 25 V at the commutator, split into two separate inputs of 5 V and 20 V. The commutator circuit was kept at room temperature for all

these tests so that the motor only was subjected to the temperature change. Therefore all the changes noted can be charged to the motor only. If curves M-2414 for -10°C ambient and M-2415 for +75°C ambient are compared it shows that the torque produced for a unit of current is almost exactly identical for the temperature extremes of the test. At cold temperature the speed at zero torque is slightly less (15,000 rpm compared with 15,400 rpm for the hot test). This is probably due to a slight increase in the bearing friction. As load is applied, the speed for the hot ambient falls off more rapidly than for the cold ambient due to the higher resistance of the armature winding at the hot temperature. This results in lower efficiency for the hot operation, the maximum for +75°C being 53% at a shaft torque of 14 g-cm compared to a maximum efficiency of 56% at 20 g-cm for the -10°C ambient. The room temperature operation falls in between these two extremes. It should be noted that the input to the sensor oscillator power supply varied slightly because it was adjusted to the minimum voltage which would properly excite all the sensor output. This situation will be discussed in greater detail in a following section.

6.4 Motor Characteristics after Environmental Testing. After the environmental tests were performed by Ogden Testing Laboratories the motor was retested to determine whether any changes resulted from the shock and vibration tests.

6.4.1 Motor Characteristics as Received. The test for comparative performance of the motor was made at 25 V and room temperature. The test was made on the motor as it was received back after the environmental shock, vibration etc. tests had been made. The results of this motor test are shown plotted on M-2454. These data can be compared with M-2416 data taken before the environmental tests were made. The performance is quite similar as regards current, speed, power output and input. The efficiency for the motor after environmental testing peaked out at a lower value by a few percent, but this is not a really significant change. Some change was noted in the oscillator drive requirement for the sensors which will be discussed later.

6.4.2 Motor Characteristics after Examination. The motor was disassembled for physical examination which disclosed no physical signs of damage or change resulting from the shock and vibration testing. The motor was then reassembled and remagnetized as usual. The magnetization process consists of placing the motor between the poles of an electromagnet and applying a field of approximately 18,000 At across the motor diameter. The position of the poles in line with the magnetizing field is first established by passing a low current through the magnetized coils which will rotate the rotor magnet until its field lines up with the magnetizer field. The results of a load test similar to the previous section is shown on M-2455. There are some minor

differences between the data of M-2454 and M-2455. The current at the low torque on the latest test M-2455 are slightly higher with accompanying higher power input at the same torque output and therefore lower efficiency. Thus the efficiency peak is about 50% compared to 52.5% for the motor before disassembly. At torques over 25 g-cm, the difference between the data begins to disappear. No explanation can be made which is consistent with the known data. It is possible that the new magnetization resulted in slightly less magnetic strength of the rotor but it would also be necessary to have slightly higher friction losses so that the no-load speed would not also be higher.

6.5 Motor Operation in Pulse Stepping Mode.

6.5.1 General. The Work Statement (3, iii) calls for measurement of the stepping characteristics of the motor with a rectangular input pulse of 50 V having a duration of 1 ms. By trial of this type of input where the motor is stalled, it was found that a voltage of 24 V (+5 V and -19 V) gave a current of roughly 400 mA in the motor which was judged ample for the test purposes as regards uniformity of response and represented a reasonable upper limit of current in the commutating transistors without unduly stressing them. For purposes of making the test, the pulse control circuit used is shown in the schematic A-2921. This circuit controls the TI 1135 transistor and

makes it conduct for a single short time interval which can be adjusted for length of pulse by changing the value of the capacitor shown. When the switch is thrown to the "on" position, a voltage pulse is inserted into the single-shot circuit turning the transistor on until the other side of the circuit turns off. The T I 1135 transistor thus acts as a switch in the negative voltage line input to the commutator control circuit. The pulses produced by this circuit are very similar in terms of length of "on time" as far as can be compared on an oscilloscope. In most cases the deviation was less than 10%. As will be seen, the test results showed deviations far in excess of this amount, so that it did not seem necessary to measure or refine the accuracy of the pulse input any further at this time.

6.5.2 Performance.

6.5.2.1 Current Pulses. Oscillograms of the current pulses obtained with a 24 V input are shown on the next page. For the upper oscillograms, the time that the maximum current is on is 1.1 ms and the time for start to finish of the pulse is 1.3 ms which makes the rise and fall time approximately 0.1 ms each. The average pulse length would thus be 1.2 ms. The lower oscillograms have a full current on time of 2.1 ms and the total time of 2.4 ms, with an average of approximately 2.3 ms. It should be emphasized that these are actual currents through the motor and not the voltage applied across it. The motor was pulsed with the approximate 1 ms and 2 ms

HERBERT C. ROTERS ASSOCIATES, INC.

OSCILLOGRAMS OF MOTOR ARMATURE CURRENT PULSES

JPL #951463

Unit #159 DC Brushless Motor

24 Volts Input to Armature Circuit (+5 and -19 V)

A-2921 Circuit

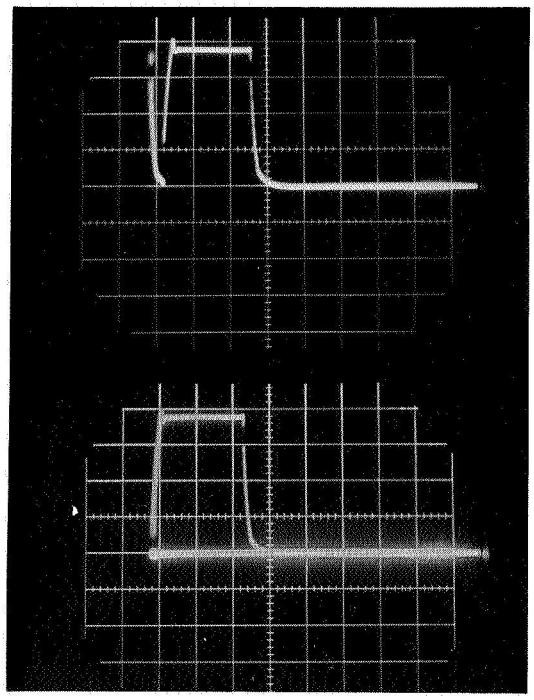

#1

Current Pulse 1.2 ms (approx)

(Voltage across 1Ω series resistor)

| | |
|---|---|
| Vertical | 100 mV/cm |
| Horizontal | 0.5 ms/cm |

Trial A

Trial B

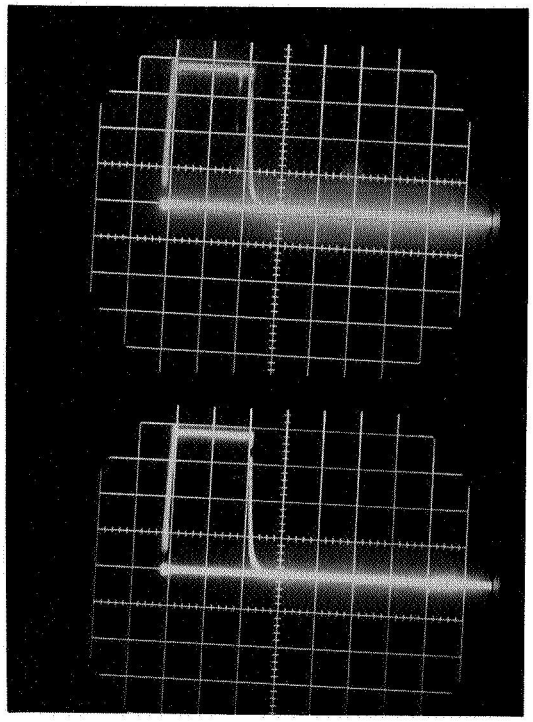

#2

Current Pulse 2.4 ms (approx)

(Voltage across 1Ω series resistor)

| | |
|---|---|
| Vertical | 100 mV/cm |
| Horizontal | 1 ms/cm |

Trial A

Trial B

HERBERT C. ROTERS ASSOCIATES, INC.

ARMATURE ROTATION WITH PULSE VOLTAGES APPLIED

JPL #951463

Unit #159 Brushless DC Motor

Armature position after applying one pulse of current from circuit A-2921 with 24 volts on the circuit (+5 and -19 volts), see Oscillograms #1 and #2

1.2 ms pulse
380 mA

| Position Deg | Displacement Deg |
|---|---|
| 0 | 50 |
| 50 | 115 |
| 165 | 50 |
| 215 | 105 |
| 320 | 40 |
| 0 | 70 |
| 70 | 105 |
| 175 | 70 |
| 245 | 100 |
| 345 | 25 |
| 10 | 90 |
| 100 | 80 |
| 180 | 70 |
| 250 | 100 |
| 350 | 55 |
| 45 | 115 |
| 160 | 45 |
| 205 | 85 |
| 290 | 65 |
| 355 | 70 |
| 65 | 100 |
| 165 | 50 |
| 215 | 100 |
| 315 | 45 |
| 0 | |

2.4 ms pulse
380 mA

| Position Deg | Displacement Deg |
|---|---|
| 0 | 220 |
| 220 | 280 |
| 140 | 220 |
| 0 | 225 |
| 225 | 275 |
| 140 | 223 |
| 3 | 237 |
| 240 | 285 |
| 165 | 200 |
| 5 | 265 |
| 270 | 270 |
| 180 | 210 |
| 30 | 250 |
| 280 | 255 |
| 175 | 200 |
| 15 | 260 |
| 275 | 260 |
| 175 | 215 |
| 30 | 250 |
| 280 | 255 |
| 175 | 220 |
| 35 | 260 |
| 295 | 240 |
| 175 | 215 |
| 30 | 250 |
| 280 | 255 |
| 175 | 220 |
| 35 | 255 |
| 290 | |

pulse lengths shown by the oscillograms. The observations made for the angle of armature position after each pulse for a series of these pulses is shown in the table on a succeeding page. The 1 ms pulses shows stepping motions from a low of 25° to a high 115°. There is some evidence that a preferential locking point exists in or around the zero degree position. Thus, the angular travel when starting from the zero position is less than when starting from a position like 240°. For 2 ms pulses, the angular interval of travel is more uniform but still erratic enough to vary from 200° to 285°.

6.5.2.2 Magnetization Procedure Effects on Stepping Performance. The rotor magnet is magnetized in place while it is assembled in the motor so that there may be a tooth pattern formed on the magnet which results in some lock points during a revolution. To try to eliminate this, the magnetizing field was increased in strength to 24,000 At across a 3/4" gap (Motor OD). The magnetizer has 3" diameter pole cores terminating in 2-1/2" diameter ferro-cobalt pole face pieces. Thus the magnetic intensity in the gap is approximately 32,000 At/in corresponding to an air flux density of 102 kMx/in$^2$ or 15.8 kG. However, this still did not eliminate the lock points. Therefore to study the operation with a tooth pattern and lock points eliminated, the rotor was disassembled and magnetized outside of the stator. This produces a very uniform magnetization in the cylindrical magnet rotor and eliminated any lock

points caused by the teeth. Test of the angular steps resulting with this magnetization showed that the length of angular travel ranged from 50° to 100° per pulse depending on the position, for 1 ms pulses. This performance is slightly better than with the rotor magnetized in place. It shows that some other factor is causing the erratic amount of angular step motion.

6.5.2.3 Time of Stepping Motion. The actual time for mechanical motion was not studied. It is theoretically much longer than the pulse length because as long as the current exists in the motor, torque is developed and the rotor will accelerate. When the current ceases, the rotor will be traveling at its maximum velocity and coast to a stop while decelerated by any braking forces present. Since the current wave form input to the motor is quite flat, the velocity of the rotor is insufficient to cause enough generated voltage sufficiently large to decrease this current. The current amplitude is determined by the armature resistance and inductance and the cut-off level of the commutation and control circuits. Apparently this cut-off level of current may have been reached since the drop in the motor winding resistance for the test is 13.8 V (36Ω x 0.380 A) while the voltage input was 24 V. In any case, because the motor current was constant during the 1 ms pulse interval, it can be assumed that the torque produced would also be constant. Therefore the acceleration of the rotor would

be uniform with maximum velocity at the end of the pulse.

6.5.2.4 Continuous Stepping Input. Continuous pulses of 1 ms duration at a 500 Hz repetitive frequency rate were applied to the motor. No interruptions of rotor speed could be detected in the form of steps, and the motor seemed to run as though it were continuously excited. Some thought was given to the possibility of inserting ac pulses, but these cannot be inserted as an input to the commutation supply of the dc motor. A possible alternate method of producing accelerating and braking torques might be a reversal of torque controlled by the logic circuit. This would require that the reversal signal be applied to the commutation logic circuits during half the cycle time. Then the pulse would produce accelerating torque and the time between pulses would produce braking torque.

6.5.2.5 Conclusions on the Foregoing Performance. It is concluded for a short pulse length like 1 ms that the motor will not step in uniform increments and that the increments will be dependent on the rotor starting position and that this disparity is roughly 2:1. It does not appear that one-sided dc pulses will lead to fast and accurate mechanical action times unless some method of introducing braking pulses is devised. When a 1 ms pulse of current is applied, the rotor accelerates during the entire 1 ms "on time" and at the end of the interval is traveling at maximum velocity. In order to bring the rotor

to a halt, an equal or greater braking effort must be applied for the "off time" interval. Therefore one problem will be to insert such a braking pulse. For example the motor can generate current backwards through the commutation supply transistors if the motor input terminals could be shorted. Unless these input terminals are shorted, there is no place for the current to go except to the battery. This is impossible because the battery voltage always exceeds the motor generated voltage. Undoubtedly there are ways to accomplish this braking but the methods may be complex and not justifiable by absolute need for such a device. The previously mentioned method of splitting the pulse into an accelerating torque phase and a decelerating torque phase by controlling the logic reversal is such a scheme. It is suspected that the actual circuit could be quite tricky.

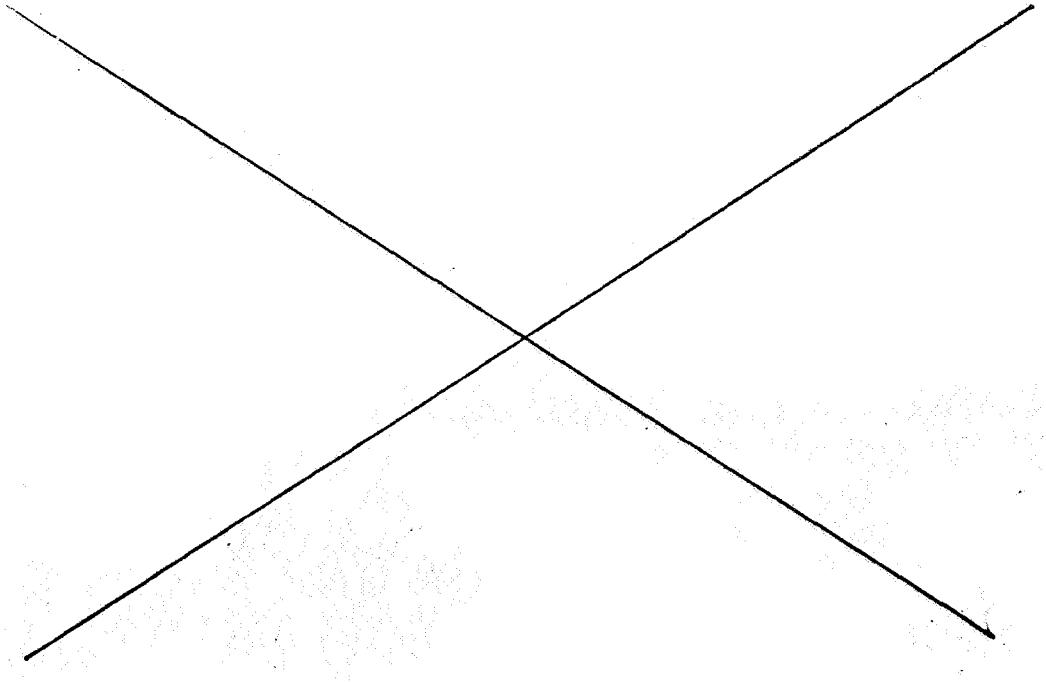

6.6 Stability of Motor Performance.

6.6.1 General. During the experimental work on the motor, some changes in the performance characteristics of the sensor took place. This change, reason unknown, resulted in a gradual rise in the exciting voltage required to drive the sensor primary exciting coil so that sufficient voltage output on the sensor secondary was obtained to drive the commutation circuit. A basic cause of the increase in excitation could be an increase in the internal air gaps of the ferrite magnetic parts which make up the sensor or to uncertainty of the axial air gap due to the end play allowed in the bearings. The internal air gaps between the ferrite parts are dependent upon the stability of the encapsulating material with time, temperature and vibration of the unit.

6.6.2 Dimensional Stability. The motor, as originally made and tested had an axial end play of approximately 0.001" as to not preload the bearings. To eliminate this end play as a cause of changes in the sensor characteristic, a spring was made to give a preload force on the bearings. This spring is shown on the detail drawing A-3008 as it was finally made, after experimentation to modify the paper design and obtain the desired force of 8 oz. The shoulder on the shaft at the shaft extension end was turned off to leave approximately 0.020" axial space. This space is now occupied by the above spring plus a spacer washer. The thickness of the spacer washer was adjusted so that the axial motion was limited to 0.001" if the axial force on the shaft exceeded the 8 oz preload. The minimum axial air gap between the sensor armature and the pole is established by the fixed mechanical dimensions of

the parts having interface contacts. This gap will be maintained at its minimum value by the spring force.

6.6.3 Environmental Stability. The stationary structure of the sensor was built up of separate ferrite parts which were encapsulated into an integral structure. There is an air gap between the Ferrite Pole A-2778 and the Ferrite Core A-2763. Such a surface to surface contact usually appears to be at least a 0.001" air gap as regards magnetic permeance. There is a possibility that gradual changes may occur in such a gap due to dimensional changes in the encapsulating material and shifts in the ferrite parts making up the structure. The unit has already undergone a long series of tests for performance and an actual shake and vibration test series. However, if the unit were not already stabilized, a series of 10 cycles of temperature fluctuations such as specified in MIL-STD-202C, Method 102A could cause a further mechanical shift of parts in the encapsulated sensor. Therefore, the motor with the added preload spring installed was given ten cycles, each cycle consisting of 1 hour minimum in 85° C ambient, 1 hour minimum in -15° C ambient. The unit was shifted directly between ambients without a hold time at room temperature.

6.6.4 Stability Evaluation. In order to check the effect of the treatment of paragraph 6.6.3, on the sensor stability, the motor and sensor performance were checked before and after the temperature cycling. One of the changes noted in the past was in the minimum required dc voltage applied to the sensor oscillator circuit. If this voltage were too low, one or more of the commutation transistors would cut off due to

insufficient sensor signal output. Therefore, the minimum acceptable operating level will be when all output transistors are just conducting. This was measured by gradually raising the oscillator dc input voltage with the motor operating at a 25 volt dc input and a shaft load of roughly 25 g-cm until all signs of cutoff had disappeared. Another set of readings were taken with the oscillator dc input raised roughly two volts. These data were taken before and after temperature cycling. In addition, the motor operating data were taken at no-load and 25 g-cm shaft load with 25 volts dc applied to the motor commutation circuit.

6.6.5 Stability Evaluation Results. The results of the experimentation of the previous paragraph are summarized in the tables on the following pages. The first table compares the output of each sensor coil before and after the temperature cycling for the minimum oscillator driving level and at a dc input roughly two volts higher than the minimum. The ac sensor coil output voltage are shown for the minimum and maximum output as the armature is slowly turned by hand. The dc output from the rectifier circuit connected to the sensor coil is also shown for the min imum and maximum output voltage. The minimum dc voltage is only included for completeness to verify that the rectified sensor voltage output goes to zero. The second table compares the motor performance before and after the temperature cycling with the motor operating at no shaft load output and also at a nominal load of 25 g-cm (approximately).

6.6.5.1 Conclusions on Sensor Stability During Temperature Cycling. An examination can be made of the effect of temperature cycling by direct comparison of the first four colums

## EFFECT OF TEMPERATURE CYCLING + ON COMMUTATION SENSOR
## COMPARISON OF SENSOR OUTPUT VOLTAGE
## (AFTER INSTALLATION OF A-3008 BEARING PRELOAD SPRING)
## TESTS WITH STATIONARY ARMATURE

| Sensor Coil | Before Temperature Cycling | | | | + After Temperature Cycling | | | |
|---|---|---|---|---|---|---|---|---|
| | AC Sensor Coil Output Voltage rms Volts | | DC Sensor Rectifier Output Voltage-Volts | | AC Sensor Coil Output Voltage rms Volts | | DC Sensor Rectifier Output Voltage-Volts | |
| | Max | Min | Max | Min | Max | Min | Max | Min |
| | Oscillator Circuit Input 25.2 V 7.38 mA, f = 105 kHz | | | | Oscillator Circuit Input 24.8 V 7.02 mA, 105 kHz | | | |
| Green | 1.25 | 0.225 | 0.90 | 0 | 1.23 | 0.207 | 0.88 | 0 |
| Bl-Wh | 1.25 | 0.245 | 0.92 | | 1.24 | 0.225 | 0.84 | |
| Blue | 1.29 | 0.245 | 0.93 | | 1.26 | 0.226 | 0.86 | |
| Black | 1.27 | 0.226 | 0.91 | | 1.25 | 0.219 | 0.82 | |
| Violet | 1.29 | 0.250 | 0.94 | | 1.30 | 0.184 | 0.86 | |
| Brown | 1.28 | 0.225 | 0.92 | | 1.25 | 0.219 | 0.86 | |
| Purple | 1.25 | 0.230 | 0.90 | | 1.23 | 0.220 | 0.85 | |
| Yellow | 1.30 | 0.235 | 0.94 | | 1.30 | 0.186 | 0.89 | |
| White | 1.21 | 0.226 | 0.86 | | 1.25 | 0.165 | 0.80 | |
| Orange | 1.20 | 0.194 | 0.86 | | 1.18 | 0.189 | 0.825 | |
| Gray | 1.25 | 0.215 | 0.92 | | 1.25 | 0.214 | 0.870 | |
| Red | 1.30 | 0.240 | 0.90 | | 1.29 | 0.234 | 0.890 | |
| Average | 1.262 | 0.230 | 0.908 | | 1.253 | 0.211 | 0.854 | |
| | Oscillator Circuit Input 27.2 V 7.80 mA; f = 105 kHz | | | | Oscillator Circuit Input 27.2 V 7.79 mA; f = 105 kHz | | | |
| Green | 1.31 | 0.225 | 0.99 | 0 | 1.35 | 0.229 | 0.965 | 0 |
| Bl-Wh | 1.34 | 0.247 | 1.00 | | 1.36 | 0.250 | 0.96 | |
| Blue | 1.36 | 0.245 | 1.02 | | 1.40 | 0.250 | 0.97 | |
| Black | 1.35 | 0.238 | 1.00 | | 1.36 | 0.240 | 0.96 | |
| Violet | 1.35 | 0.245 | 1.04 | | 1.45 | 0.202 | 1.00 | |
| Brown | 1.35 | 0.236 | 1.01 | | 1.37 | 0.240 | 1.00 | |
| Purple | 1.31 | 0.239 | 1.00 | | 1.35 | 0.242 | 0.97 | |
| Yellow | 1.35 | 0.245 | 1.02 | | 1.44 | 0.206 | 1.00 | |
| White | 1.29 | 0.237 | 0.92 | | 1.35 | 0.183 | 0.93 | |
| Orange | 1.26 | 0.204 | 0.92 | | 1.30 | 0.206 | 0.92 | |
| Gray | 1.33 | 0.226 | 0.98 | | 1.36 | 0.231 | 0.965 | |
| Red | 1.39 | 0.253 | 1.01 | | 1.40 | 0.255 | 1.00 | |
| Average | 1.333 | 0.237 | 0.993 | | 1.374 | 0.228 | 0.970 | |

+ (10) Temperature Cycles -15° C to 85° C to -15° C, one hour minimum at each temperature.

EFFECT OF TEMPERATURE CYCLING + ON MOTOR PERFORMANCE
(AFTER INSTALLATION OF A-3008 BEARING PRELOAD SPRING)
25 VOLTS DC APPLIED TO MOTOR CIRCUITS

| | | Before Temperature Cycling | | After Temperature + Cycling | |
|---|---|---|---|---|---|
| | | Minimum Oscillator Input | 27.2 V Oscillator Input | Minimum Oscillator Input | 27.2 V Oscillator Input |
| Oscillator DC Input | | | | | |
| Voltage | V | 25.2 | 27.2 | 24.8 | 27.2 |
| Current | mA | 7.22 | 7.88 | 7.02 | 7.76 |
| Power | mW | 182 | 214 | 174 | 211 |
| | | NO LOAD | | | |
| Motor | | | | | |
| Battery Input Current | mA | 44.6 | 51 | 45.9 | 50.9 |
| Battery Input Power | mW | 1117 | 1275 | 1144 | 1270 |
| Motor Shaft Torque | g-cm | 0 | 0 | 0 | 0 |
| Speed | rpm | 14320 | 14600 | 14160 | 14400 |
| | | 25.7 g-cm Shaft Load | | | |
| Battery Input Current | mA | 213 | 214 | 211 | 219 |
| Battery Input | mW | 5330 | 5355 | 5285 | 5475 |
| Motor Shaft Torque | g-cm | 25.7 | 25.7 | 25.7 | 25.7 |
| Speed | rpm | 10400 | 10600 | 10120 | 10450 |
| Shaft Power Output | mW | 2747 | 2800 | 2674 | 2761 |
| Efficiency | % | 51.5 | 52.3 | 50.6 | 50.4 |

+ (10) Temperature cycles -15° C to 85° C to -15°C, one hour minimum at each temperature

(before) to the last four columns (after). An averaged value of the twelve sensor readings is included. Individual coil values are somewhat erratic because it is difficult to obtain the true maximum reading. The minimum dc oscillator input voltage required for complete commutation appears to show a drop to 24.8 volts after temperature cycling compared to 25.2 volts before. This is believed to be a result of the difficulty in setting an exact minimum value to the current cutoff of the commutation transistor. The dc sensor circuit output voltage after temperature cycling is quite a bit lower, 0.854 volts as compared to the 0.908 volts before. Such a difference could be interpreted to mean that the electronic commutation circuit had changed and not that the sensor had altered characteristics. A lower dc oscillator input will normally produce a lower dc rectified sensor output. A better comparison can be made from the average values for a 27.2 volt dc oscillator input. There is virtually no change in the oscillator input current and very little change in the sensor outputs. In fact, for the 27.2 volt input, while the average dc sensor coil output has increased 3% after temperature cycling, the dc rectified sensor coil output has decreased 2.4%. For all practical purposes, it is concluded that the temperature cycling has not affected the performance of the sensor.

6.6.5.2 Conclusions on Motor Performance Stability During Temperature Cycling. The results summarized in the second table for motor performance before and after temperature

cycling show no significant changes in any of the parameters such as motor current and motor speed. Any changes can be the combination of experimental error in readings plus the possibility of variation in bearing friction. Therefore it is concluded that the temperature cycling has had no effect on the motor performance.

6.6.5.3 Final Conclusion on Sensor Stability. From the past history of the motor-sensor unit it is concluded that the unit is now stable and that this stability is a result of:

a) Passage of time plus vibration and shock testing

b) More precise axial positioning of the shaft and preloading of the bearings.

The temperature cycling had no further effect on the unit. The value of performing a temperature cycling operation can be determined only on a new motor unit in combination with the condition (b) above. On such a fresh unit it can be conceived that the temperature cycling will help stabilize the unit without the operation of (a) conditions above. Such a temperature cycling operation should be specified on any further motors of this type.

6.7 Speed Control. The theoretical mode of operation of the speed control circuit is described in section 5.1 of the report.

6.7.1 Test of One-Shot Multivibrators. The desired frequencies at the speed governing point are as follows:

| | | | | | |
|---|---|---|---|---|---|
| Motor Speed | rpm | 8000 | 4500 | 2000 | 200 |
| Control Frequency (OS-1) | Hz | 4260 | 2400 | 1065 | 106.5 |
| Motor Speed Frequency (OS-2) | Hz | 1600 | 900 | 400 | 40 |

The motor speed frequency is based upon generating 12 pulses per revolution of the shaft and is equal to rpm x $\frac{12}{60}$. The one-shot multivibrators will be referred to as OS-1 for the speed control frequency signal and OS-2 for the motor speed frequency signal. An initial test of these units was performed with the results shown on M-2348 which shows the filtered output voltage from the one-shot multivibrator (this is also the input to the differential amplifier) versus the input frequency to the one-shot multivibrator. The input frequency was obtained from a sine wave oscillator for these tests. The solid line curves show actual data for the two units and is reasonably linear. For comparison purposes, the data for OS-1 was replotted (dashed curve) to show the output voltage at a frequency ratio of 900/2400. At any frequency, for perfect speed control, the voltage of OS-1 and OS-2 should be equal. Although this is not quite true, it will be possible to correct the major difference by adjusting the circuit parameters to achieve the same curve slope. At very slow speeds, the curves appear slightly different in shape and may require an added correction. The basic concept of a signal output proportional to frequency input looks sufficiently workable to use for speed control purposes over a considerable range.

6.7.2 Final Status of Speed Control Circuit. Further work on the speed control circuit was stopped in favor of additional work on the sensor stability discussed in Section 6.6. The present condition of the speed control circuit is shown on A-2972. This circuit does not successfully control the motor speed because the motor hunts violently in speed. This unstable condition appears when the servo loop is closed and the motor speed signal is fed into the control circuit at OS-2.

6.7.3 General Remarks. In the test work on the speed control circuit, there has been a relatively high rate of failure of various semiconductor components, the cause of which is unknown. Some failures have also occurred in normal motor testing without the speed control circuit. These failures have occurred mostly in the commutation transistors $Q_1$ and $Q_3$ of A-2780A, and several failures in the logics circuit SG 220 (AG-2) of A-2780A. These breakdowns have continued even after various precautionary circuit protections such as reverse current diodes have been installed. It would be advantageous if any further work were to be done, to start analysis with a lower frequency motor speed signal obtained by using only one-half or less of the commutation circuits to produce the motor speed signal.

## 7.0 CONCLUSIONS AND RECOMMENDATIONS

7.1 Motor. From the design and performance of the test unit the following conclusions are drawn:

a) The motor output performance is very good and in agreement with calculated values.

b) The use of a ring armature winding has been satisfactory and has produced no unknown extra losses.

c) The elimination of the mounting hole in the rotor magnet is quite important to obtain the best performance in a motor with a small diameter such as the subject one.

d) The method of rotor construction with a two-piece shaft is stable mechanically and has not distorted with time, temperature cycling and shock and vibration tests.

e) The motor cannot be used in stepping operations with its present method of commutation and control and no simple method of achieving a stepping action has been devised.

7.2 Sensor. The following conclusions are made respecting the sensor and its performance:

a) It is possible to build an operable electromagnetic twelve pick-off sensor within the allowed 3/4" diameter.

b) Some aging changes have been noted in the performance characteristics of the sensor which may be a result of either time or the environmental tests or both.

c) Temperature cycling operations per MIL-2020 produce no further effect after the changes of (b) above have occurred.

d) It is believed possible to bring about an earlier stabilization by performing such a temperature cycling operation immediately after assembly.

e) The use of a bearing preloading spring is desirable for stability of sensor performance.

f) The present shielding method has yielded almost completely satisfactory conformance to the radio interference specifications.

g) A two terminal oscillator as designed has proved to be simple and reliable.

7.3 Logic. With regard to the logic portion of the circuit, it is concluded that:

a) The method of obtaining a reversal of motor rotation by logic switching semiconductors is completely workable.

b) Although the power consumed may be considered relatively high, except for a laboratory model, such power consumption should be capable of reduction in new designs.

c) The frequency of component failure has been higher than would be expected in normal usage.

7.4 Commutation Circuit. For the commutation circuit it is concluded that:

a) The final circuit is satisfactory as regarding yielding good motor performance.

b) The failure of semiconductor components in the commutation portion of the circuit has been much more frequent than expected and the reasons are not known.

7.5 Recommendations. From the experience gained in the performance of this job it is recommended that:

a) The motor and sensor construction for any future experimental work should be made to use fewer armature coils, slots and sensor output coils so that the accompanying electronic circuits will be fewer in number and easier to experiment with.

b) When less sensor coils are used, construction methods using one piece ferrite magnetic circuits may be possible. This will avoid the problem of possible changes in air gaps in composite ferrite assemblies in the sensor.

c) Where multiple composite ferrite assemblies are used in a sensor construction, careful consideration should be given to the temperature-time stability of the encapsulating resin.

A temperature cycling operation should be the first step after an encapsulation assembly operation to assist stabilization.

d) Further work is needed on the reliability of the various logic and commutation semiconductors and the effect of the circuit operation. Higher voltage transistors should be an initial improvement trial on actual hardware coupled with a thorough circuit analysis and circuit current and voltage measurements as a parallel effort.

# APPENDIX I
## MOTOR DESIGNS

This section is included as a brief discussion of the preliminary designs made before the final unit design. The first design #1 demonstrated that it was almost a necessity to find a method for eliminating the shaft mounting hole in the magnet and thus obtain a larger magnet cross section area.

Design #2 introduced the change to a solid magnet rotor (no shaft hole) which provided a large increase in available magnet flux. The yoke ring was changed to silicon steel because of its higher flux carrying ability compared to nickel-iron. The length was reduced to 0.30" to approach the desired overall motor length of 1-1/4". 11 slots were picked as a reasonable number considering problems of leads and sensor coils. M-2276 shows the computed performance.

Design #3 is similar in all respects to #2 except that the stator length is increased to 0.372" and the winding changed accordingly. M-2275 shows the computed performance and the relatively large improvement in efficiency at the higher load levels. For example, at 0.5 oz-in the efficiency for the 0.372" stator length is 32% compared to 23% for the 0.30" stator length. Since the stator length is a small part of the overall motor length, the longer stack was chosen by mutual agreement with JPL. The axial length of the motor is distributed roughly as follows:

| | | |
|---|---|---|
| 1. | Back end cover | 0.025" |
| 2. | Clearance to end connections | 0.010" |
| 3. | Back end connection | 0.171" |
| 4. | Stator stack length | 0.372" |
| 5. | Stator stack end insulators | 0.020" |
| 6. | Front end connections | 0.171" |
| 7. | Clearance between front end connections and bearing support plate | 0.015" |
| 8. | Front bearing support plate | 0.025" |
| 9. | Clearance between front bearing support plate to sensor rotor support plate | 0.050" |
| 10. | Rotor support plate | 0.050" |
| 11. | Sensor rotor, axial thickness | 0.050" |
| 12. | Sensor coil space | 0.278" |
| 13. | Sensor yoke | 0.050" |
| 14. | Front case cover | 0.025" |
| | Total Length | 1.312" |

Design #4 is the final design and is modified to have a 12 slot stator, a ferrocobalt yoke ring, the stator lamination material changed to silicon steel and a thinner rotor magnet housing which permits a 0.015" effective rotor-stator radial air gap. The computed performance is shown on M-2283 and is roughly comparable with Design #3. The motor construction and performance are described in the main body of the report. A tabulation of the important mechanical sizes and parts material for each of the designs is listed below.

| | | Design #1 | Design #2 | Design #3 | Final |
|---|---|---|---|---|---|
| OD Stator | in | 0.719 | 0.688 | 0.688 | 0.700 |
| ID Stator | in | 0.322 | 0.372 | 0.372 | 0.342 |
| Length Stator | in | 1/2 | 0.300 | 0.372 | 0.372 |
| Number of teeth | | 15 | 11 | 11 | 12 |
| Tooth Width | in | 0.059 | 0.037 | 0.037 | 0.028 |
| Gross Slot Area | $in^2$ | 0.0054 | 0.00851 | 0.00851 | 0.0102 |
| Turns per coil | | | 121 | 98 | 82 |
| Wire Size | | #43 | #40 | #39 | #38 |
| Armature Resistance (brush-brush) | Ω | - | 71.0 | 45.6 | 36.0 |
| Stator Material | | Nickel Iron | Nickel Iron | Nickel Iron | Silicon |
| Yoke Ring Material | | | Silicon Steel | Silicon Steel | Ferrocobalt |
| Rotor OD | in | 0.312 | 0.312 | 0.312 | 0.312 |
| Rotor ID | in | 0.125 | 0 | 0 | 0 |
| Rotor Length | in | 0.500 | 0.300 | 0.372 | 0.372 |
| Material | | Alnico IX | Alnico IX | Alnico IX | Alnico IX |
| Radial Air Gap | | 0.005" | 0.020" | 0.020" | 0.015" |
| Computed Performance | | - | M-2276 | M-2275 | M-2283 |

Design

#1 Abandoned because teeth too large, winding too fine wire

#2 " " too long

#3 Decided to make 12 slots, change to Ferrocobalt yoke and thinner case wall

## APPENDIX II

## EXPERIMENTAL EVALUATION OF THE LOGIC, AND COMMUTATION CIRCUITS

The following section describes the principal changes in the circuitry for the motor power supply from the early conception stage to the final delivered stage.

The commutation circuit in its first complete outline is shown on A-2760. The final circuit is shown on A-2780A and the following described changes were made at various times.

1. The sensor output rectifier-filter circuit ($C_1$ + $R_1$ of A-2780A) was made 0.1 $\mu$F and 10 k to speed up the response of the sensor rectified signal output.
2. Decoupling inductors were added ($L_1$ and $L_2$) and a filtering capacitor $C_3$ to eliminate a tendency of some bar circuits to oscillate.
3. Resistance $R_3$ and $R_4$ were added to limit the base currents in $Q_1$ and $Q_2$ and $AG_2$.
4. Reverse polarity diodes $CR_3$, $CR_4$, $CR_5$ and $CR_6$ were added to help dissipate any pump-back of current through the output transistors $Q_3$, $Q_4$, $Q_5$ and $Q_6$. Such a reverse direction voltage might arise when the opposite bridge transistors $Q_4$ and $Q_5$ clamp off and the inductance of the winding generates a voltage from $M_2$ to $M_1$ with $M_1$ possibly rising higher than the 5 volt bus voltage.

5. The output signals from each half of the bar circuit were brought out separately to each other. When all the outputs of the six bar circuits were brought to a common, there was too much interference between the commutator circuits resulting in false switching and other problems.
6. The Pulse Isolation Amplifier of A-2865 was added to each bar output (12 outputs) to eliminate the feedback problem of Item 5.

## APPENDIX III

## ENVIRONMENTAL TESTS

This appendix consists of the report of the environmental tests "Originators Report No 6D108-4" performed by Ogden Technology Laboratories, Inc., OT L Job Number 7667, Herbert C Roters Associates, Inc. purchase order 1940. All tests were passed except for the radio interference test where some interference exceeding the limit as noted at various points as discussed in the Ogden report section 4.1.1. Their Figure 1 shows the amount of excess over the specification, a maximum of perhaps 12% at some points. No comment will be made about the importance of these results or the need for improvement.

# PROPOSED CIRCUIT FOR REGULATING THE MOTOR-SPEED IN RESPONSE TO A VARIABLE-FREQUENCY SQUARE WAVE SIGNAL

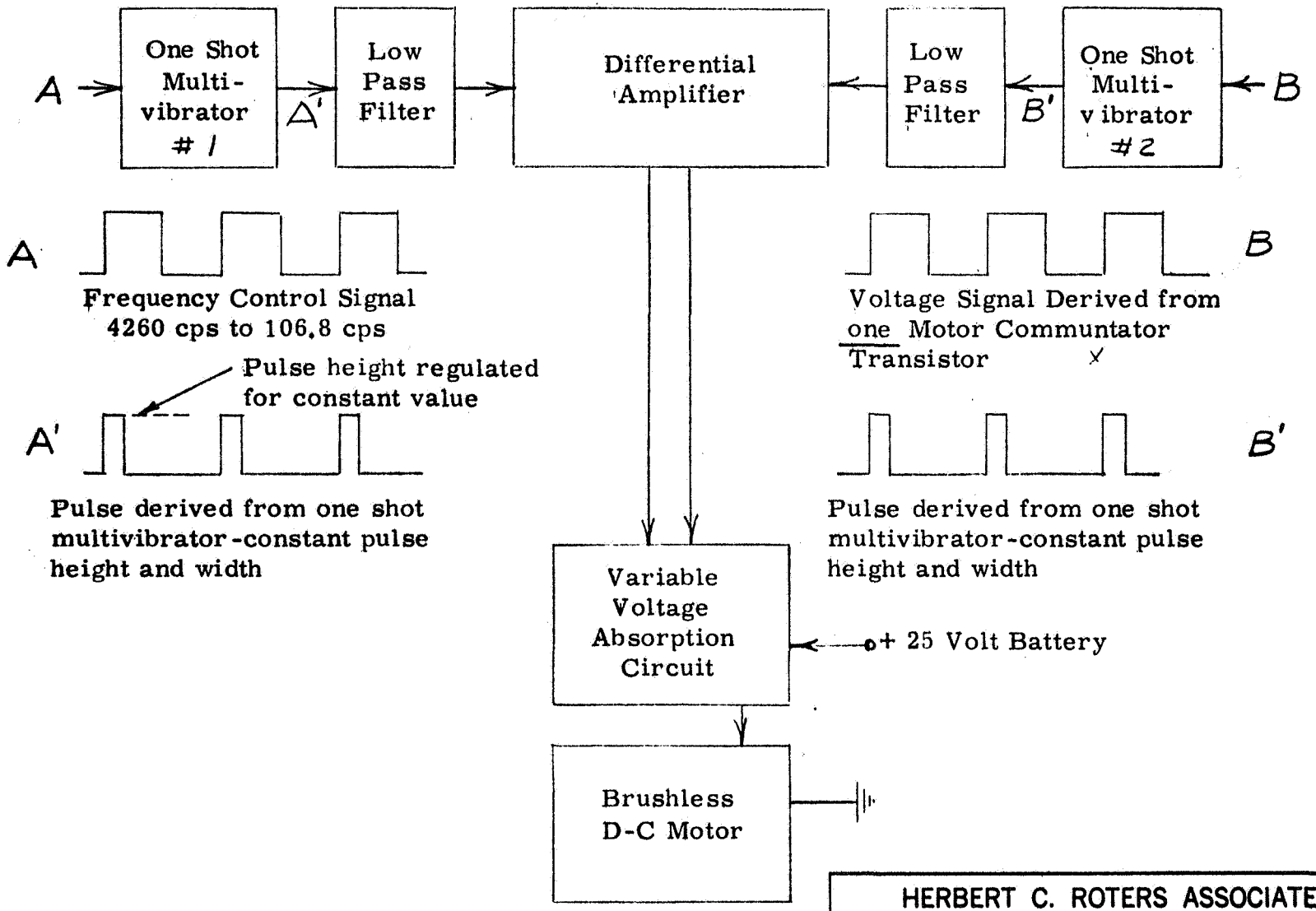


| NO. | BY | DATE | REVISION |
|---|---|---|---|
| A | HOJ | 2-28-63 | ADDED #1 & #2 |

TOLERANCES
FRACT. ± 1/64 DEC. ± .005 ANG. ± 1/2°
UNLESS OTHERWISE SPECIFIED

HERBERT C. ROTERS ASSOCIATES, INC.

TITLE: See Above

DR. BY: DATE 8-65

CH. BY: DATE

MATERIAL

SCALE

No. A-2667

No. A-2667

No. A-2667

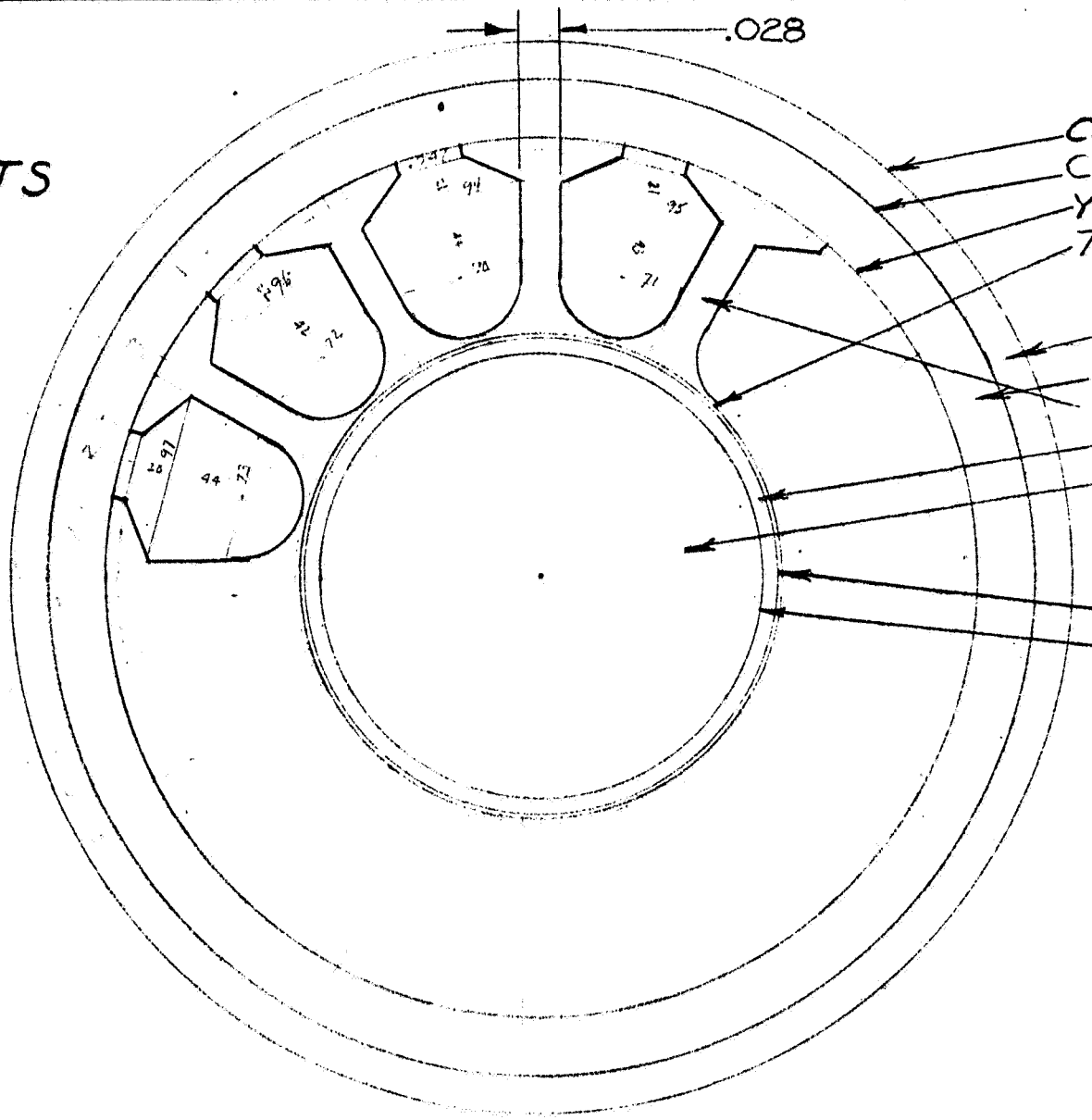


No. A-2737

No. A-2737

HERBERT C. ROTERS ASSOCIATES, INC.

TITLE: LAMINATION LAYOUT showing Case and Rotor

DR. BY: HCR DATE 5-11-66

CH. BY: DATE

MATERIAL

SCALE 8X

No. A- 2737

TOLERANCES
FRACT. ± 1/64 DEC. ± . ANG. ± 1/2°
UNLESS OTHERWISE SPECIFIED

| NO. | BY | DATE | REVISION |
|---|---|---|---|
| | | | |
| | | | |
| | | | |

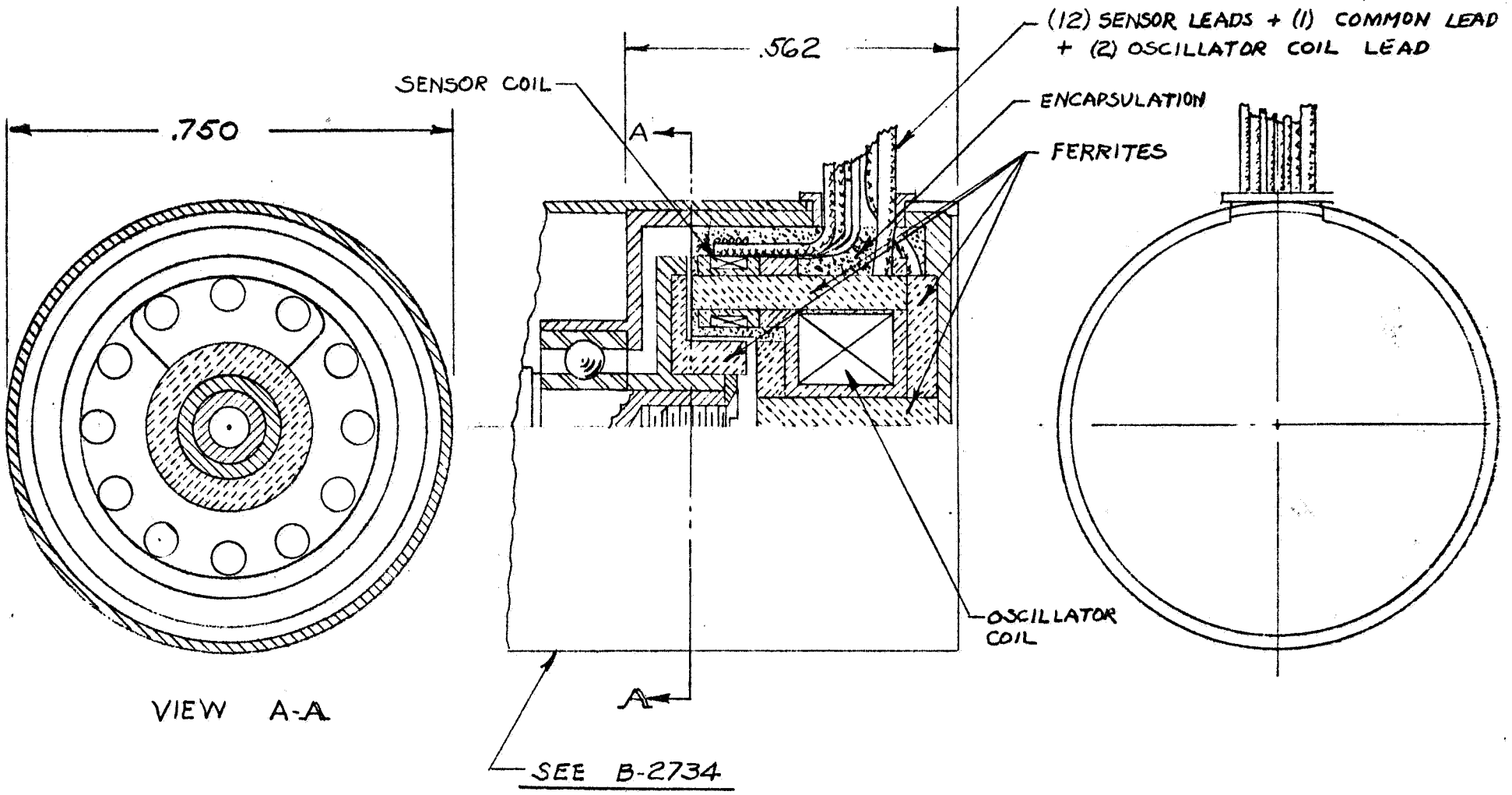


No. A-2742

No. A-2742

| NO. | BY | DATE | REVISION |
|---|---|---|---|
| | | | |

TOLERANCE
FRACT. ± 1/64 DEC. ± ANG. ± 1/2°
UNLESS OTHERWISE SPECIFIED

HERBERT C. ROTERS ASSOCIATES, INC.

TITLE: SENSOR ASSEMBLY LAYOUT I
DC. BRUSHLESS MOTOR JPL#951463

| DR. BY: | DATE | MATERIAL |
|---|---|---|
| HOJ | 5-10-66 | ~ |
| CH. BY: | DATE | |
| | | SCALE 4:1 |

No. A-2742

OGILVIE PRESS, INC., BROOKLYN 17, N. Y. ULTRAVEL NO. 490M

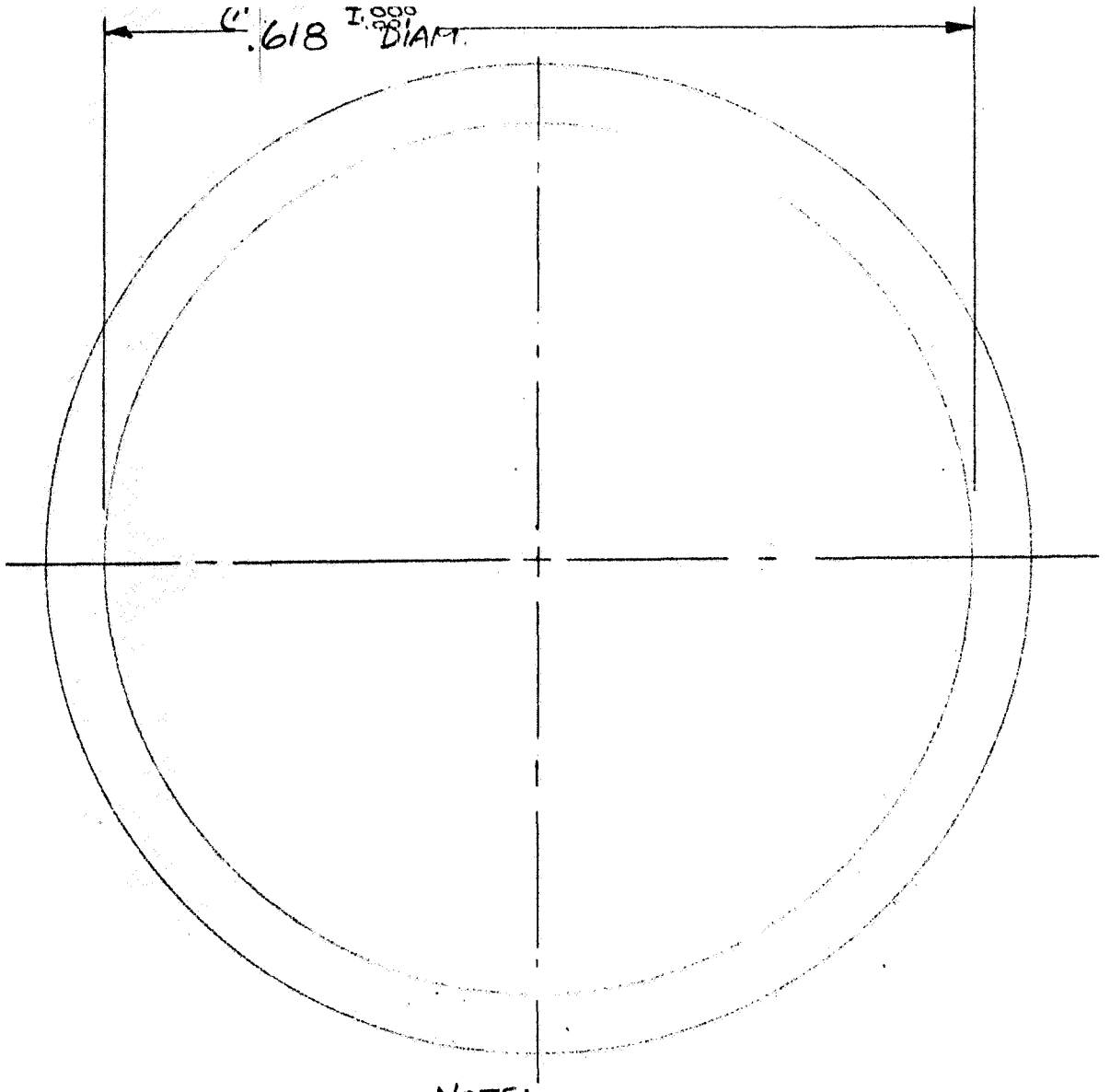


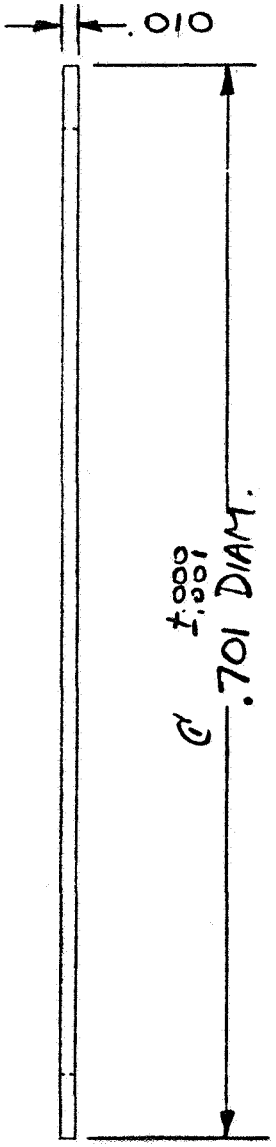


NOTE:
1. LAMINATIONS TO BE FLAT & FREE FROM BURRS
2. DIAMS. MARKED Ø TO BE CONCENTRIC WITHIN .001 F.I.R.

| NO. | BY | D | REVISION |
|---|---|---|---|
| | | | |
| | | | |
| | | | |

TOLERANCES
FRACT. ± 1/64 DEC. ± ANG. ± 1/2°
UNLESS OTHERWISE SPECIFIED

**HERBERT C. ROTERS ASSOCIATES, INC.**

TITLE: YOKE RING LAMINATION
JPL 951463

| DR. BY: | DATE | MATERIAL |
|---|---|---|
| J.A.F. | 6-26-66 | .010 THICK FERROCOBALT |
| CH. BY: | DATE | |
| HOJ | 6-28-66 | |
| SCALE 8:1 | | No. A-2752 |

No. A-2752

No. A-2752

OGILVIE PRESS, INC., BROOKLYN 17, N. Y. ULTRAVEL NO. 490M

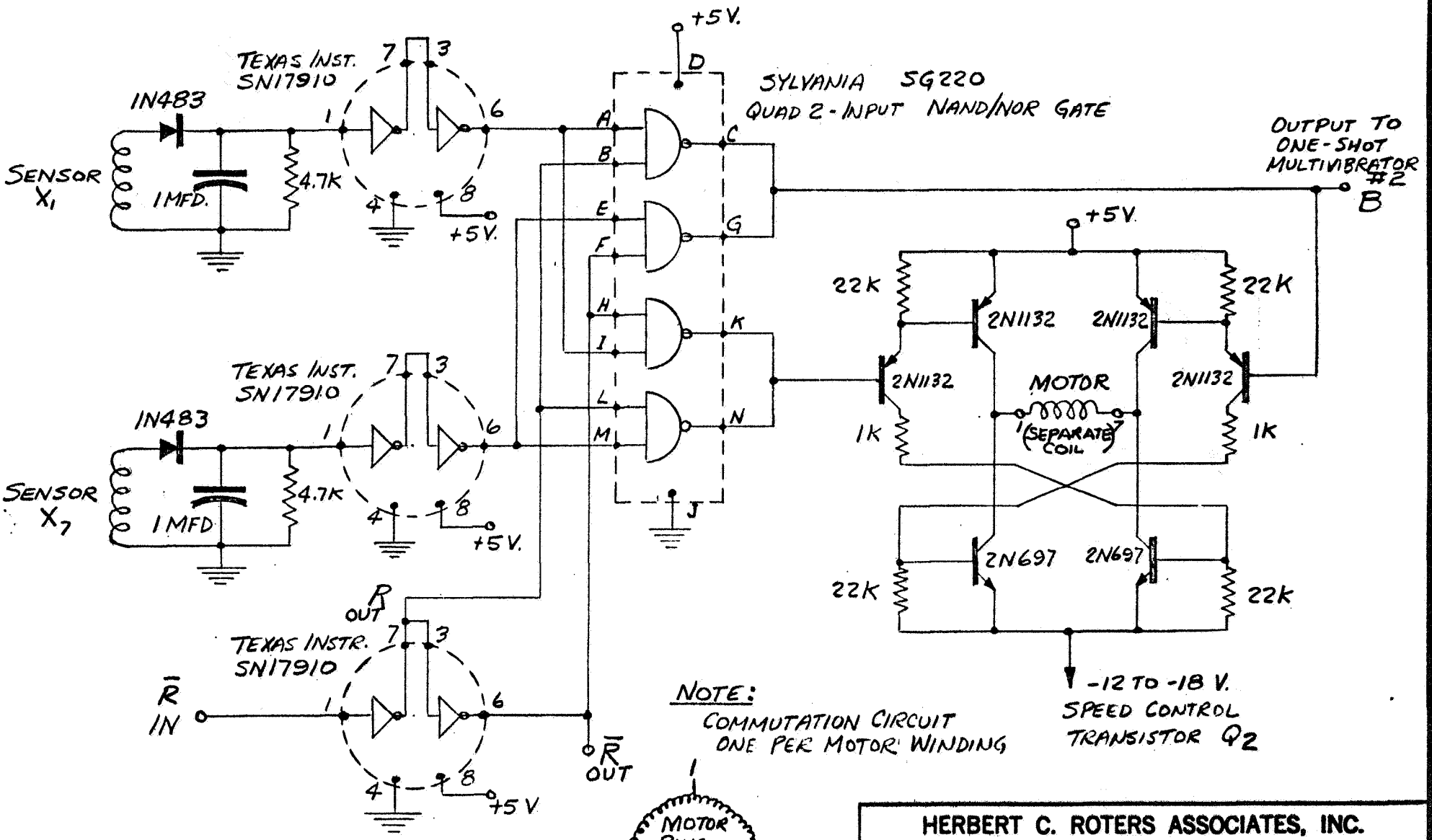


| NO. | BY | | REVISION |
|---|---|---|---|
| A | HOJ | 8-15-66 | ADDED RING WINDING |

TOLERANCES
FRACT. ± 1/64 DEC. ± ANG. ± 1/2°
UNLESS OTHERWISE SPECIFIED

HERBERT C. ROTERS ASSOCIATES, INC.

TITLE: COMMUTATION CIRCUIT - (PRELIMINARY)
BRUSHLESS D.C. MOTOR

| DR. BY: | DATE | MATERIAL |
|---|---|---|
| J.A.F. | 8-4-66 | — |
| CH. BY: | DATE | |
| HOJ | 8-8-66 | |
| SCALE — | | No. A-2760 |

No. A-2760

No. A-2760

OGILVIE PRESS, INC., BROOKLYN 17, N. Y. ULTRAVEL NO. 490M

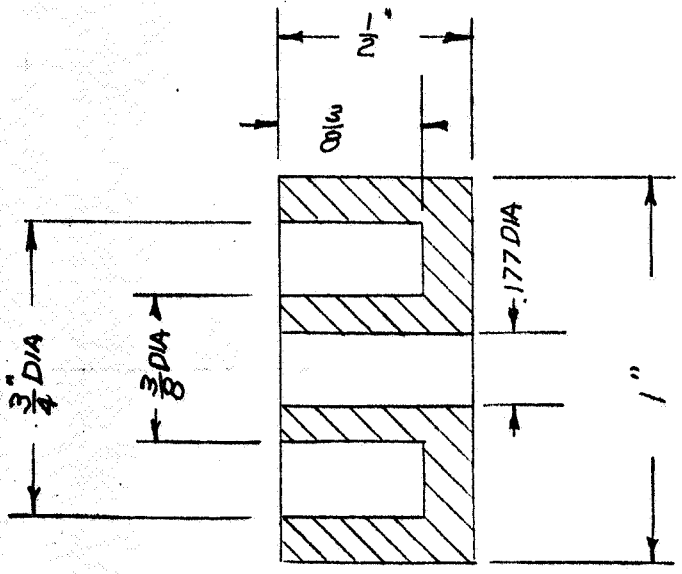


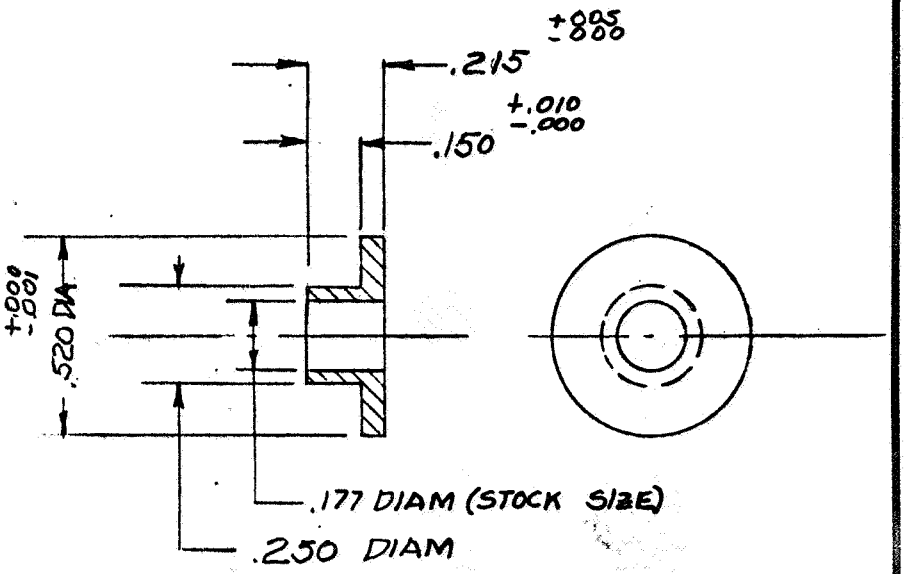


## MATERIAL DESCRIPTION

STANDARD CUP CORE CF 202 # F975
MATERIAL "H" FERRITE
INDIANA GENERAL CORP.

A-2763 PART

No. A-2763

No. A-2763

| NO. | BY | D | REVISION |
|---|---|---|---|
| | | | |

TOLERANCES
FRACT. ± 1/64 DEC. ± ANG. ± 1/2°
UNLESS OTHERWISE SPECIFIED

HERBERT C. ROTERS ASSOCIATES, INC.

TITLE: SENSOR CORE - DC BRUSHLESS MOTOR

| DR. BY: | DATE | MATERIAL |
|---|---|---|
| HOJ | 8-5-66 | SEE ABOVE CF 202 # F975 |
| CH. BY: | DATE | SCALE 2:1 |
| | | No. A-2763 |

OGILVIE PRESS, INC., BROOKLYN 17, N. Y. ULTRAVEL NO. 490M

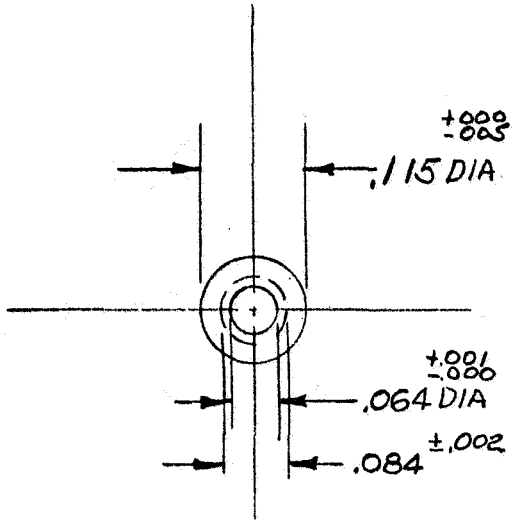


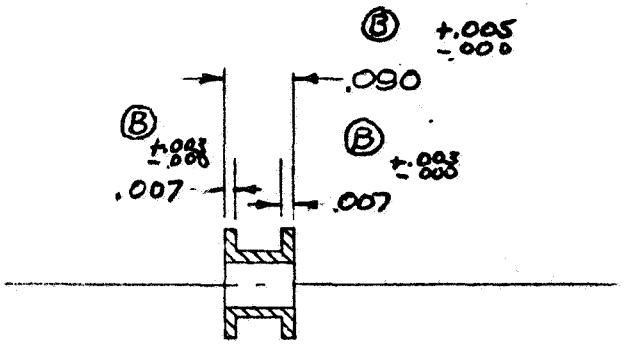


| NO. | BY | D | REVISION |
|---|---|---|---|
| B | HOJ | 8/31/67 | WAS ±.005; WAS .010 ±.003 |
| A | HOJ | 12/2[illegible] | WAS .090, .012, .094 |

TOLERANCES
FRACT. ± 1/64 DEC. ± ANG. ± 1/2°
UNLESS OTHERWISE SPECIFIED

HERBERT C. ROTERS ASSOCIATES, INC.

TITLE: BOBBIN- SENSOR POLE
UNIT 159 DC BRUSHLESS MOTOR

DR. BY: HOJ DATE 10-12-66
CH. BY: DATE

MATERIAL: NYLON- ZYTEL 101

SCALE 4:1

No. A-777

No. A-777

No. A-777

OGILVIE PRESS, INC., BROOKLYN 17, N. Y. ULTRAVEL NO. 490M

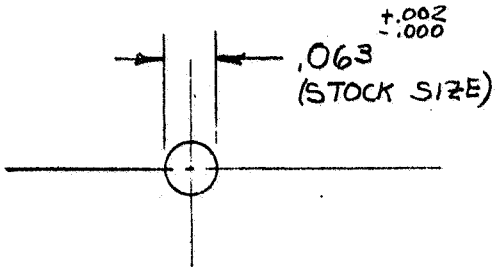


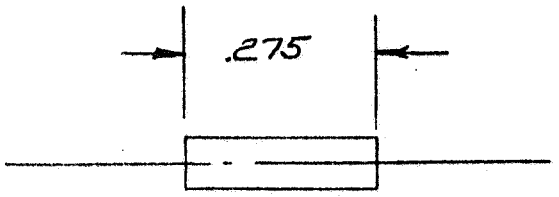


No. A-2778

No. A-2778

| NO. | BY | DA | REVISION |
|---|---|---|---|
| | | | |

TOLERANCES
FRACT. ± 1/64 DEC. ± ANG. ± 1/2°
UNLESS OTHERWISE SPECIFIED

**HERBERT C. ROTERS ASSOCIATES, INC.**

TITLE: POLE - SENSOR
UNIT 159 DC BRUSHLESS MOTOR

| DR. BY: | DATE | MATERIAL # 56-680-17/3B |
|---|---|---|
| HOJ | 10-12-66 | FERROXCUBE - KAHGAN COMPONENTS CORP |
| CH. BY: | DATE | |
| | | SCALE 4:1 — No. A- 178 |

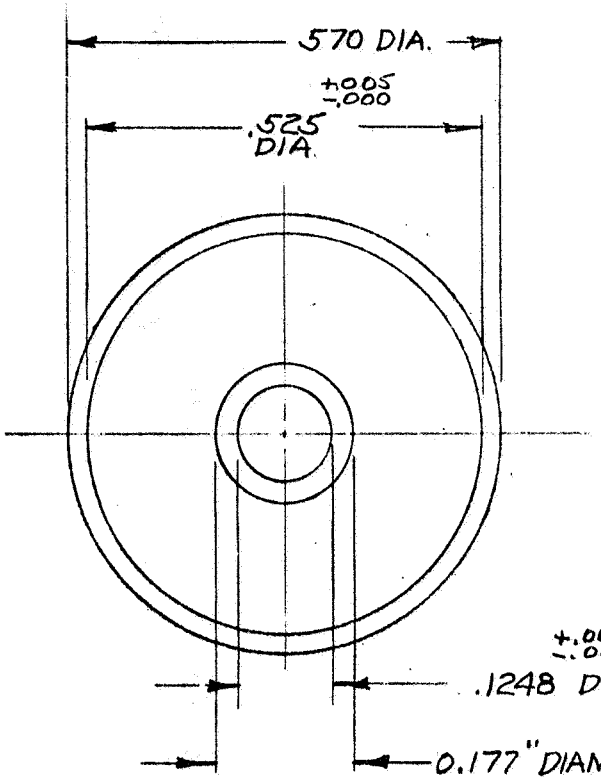


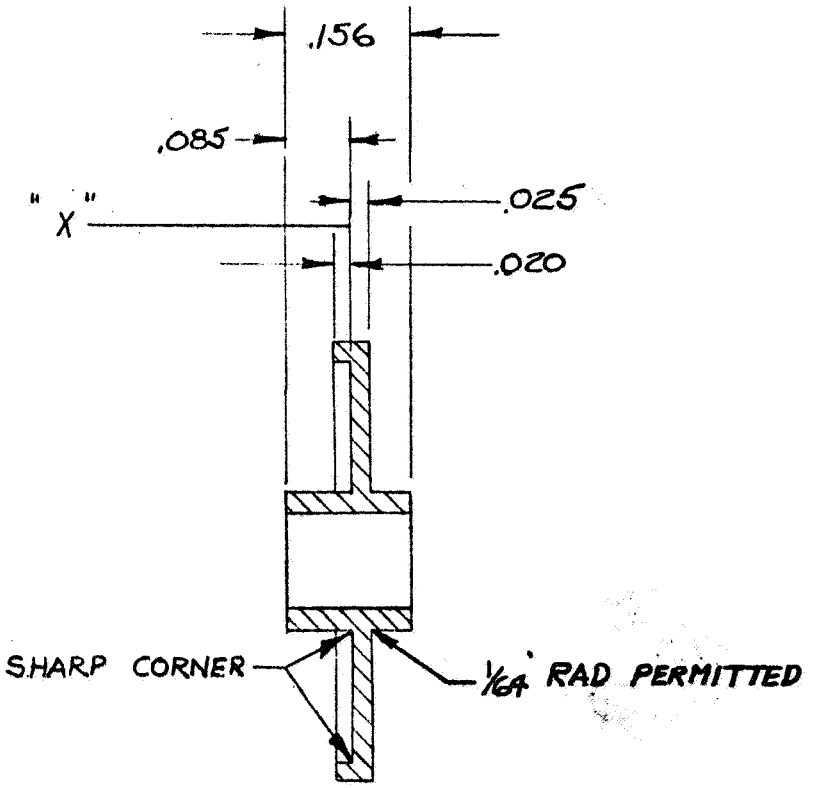


NOTES:

1. ALL DIAMS. CONCENTRIC WITHIN .001 TIR
2. SURFACE 'X' ⊥ TO .1248 DIA. WITHIN .001 TIR

No. A-2779

| NO. | BY | D | REVISION |
|---|---|---|---|
| | | | |

TOLERANCES
FRACT. ± 1/64 DEC. ± ANG. ± 1/2°
UNLESS OTHERWISE SPECIFIED

**HERBERT C. ROTERS ASSOCIATES, INC.**

TITLE: HUB - SENSOR ARMATURE
UNIT 159 DC BRUSHLESS MOTOR

| DR. BY: | DATE | MATERIAL |
|---|---|---|
| HOJ | 10-12-66 | 2024-T4 ALUM |
| CH. BY: | DATE | |
| | | SCALE 4:1 |

No. A-2779

No. A-2779

OGILVIE PRESS, INC., BROOKLYN 17, N. Y. ULTRAVEL NO. 490M

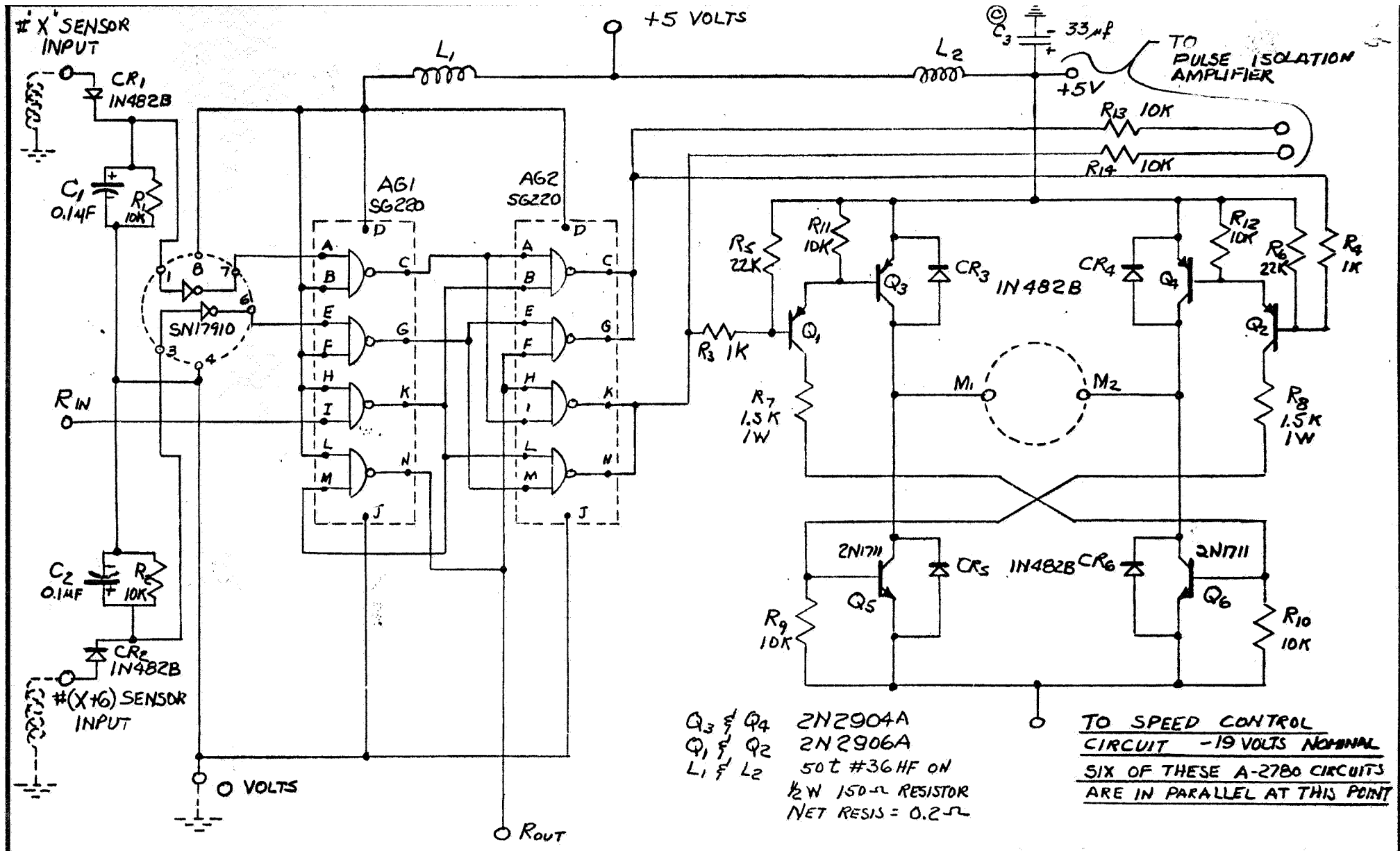


| NO. | BY | DATE | REVISION |
|---|---|---|---|
| E | HOJ | 3-9-69 | ADDED $R_{13}$, $R_{14}$ |
| D | TJL | 8-13-68 | CHANGED $R_5$ & $R_6$ FROM 10K Ω |
| C | TJL | 7-30-68 | RELOCATED $C_3$ |
| B | TJL | 12-12-67 | RELOCATED $C_3$ |
| A | HOJ | 10-13-67 | REDRAWN |

TOLERANCES
FRACT. ± 1/64 DEC. ± ANG. ± 1/2°
UNLESS OTHERWISE SPECIFIED

HERBERT C. ROTERS ASSOCIATES, INC.

TITLE: COMMUTATOR SCHEMATIC (TWO COMMUTATION POINTS)

| DR. BY: | DATE | MATERIAL |
|---|---|---|
| HOJ | 10-13-67 | |
| CH. BY: | DATE | SCALE — |
| TJL | 10-18-67 | No. A-2780A |

No. A-2780A

No. A-2780A

OGILVIE PRESS, INC., BROOKLYN 17, N. Y. ULTRAVEL NO. 490M

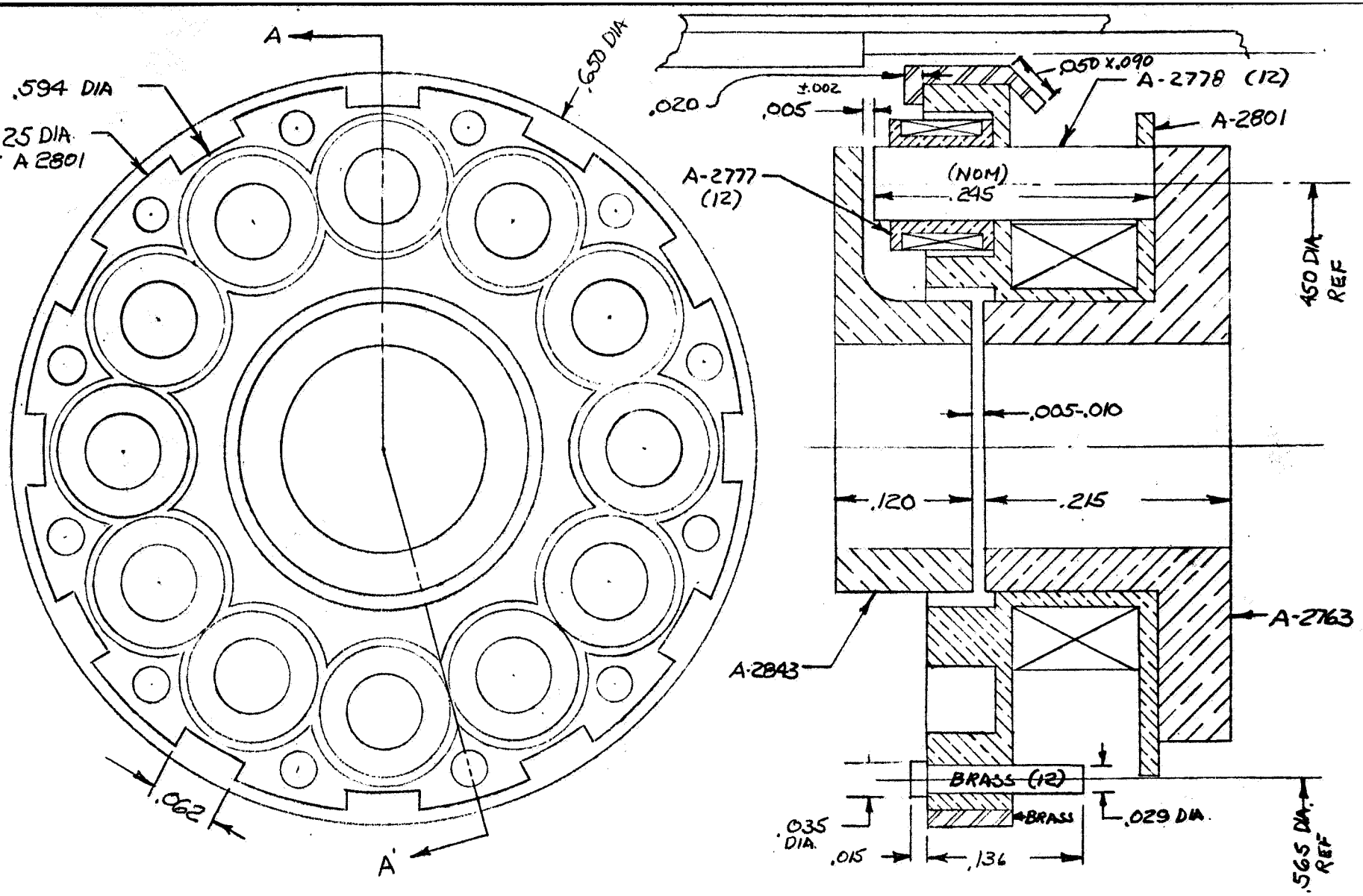


| NO. | BY | DATE | REVISION |
|---|---|---|---|
| A | HOJ | 2-21-68 | ADDED DIMENSIONS, CHANGED OUTLINE |

TOLERANCES
FRACT. ± 1/64 DEC. ± ANG. ± 1/2°
UNLESS OTHERWISE SPECIFIED

HERBERT C. ROTERS ASSOCIATES, INC.

TITLE: SENSOR LAYOUT- UNIT 159 DC BRUSHLESS MOTOR

| DR. BY: | DATE | MATERIAL |
|---|---|---|
| HOJ | 1-4-67 | ~ |
| CH. BY: | DATE | |
| | | SCALE 8:1 |

No. A-2800

No. A-2800

OGILVIE PRESS, INC., BROOKLYN 17, N. Y. ULTRAVEL NO. 490M

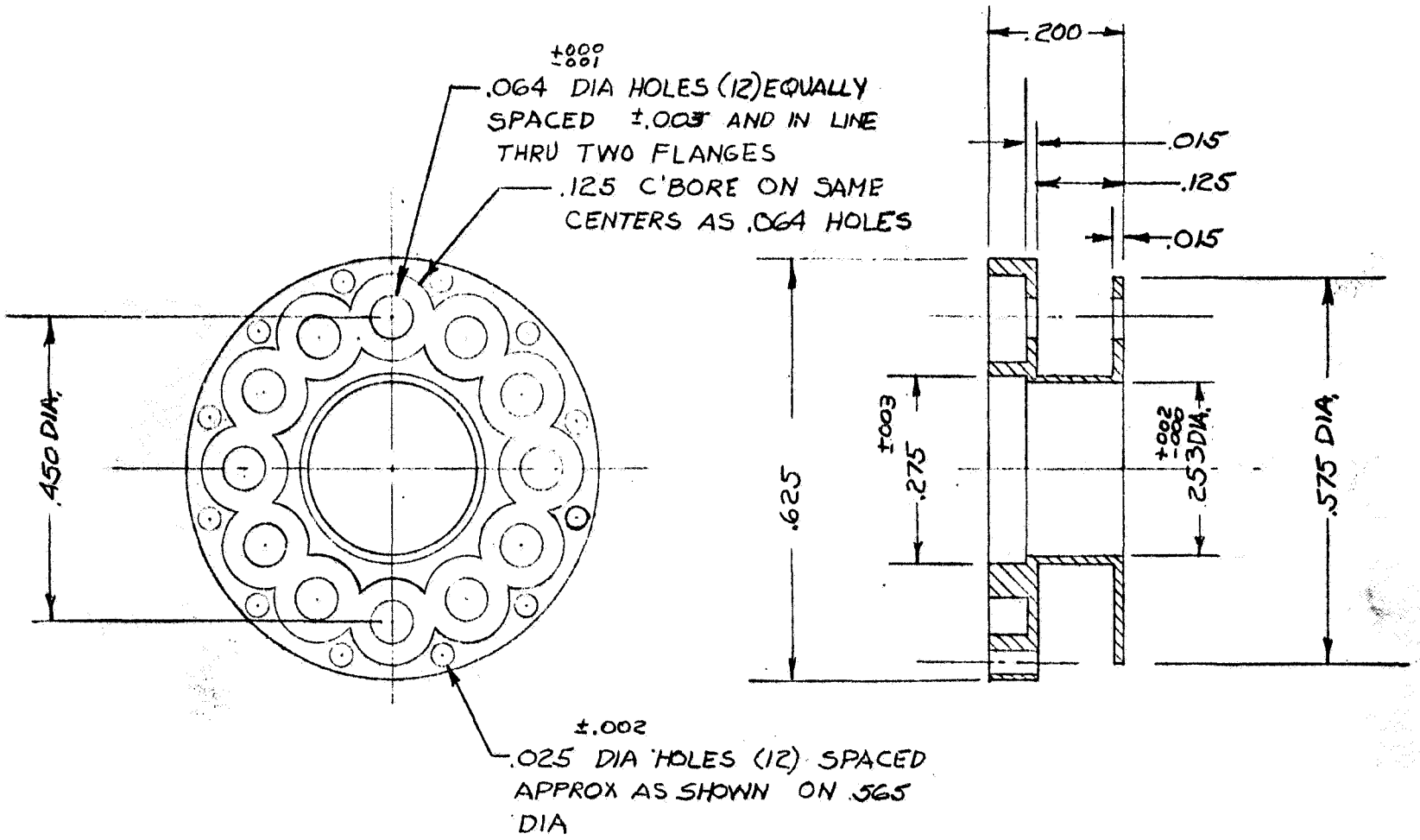


| NO. | BY | DA.. | REVISION |
|---|---|---|---|
| | | | |

TOLERAN
FRACT. ± 1/64 DEC. ± ANG. ± 1/2°
UNLESS OTHERWISE SPECIFIED

**HERBERT C. ROTERS ASSOCIATES, INC.**

TITLE: BOBBIN - OSCILLATOR COIL, UNIT 159

| DR. BY: | DATE | MATERIAL |
|---|---|---|
| HDJ | 1-4-67 | NYLON - ZYTEL 101 |
| CH. BY: | DATE | |
| | | SCALE 4:1 |

No. A-2801

No. A-2801

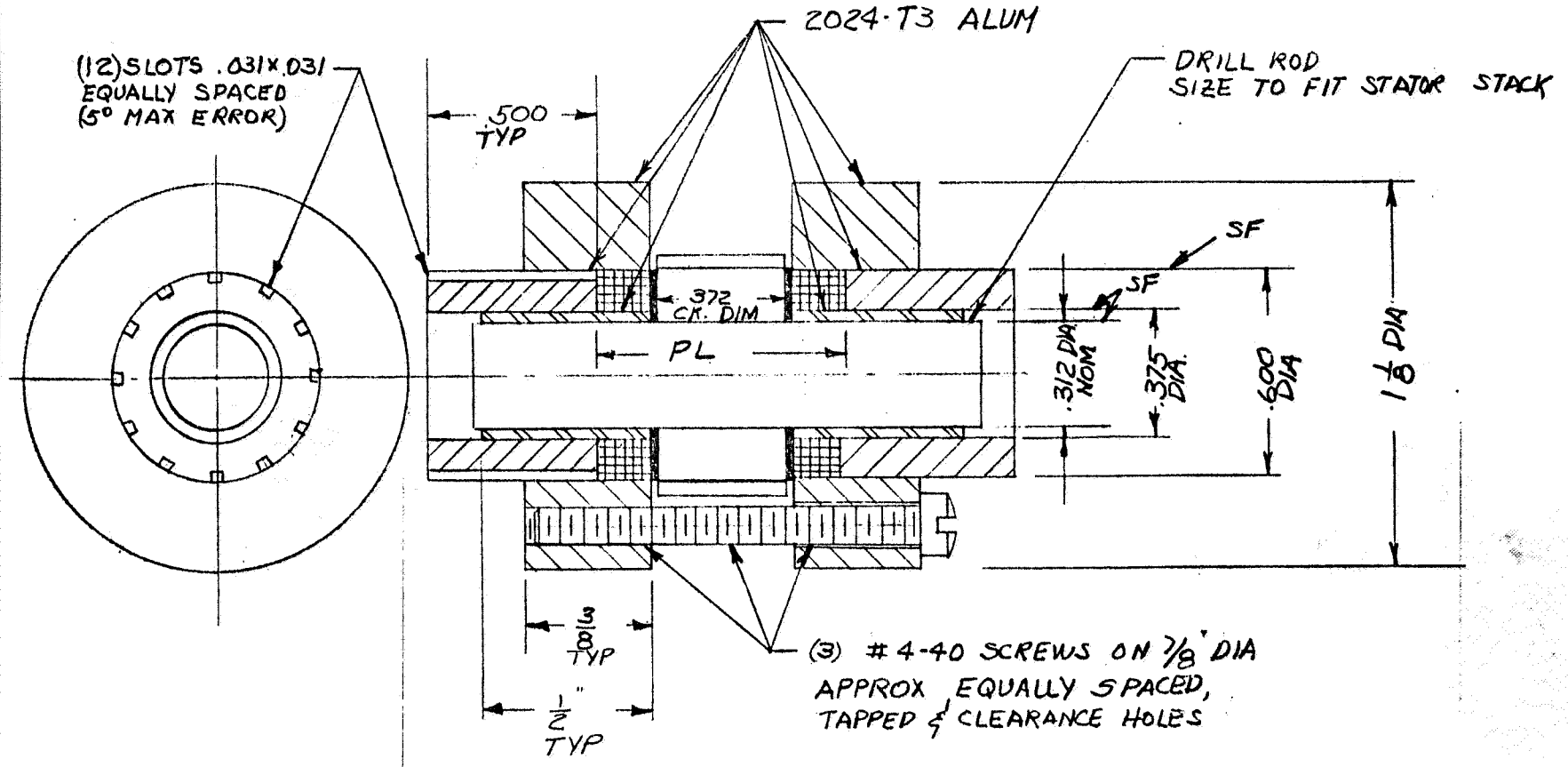


NOTE:

1. SF MEANS SLIDE FIT
2. PL MEANS MAX. PRESSED WINDING LENGTH = 0.735"

| NO. | BY | DATE | REVISION |
|---|---|---|---|
| | | | |

TOLERANCES
FRACT. ± 1/64 DEC. ± .005 ANG. ± 1/2°
UNLESS OTHERWISE SPECIFIED

**HERBERT C. ROTERS ASSOCIATES, INC.**

TITLE: WINDING PRESSING FIXTURE
UNIT 159 DC BRUSHLESS MOTOR

| DR. BY: | DATE | MATERIAL |
|---|---|---|
| HOJ | 2-15-67 | 2 |
| CH. BY: | DATE | |
| | | SCALE 2:1 |

No. A-2812

No. A-2812

DARK PARTS ARE
ENCAPSULATION FIXTURE
ADDED PARTS

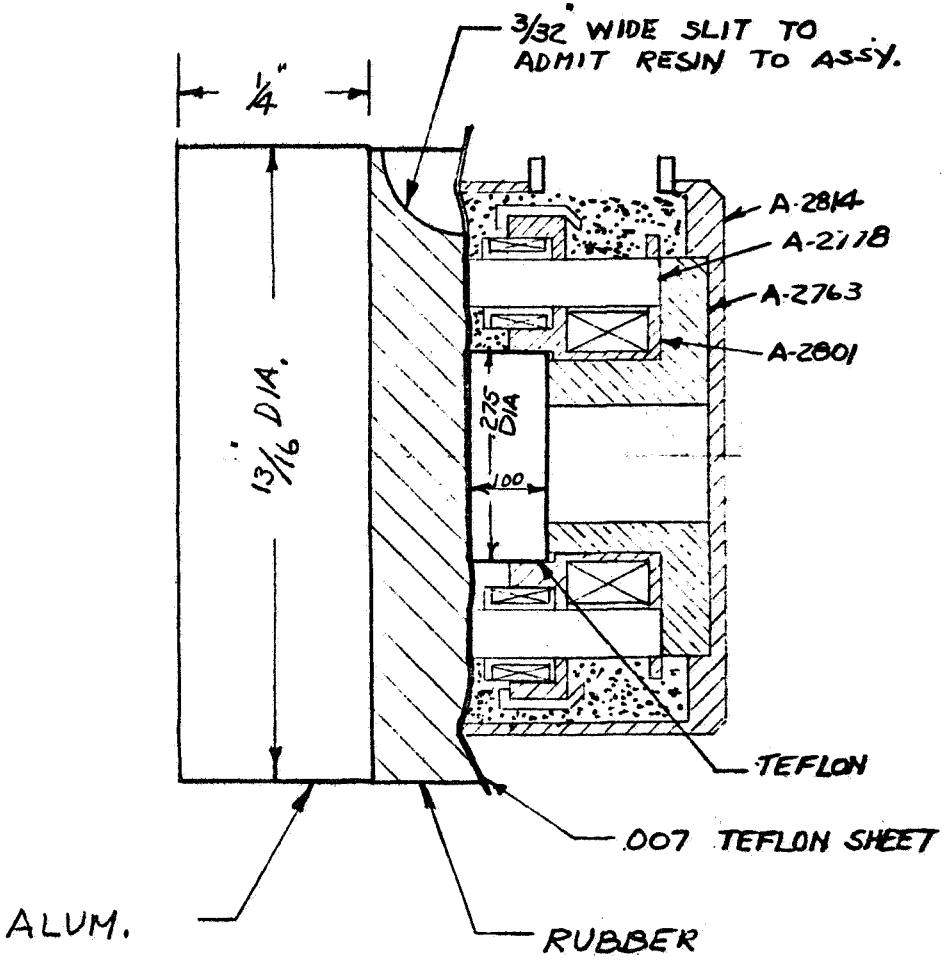


No. A-2813

| NO. | BY | D | REVISION |
|---|---|---|---|
| | | | |

TOLERANCES UNLESS OTHERWISE SPECIFIED
FRACT. ± 1/64 DEC. ± ANG. ± 1/2°

HERBERT C. ROTERS ASSOCIATES, INC.

TITLE: ENCAPSULATION FIXTURE - SENSOR ASSY
UNIT 159 DC BRUSHLESS MOTOR

| DR. BY: | DATE | MATERIAL |
|---|---|---|
| HOJ | 2-20-67 | ~ |
| CH. BY: | DATE | |
| | | SCALE 4/1 |

No. A-2813

OCULUS PRESS, INC. BROOKLYN 17, N. Y. ULTRAVEL NO. 480M

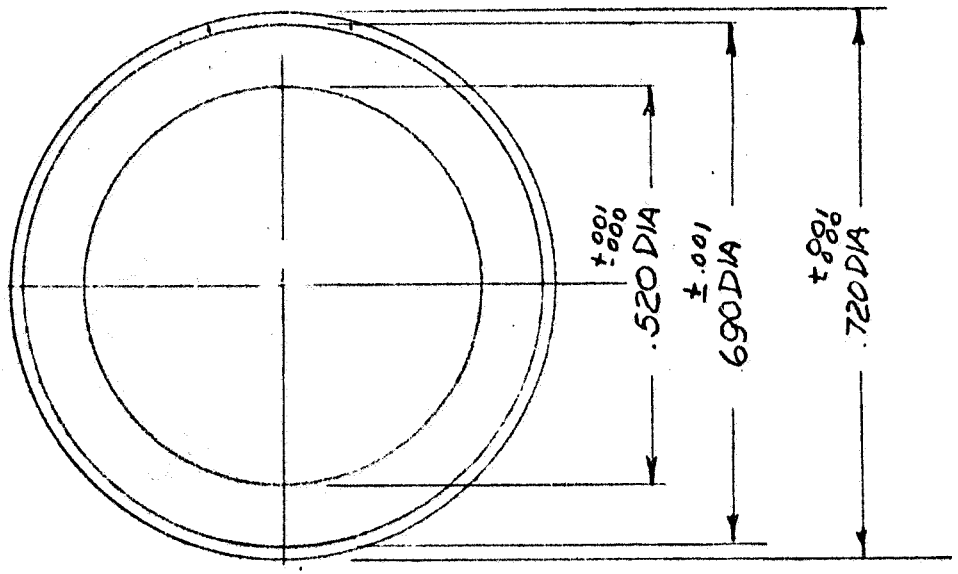


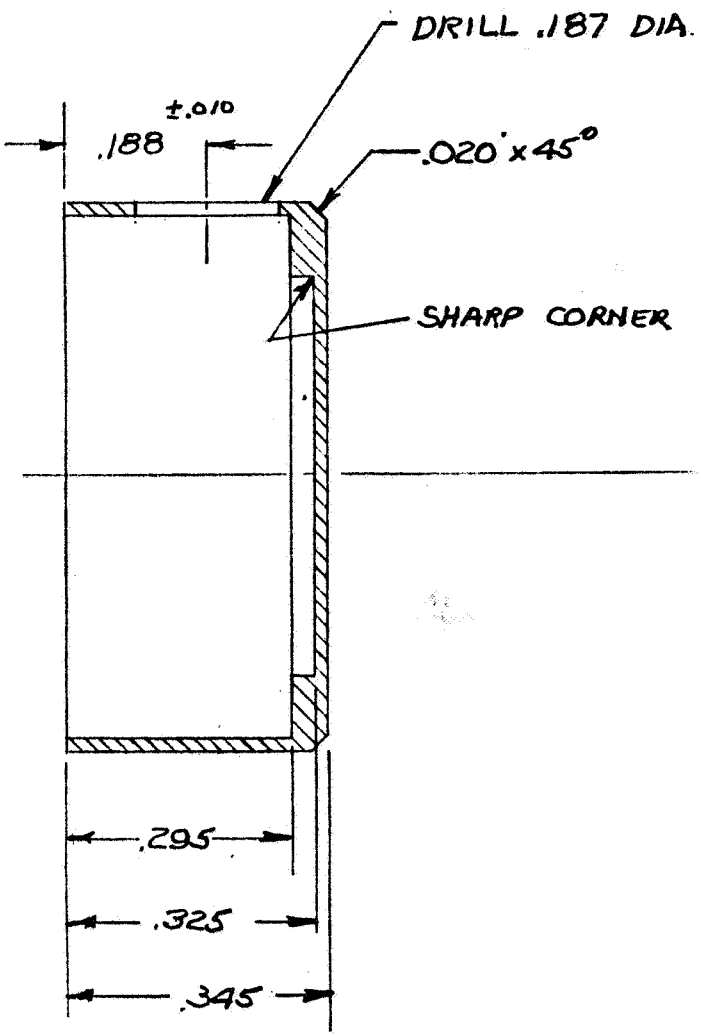


NOTES:

1. .520 & .720 DIAMS TO BE CONCENTRIC WITHIN .001 TIR

No. A-2814

No. A-2814

| NO. | BY | DA | REVISION |
|---|---|---|---|
| | | | |

TOLERANCES
FRACT. ± 1/64 DEC. ± ANG. ± 1/2°
UNLESS OTHERWISE SPECIFIED

HERBERT C. ROTERS ASSOCIATES, INC.

TITLE: SENSOR CASE
UNIT 159 DC BRUSHLESS MOTOR

| DR. BY: | DATE | MATERIAL |
|---|---|---|
| HOJ | 2-15-67 | 2024-T3 ALUM |
| CH. BY: | DATE | |
| | | SCALE 4:1 |

No. A-2814

OGILVIE PRESS, INC., BROOKLYN 17, N. Y. ULTRAVEL NO. 490M

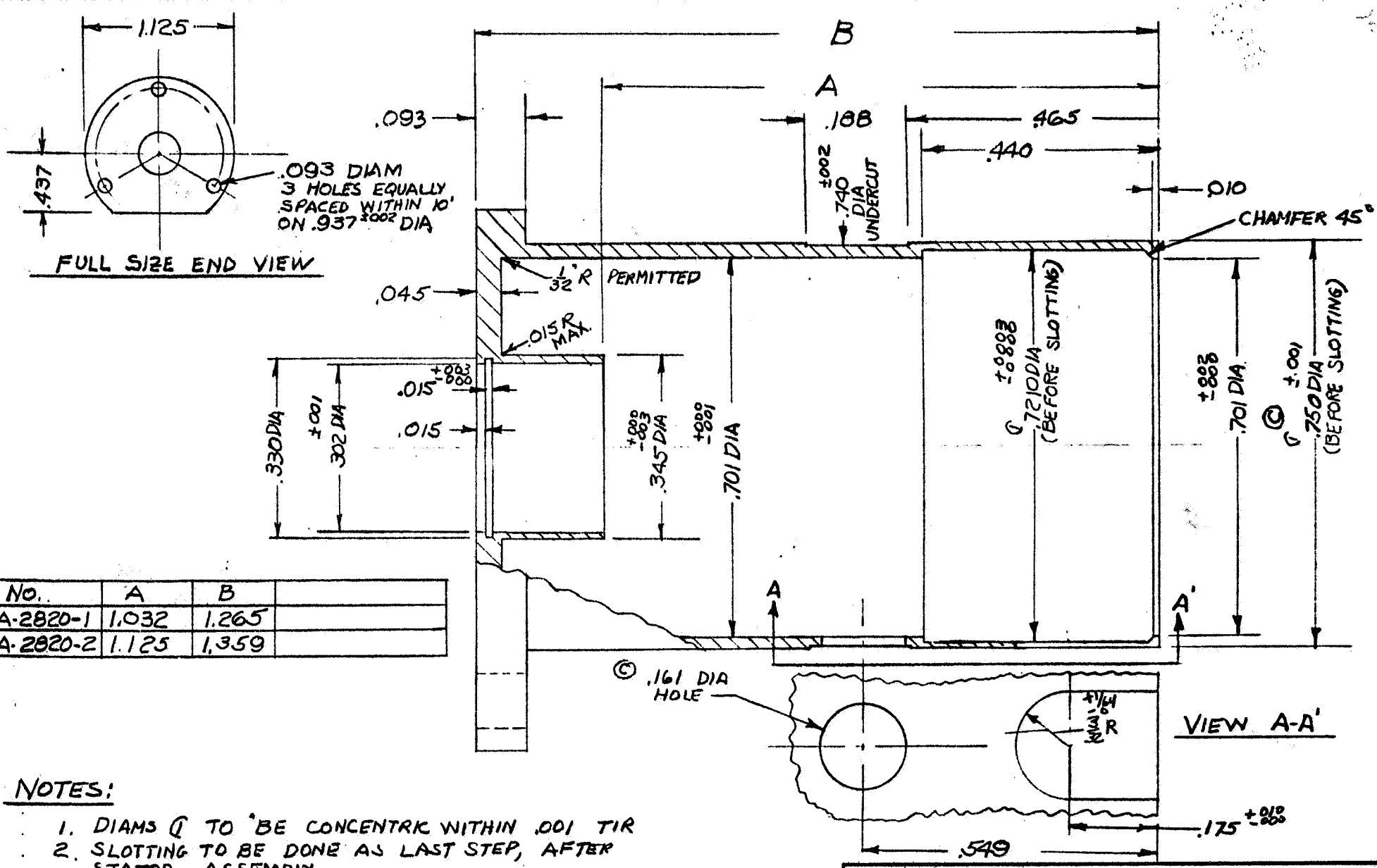


| No. | A | B | |
|---|---|---|---|
| A-2820-1 | 1.032 | 1.265 | |
| A-2820-2 | 1.125 | 1.359 | |

NOTES:

1. DIAMS © TO BE CONCENTRIC WITHIN .001 TIR
2. SLOTTING TO BE DONE AS LAST STEP, AFTER STATOR ASSEMBLY

| NO. | BY | DATE | REVISION |
|---|---|---|---|
| C | HOJ | 10/29/67 | WAS 760; WAS ±.002; WAS .156 |
| B | HOJ | 10/13/67 | TABLE ADDED |
| A | HOJ | 3/[illegible] | FLANGE OUTLINE |

TOLERANCES
FRACT. ± 1/64 DEC. ± ANG. ± 1/2°
UNLESS OTHERWISE SPECIFIED

HERBERT C. ROTERS ASSOCIATES, INC.

TITLE: HOUSING
UNIT 159 DC BRUSHLESS MOTOR
JPL 951463

| DR. BY: | DATE | MATERIAL |
|---|---|---|
| HOJ | 3-8-67 | 2024-T4 ALUM |
| CH. BY: | DATE | SCALE 4:1 |

No. A-2820

No. A-2820

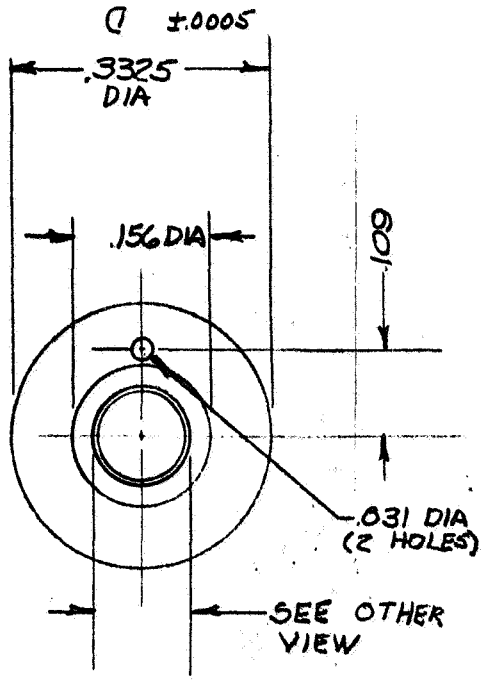


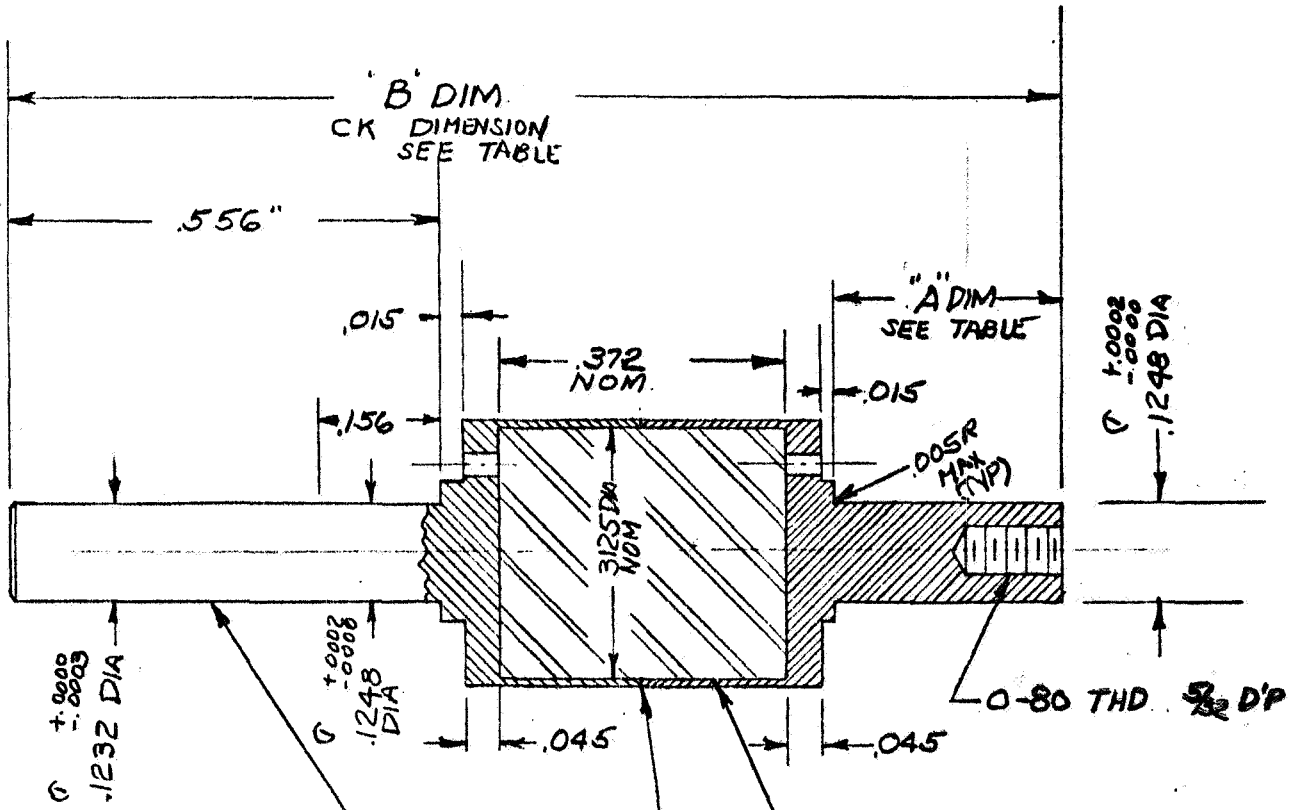


NOTES:

1. MAKE SHAFT PARTS .005 OVERSIZE ON EXTERIOR DIAMS AND .0005 LOOSE ON MAGNET
2. ASSEMBLE PARTS ON MAGNET WITH LOCKTITE "A". .031 HOLES ARE RELIEF HOLES. ALLOW TO SET
3. FINISH DIAMS AS SHOWN
4. DIAMS ℄ TO BE CONCENTRIC WITHIN .0005 TIR
5.

ALNICO IX MAGNET (MAGNETIC AXIS ON DIAM)

ADJUST GAP BETWEEN PARTS TO BE .000-.003

303 STAINLESS STEEL - SHAFT PARTS (NON-MAGNETIC)

| DWG No. | 'A' DIM | 'B' DIM |
|---|---|---|
| A-2821-1 | .290 | 1.338 |
| A-2821-2 | .383 | 1.431 |

| NO. | BY | D. | REVISION |
|---|---|---|---|
| A | HOJ | 11/13 | ADDED TABLE, WAS -1 DIMNS. |

TOLERANCES
FRACT. ± 1/64 DEC. ± ANG. ± 1/2°
UNLESS OTHERWISE SPECIFIED

**HERBERT C. ROTERS ASSOCIATES, INC.**

TITLE: ROTOR ASSEMBLY & FINISHING UNIT 159 DC BRUSHLESS MOTOR JPL 951463

| DR. BY: | DATE | MATERIAL |
|---|---|---|
| HOJ | 3-9-67 | |
| CH. BY: | DATE | |
| | | SCALE 4:1 |

No. A-2821

No. A-2821

OGILVIE PRESS, INC., BROOKLYN 17, N. Y. ULTRAVEL NO. 490M

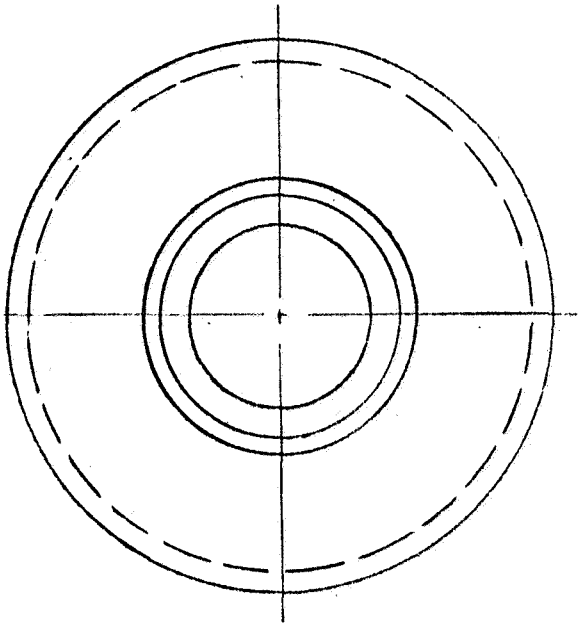

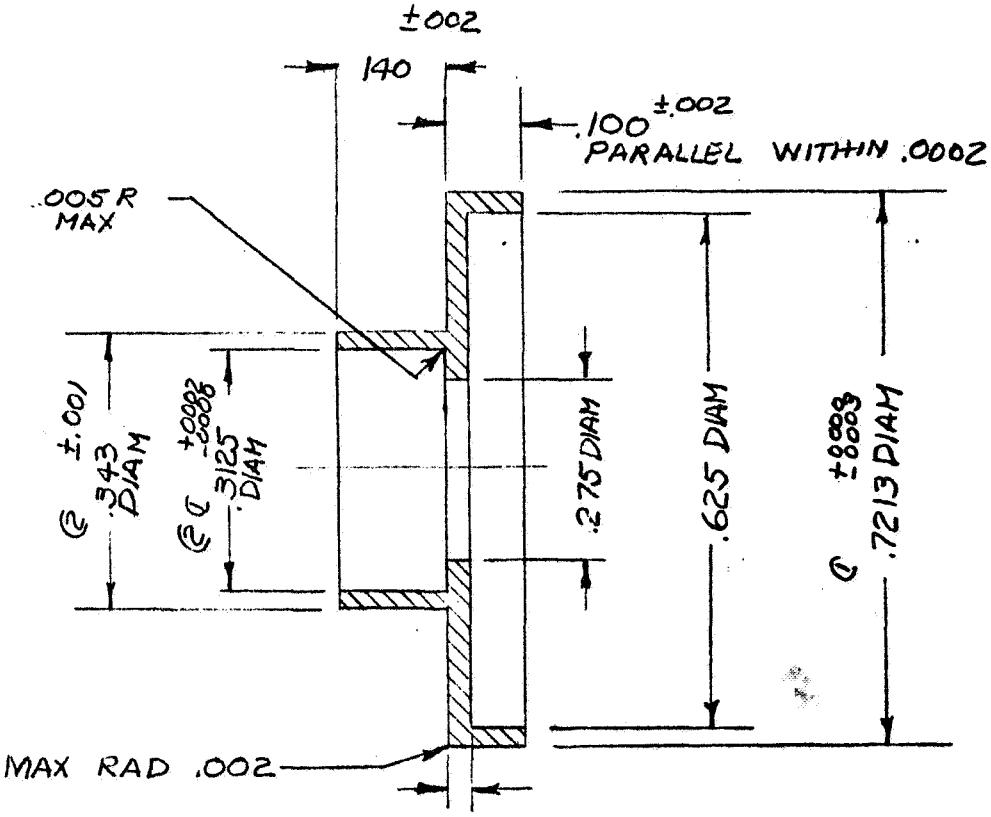


NOTES:
1. Ⓒ DIAMS CONCENTRIC WITHIN .0005 TIR
2. Ⓔ DIAMS CONCENTRIC WITHIN .002 TIR

No. A-2822

| NO. | BY | D. | REVISION |
|---|---|---|---|
| | | | |

TOLERANCES
FRACT. ± 1/64 DEC. ± ANG. ± 1/2°
UNLESS OTHERWIS. ECIFIED

HERBERT C. ROTERS ASSOCIATES, INC.

TITLE: SUPPORT - REAR BEARING
UNIT 159 DC BRUSHLESS MOTOR
JPL 951463

| DR. BY: HOJ | DATE 3- | MATERIAL |
|---|---|---|
| CH. BY: | DATE | SCALE 4:1 |

No. A- 322

No. A-2822

L - Sensor coil

C - Tuning Capacitor

$C_1, C_2, C_3, C_4$ - 1 μf 15 VDC

$R_1, R_2, R_3, R_4$ - 2200 Ω

$R_5, R_6, R_7, R_8$ - 10K Ω

$R_9, R_{10}, R_{11}, R_{12}$ - 16K Ω

$Q_1, Q_2$ - 2N 2906A

$Q_3, Q_4$ - 2N 1711

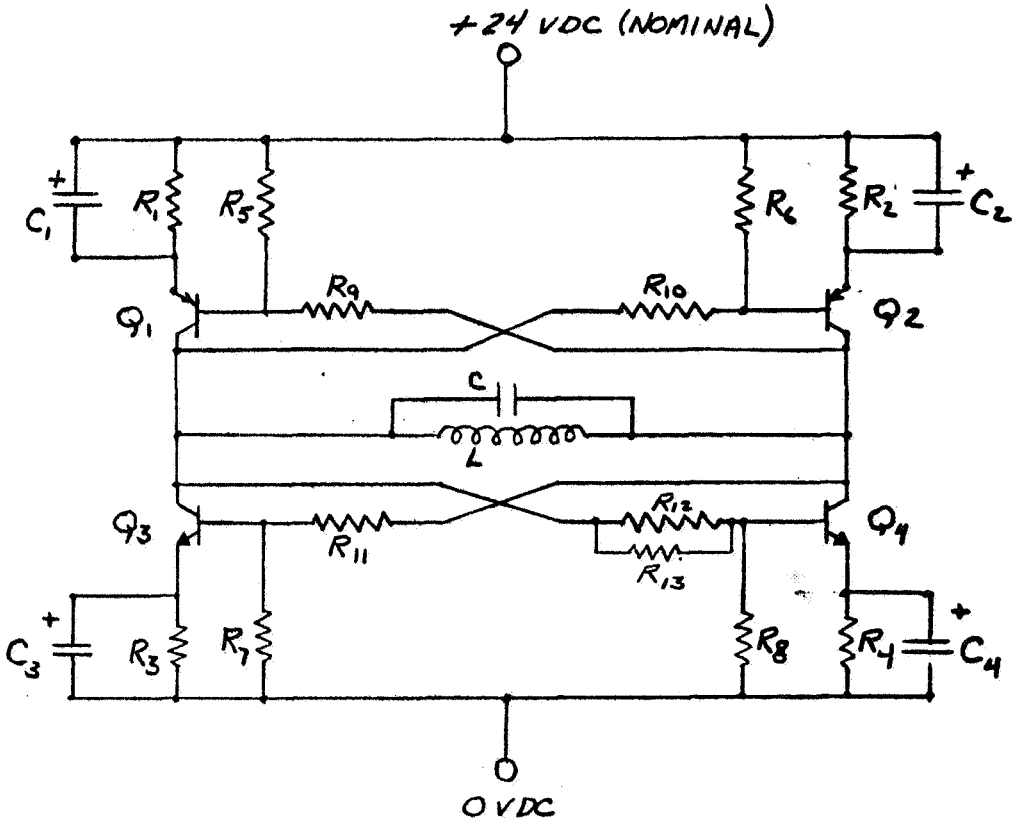


| NO. | BY | DA | REVISION |
|---|---|---|---|
| A | TJL | 4-11 | ADDED $R_{13}$ |

TOLERANCES UNLESS OTHERWISE SPECIFIED
FRACT. ± 1/64 DEC. ± ANG. ± 1/2°

HERBERT C. ROTERS ASSOCIATES, INC.

TITLE: OSCILLATOR - Schematic Diagram

| DR. BY: | DATE | MATERIAL |
|---|---|---|
| TJL | 5-31-67 | — |
| CH. BY: | DATE | |
| | | SCALE |

No. A-2839

No. A-2839

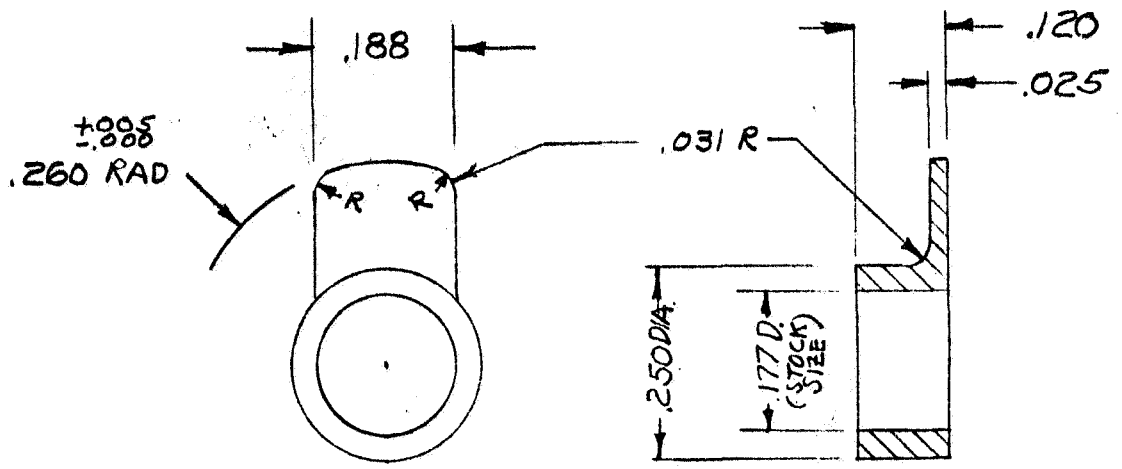


FULL SIZE VIEW OF PART

NOTES:

1. .260 RAD & .177 DIA TO BE CONCENTRIC WITHIN .005 COMMON ℄
2. .250 & .177 DIAS CONCENTRIC WITHIN .002 TIR

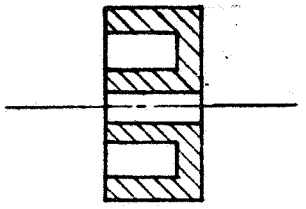

FULL SIZE VIEW OF STOCK MATERIAL
STANDARD CUP CORE CF202 # F975
MATERIAL "H" FERRITE
INDIANA GENERAL CORP

No. A-2843

No. A-2843

| NO. | BY | DA.. | REVISION |
|---|---|---|---|
| A | HOJ | 6-[illegible] | WAS A-2764 |

TOLERANCES
FRACT. ± 1/64 DEC. ± ANG. ± 1/2°
UNLESS OTHERWISE SPECIFIED

HERBERT C. ROTERS ASSOCIATES, INC.

TITLE: SENSOR ARMATURE - DC BRUSHLESS MOTOR

| DR. BY: | DATE | MATERIAL |
|---|---|---|
| HOJ | 8-5-66 | SEE ABOVE CF 202 # F[illegible] (A) |
| CH. BY: | DATE | SCALE 4:1 |
| | | No. A-2843 |

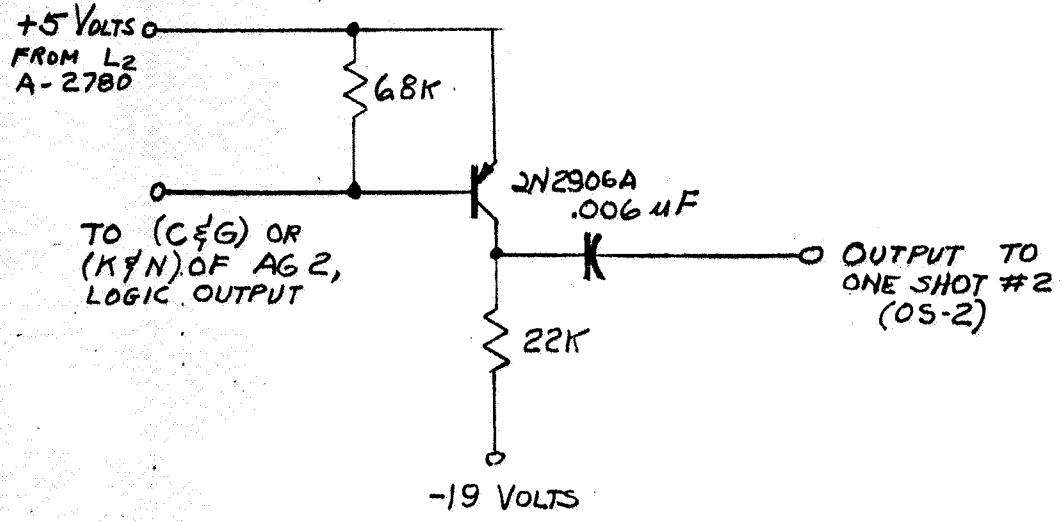


NOTE: (1) REQ. FOR EACH COMMUTATING POINT

No. A-2865

| NO. | BY | DATE | REVISION |
|---|---|---|---|
| | | | |

TOLERANCES UNLESS OTHERWISE SPECIFIED
FRACT. ± 1/64 DEC. ± ANG. ± 1/2°

HERBERT C. ROTERS ASSOCIATES, INC.

TITLE: PULSE ISOLATION AMPLIFIER

| DR. BY: | DATE | MATERIAL |
|---|---|---|
| HOJ | 10-18-67 | |
| CH. BY: | DATE | |
| TJL | 10-18-67 | |
| SCALE | | No. A-2865 |

No. A-2865

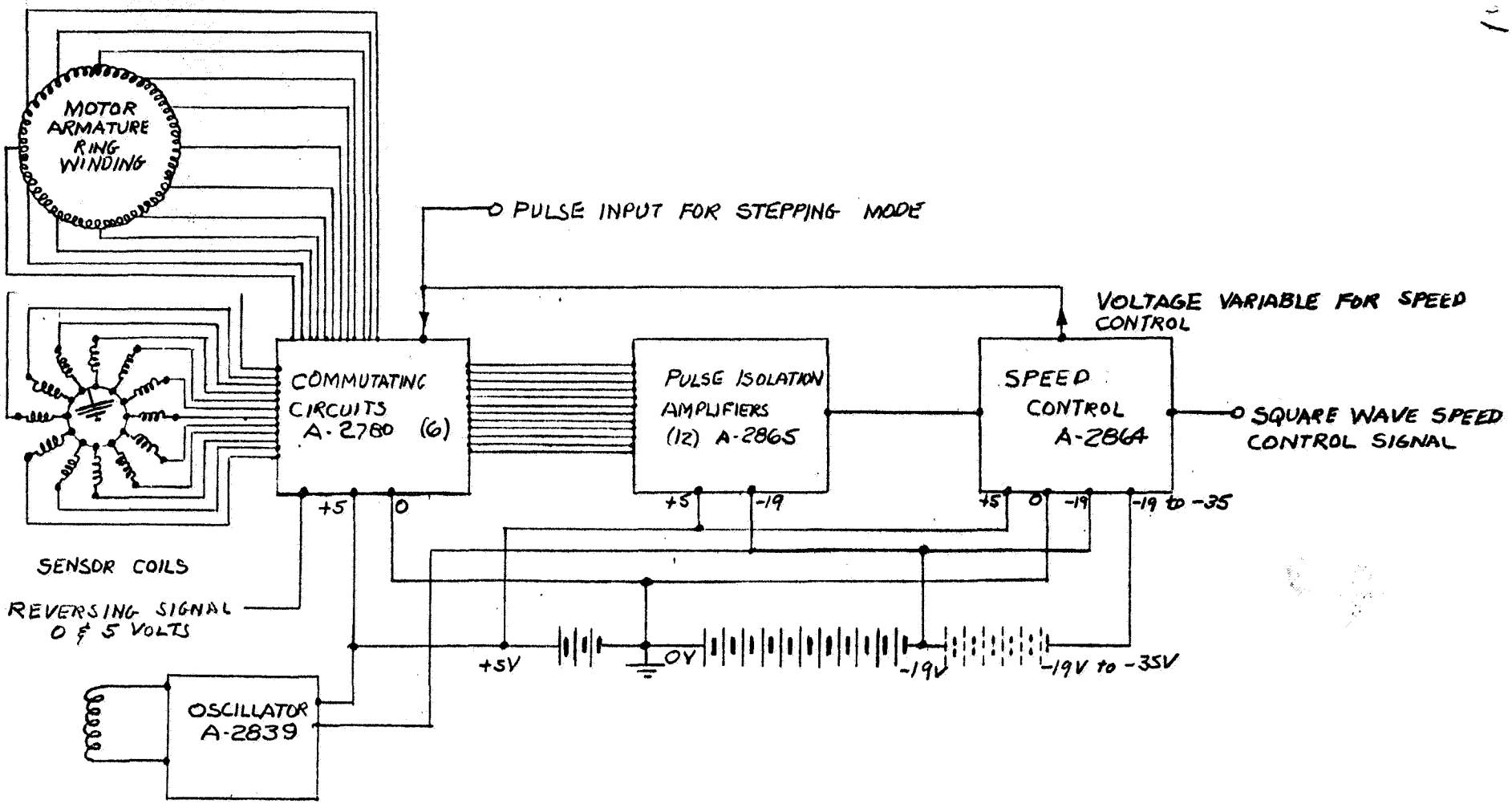


No. A-2866

No. A-2866

| NO. | BY | D | REVISION |
|---|---|---|---|
| | | | |

TOLERANCES
FRACT. ± 1/64 DEC. ± ANG. ± 1/2°
UNLESS OTHERWISE SPECIFIED

HERBERT C. ROTERS ASSOCIATES, INC.

TITLE: CIRCUIT CONNECTIONS - DC BRUSHLESS MOTOR - JPL 951463

| DR. BY: | DATE | MATERIAL |
|---|---|---|
| HOJ | 10-19/67 | |
| CH. BY: | DATE | |
| | | SCALE ~ |

No. A-2866

OGILVIE PRESS, INC., BROOKLYN 17, N. Y. ULTRAVEL NO. 490M

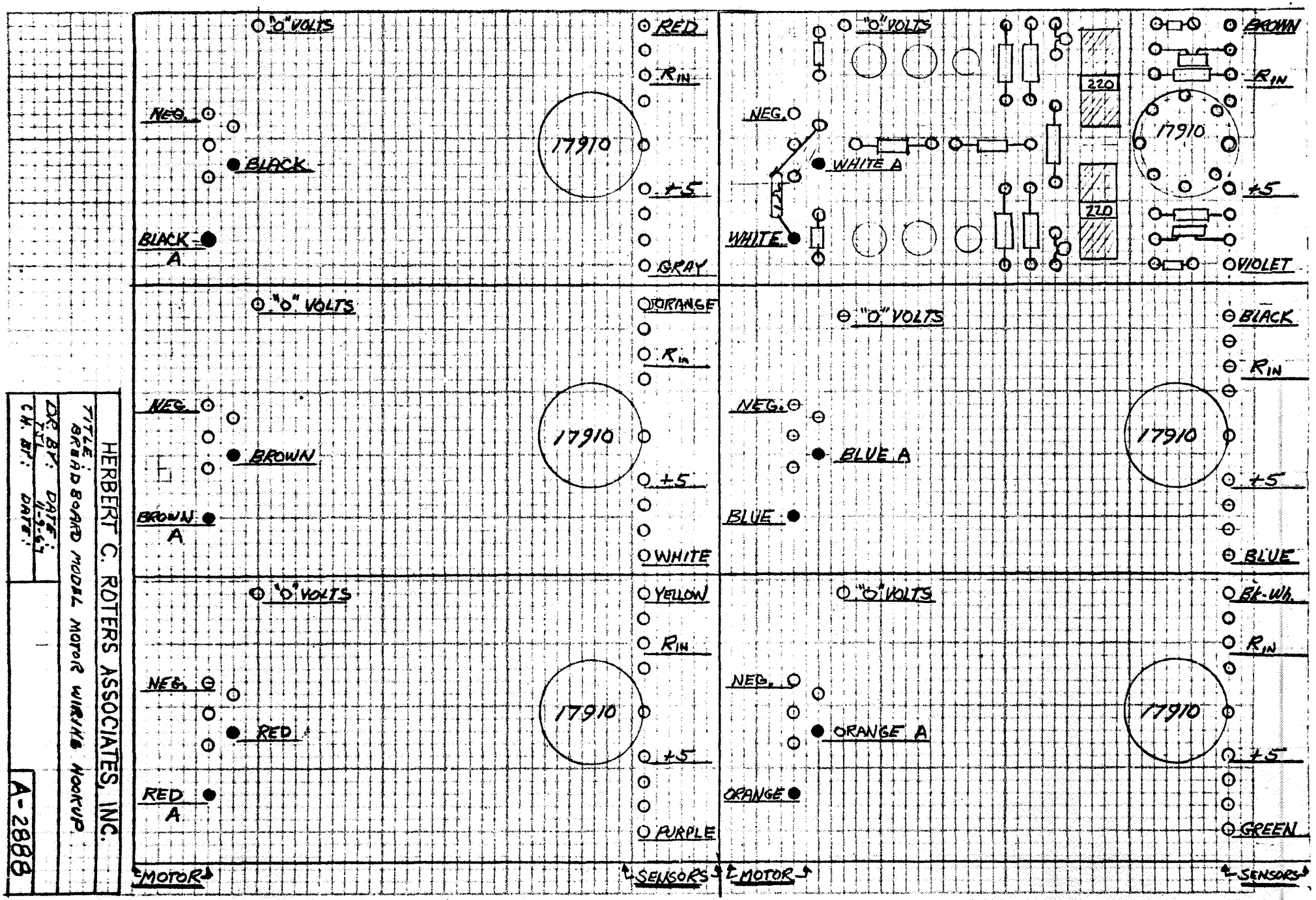


HERBERT C. ROTERS ASSOCIATES, INC.

TITLE: BREAD BOARD MODEL MOTOR WIRING HOOKUP

DR. BY: DATE: 11-2-67

CH. BY: DATE:

A-2888

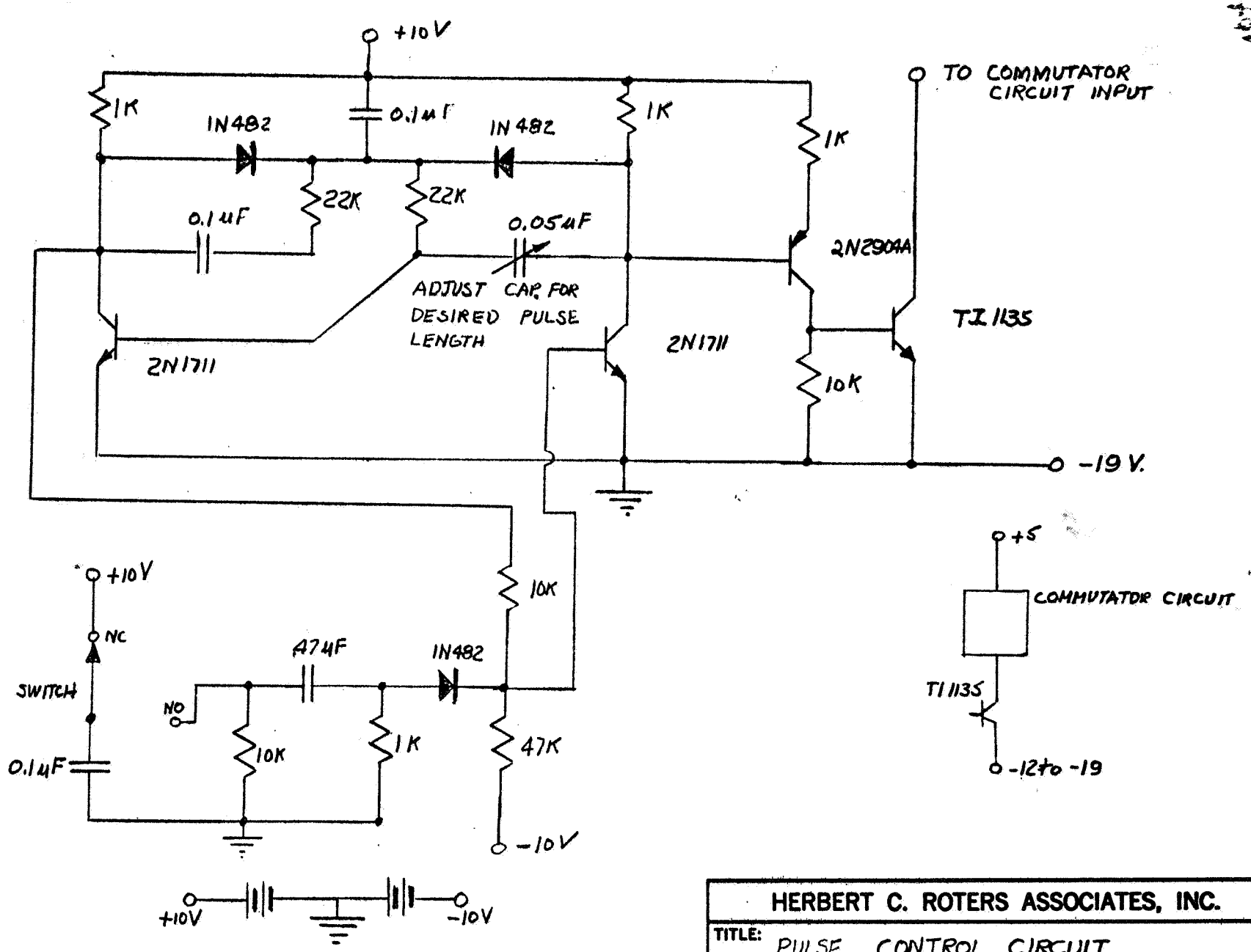


| NO. | BY | D | REVISION |
|---|---|---|---|
| | | | |

TOLERANCES
FRACT. ± 1/64 DEC. ± ANG. ± 1/2°
UNLESS OTHERWISE SPECIFIED

HERBERT C. ROTERS ASSOCIATES, INC.

TITLE: PULSE CONTROL CIRCUIT

| DR. BY: | DATE | MATERIAL |
|---|---|---|
| HDJ | 2-19-68 | 2 |
| CH. BY: | DATE | |
| TJL | 2-21-68 | |

SCALE 2 — No. A-21

No. A-2921

No. A-2921

OGILVIE PRESS, INC., BROOKLYN 17, N. Y. ULTRAVEL NO. 490M

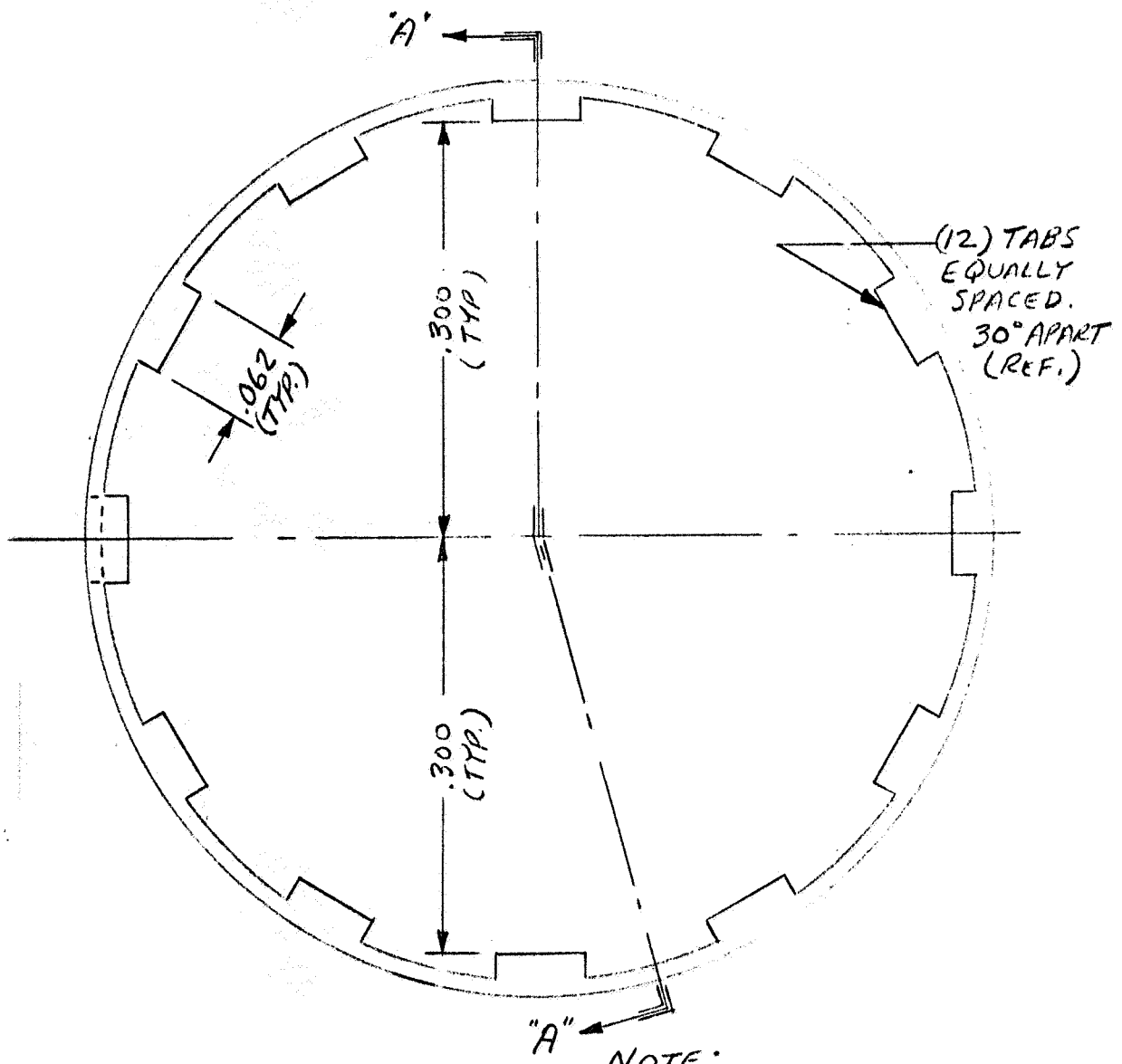


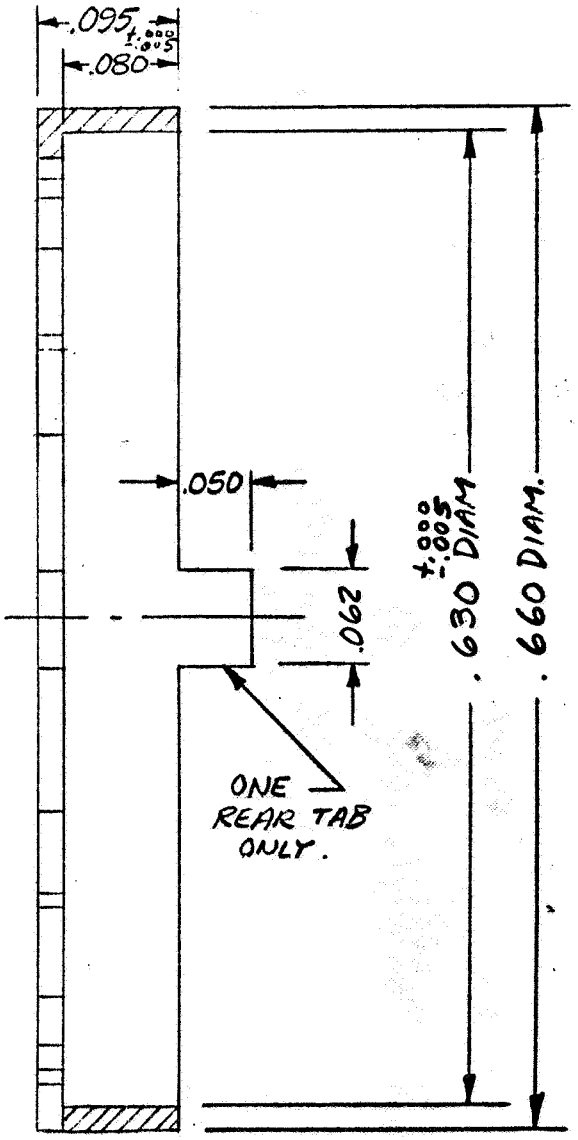


SECTION "A"-"A"

NOTE:
1. .300 DIMENSION MAY BE .300 RAD. (TYP.)

| NO. | BY | DA | REVISION |
|---|---|---|---|
| | | | |

TOLERANCES UNLESS OTHERWISE SPECIFIED
FRACT. ± 1/64 DEC. ± ANG. ± 1/2°

HERBERT C. ROTERS ASSOCIATES, INC.

TITLE: RING - CROWN TERMINAL

| DR. BY: | DATE | MATERIAL |
|---|---|---|
| J.A.F | 7-27-68 | BRASS |
| CH. BY: | DATE | |

SCALE 8:1 No. A-2967

No. A-2967

No. A-2967

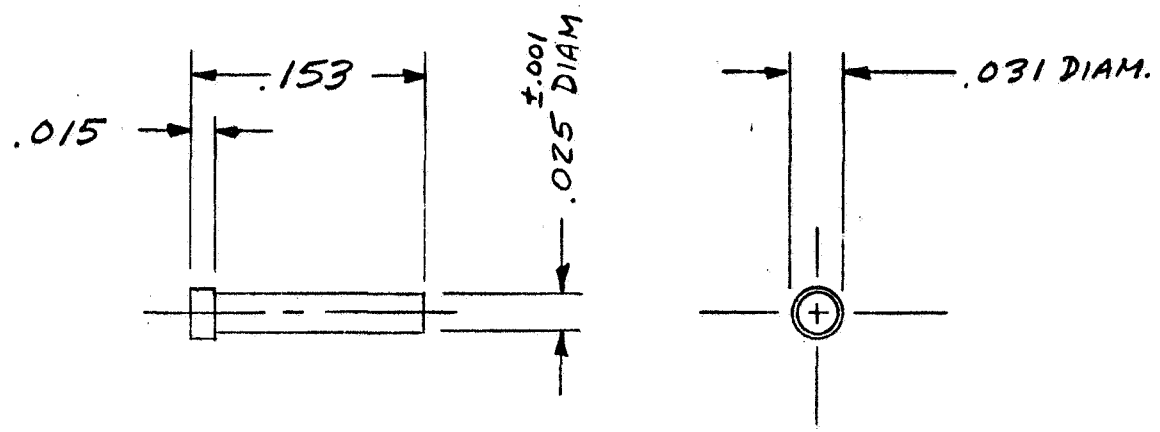


No. A-2968

| NO. | BY | D. | REVISION |
|---|---|---|---|
| | | | |

TOLERANCES
FRACT. ± 1/64 DEC. ± ANG. ± 1/2°
UNLESS OTHERWIS ECIFIED

**HERBERT C. ROTERS ASSOCIATES, INC.**

TITLE: TERMINAL PIN

| DR. BY: | DATE | MATERIAL |
|---|---|---|
| J.A.F. | 7-27-68 | BRASS |
| CH. BY: | DATE | SCALE 8:1 |

No. A-2968

No. A-2968

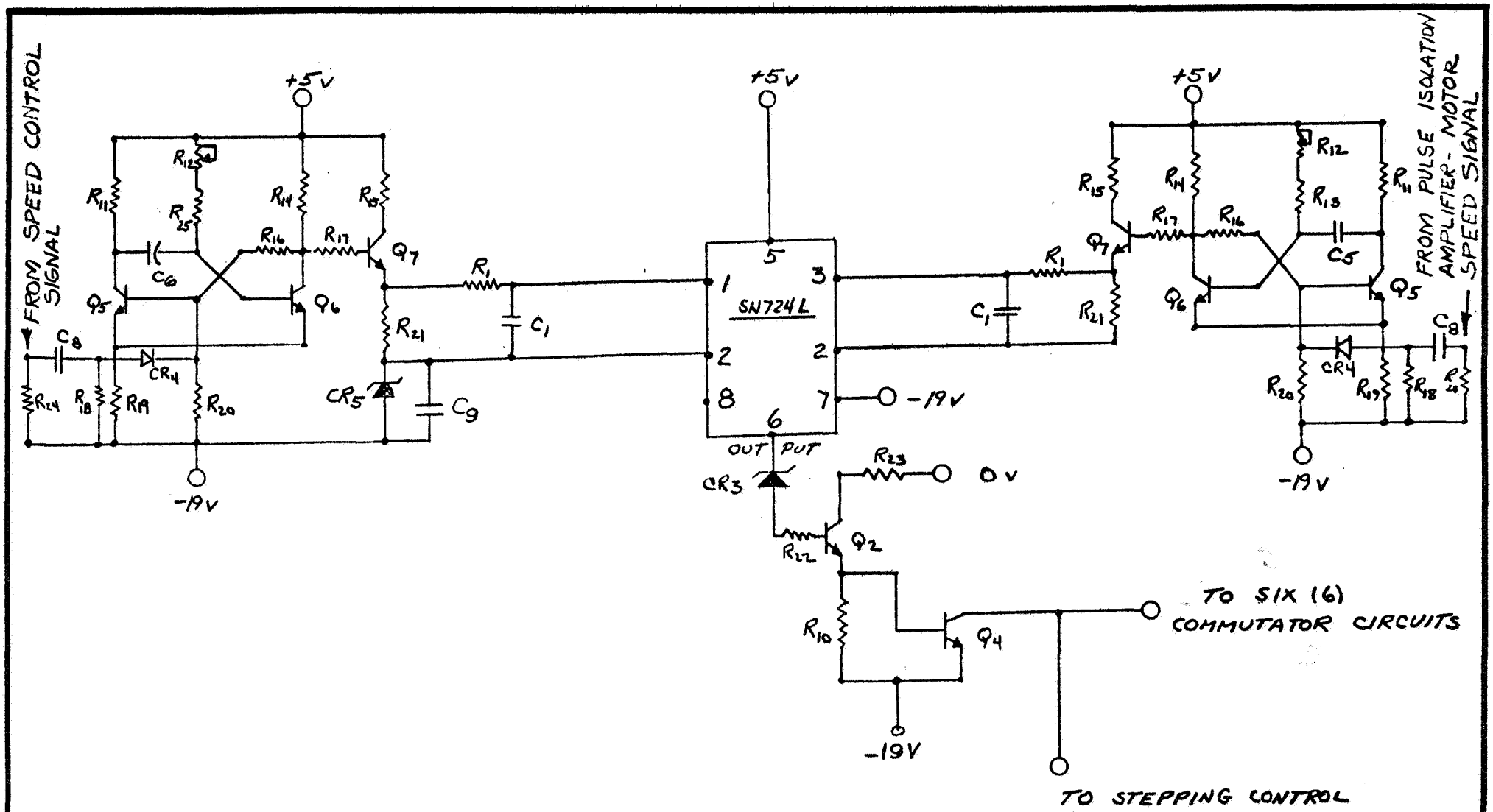


No. A-2972

No. A-2972

| NO. | BY | D. | REVISION |
|---|---|---|---|
| | | | |

TOLERANCE
FRACT. ± 1/64 DEC. ± ANG. ± 1/2°
UNLESS OTHERWISE SPECIFIED

**HERBERT C. ROTERS ASSOCIATES, INC.**

TITLE: SPEED CONTROL CIRCUIT (FINAL)

| DR. BY: | DATE | MATERIAL |
|---|---|---|
| TJL | 8-8-68 | ~ |
| CH. BY: | DATE | |
| | | SCALE ~ |

No. A-2972

# PARTS LIST FOR SPEED CONTROL CIRCUIT - A-2972 SUPP.

| | | | |
|---|---|---|---|
| $R_1$ | 2200Ω | $R_{23}$ | 150Ω |
| $R_{11}, R_{14}$ | 4700Ω | $C_1$ | 15 μF |
| $R_{10}$ | 10 KΩ | $C_5$ | 0.02 μF |
| $R_{12}$ | 7.5 KΩ Pot | $C_6$ | 0.0068 μF |
| $R_{13}$ | 22 K+ | $C_8$ | 15 μF |
| $R_{15}$ | 100Ω | $C_9$ | 1.5 μF 35 V |
| $R_{16}, R_{18}$ | 22 KΩ | $CR_3$ | 1N 752 |
| $R_{17}, R_{21}$ | 1000Ω | $CR_4$ | 1N 482 |
| $R_{19}$ | 470Ω | $CR_5$ | 11 V Zener (Tentative) |
| $R_{20}$ | 47 KΩ | $Q_2, Q_5, Q_6, Q_7$ | 2N 1711 |
| $R_{21}$ | 1000Ω | $Q_4$ | TI 1135 |
| $R_{22}$ | 82 KΩ | | |

No. A-2972 Supp

| NO. | BY | DA.. | REVISION |
|---|---|---|---|
| | | | |
| | | | |
| | | | |

TOLERAN
FRACT. ± 1/64 DEC. ± ANG. ± 1/2°
UNLESS OTHERWISE SPECIFIED

HERBERT C. ROTERS ASSOCIATES, INC.

TITLE:
PARTS LIST FOR SPEED CONTROL CIRCUIT
A-2972

| DR. BY: | DATE | MATERIAL |
|---|---|---|
| TJL | 8-8-68 | |
| CH. BY: | DATE | |
| | | SCALE |

No. A- 2972 Supp.

No. A-2972 Supp

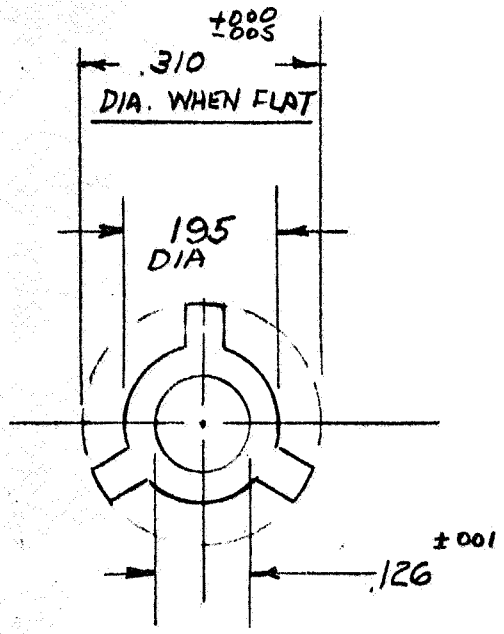



- BEND ALL THREE LEGS EQUALLY TO GIVE 8-10 oz WHEN SQUEEZED FLAT.

REMOVE ALL BURRS

No. A-3008

No. A-3008

| NO. | BY | D. | REVISION |
|---|---|---|---|
| | | | |

TOLERANCES
FRACT. ± 1/64 DEC. ± ANG. ± 1/2°
UNLESS OTHERWISE SPECIFIED

HERBERT C. ROTERS ASSOCIATES, INC.

TITLE: SPRING- PRELOAD

| DR. BY: | DATE | MATERIAL |
|---|---|---|
| HCJ | 3-15-69 | .005" PHOSPHOR BRONZE SPRING TEMPER |
| CH. BY: | DATE | |
| | | SCALE: No. A-3008 |

# PERFORMANCE CHARACTERISTICS BRUSHLESS DC MOTOR

## DESIGN NO. 2

## JET PROPULSION LABORATORIES

## CONTRACT #951463

Speed 4500 rpm

Herbert C. Roters Associates, Inc. April 3, 1966

**DATA:**

Case - 3/4" Dia x 1.312" long
Rotor - 5/16" Dia x 0.372" long, Alnico IX
Winding - 98 t/c #39 HF - 11 teeth, 0.037" wide
Resistance between terminals - 45.6Ω
Air Gap - 0.020" radial

Note: Performance shown does not include power requirement for obtaining commutation signal and transistor drive.

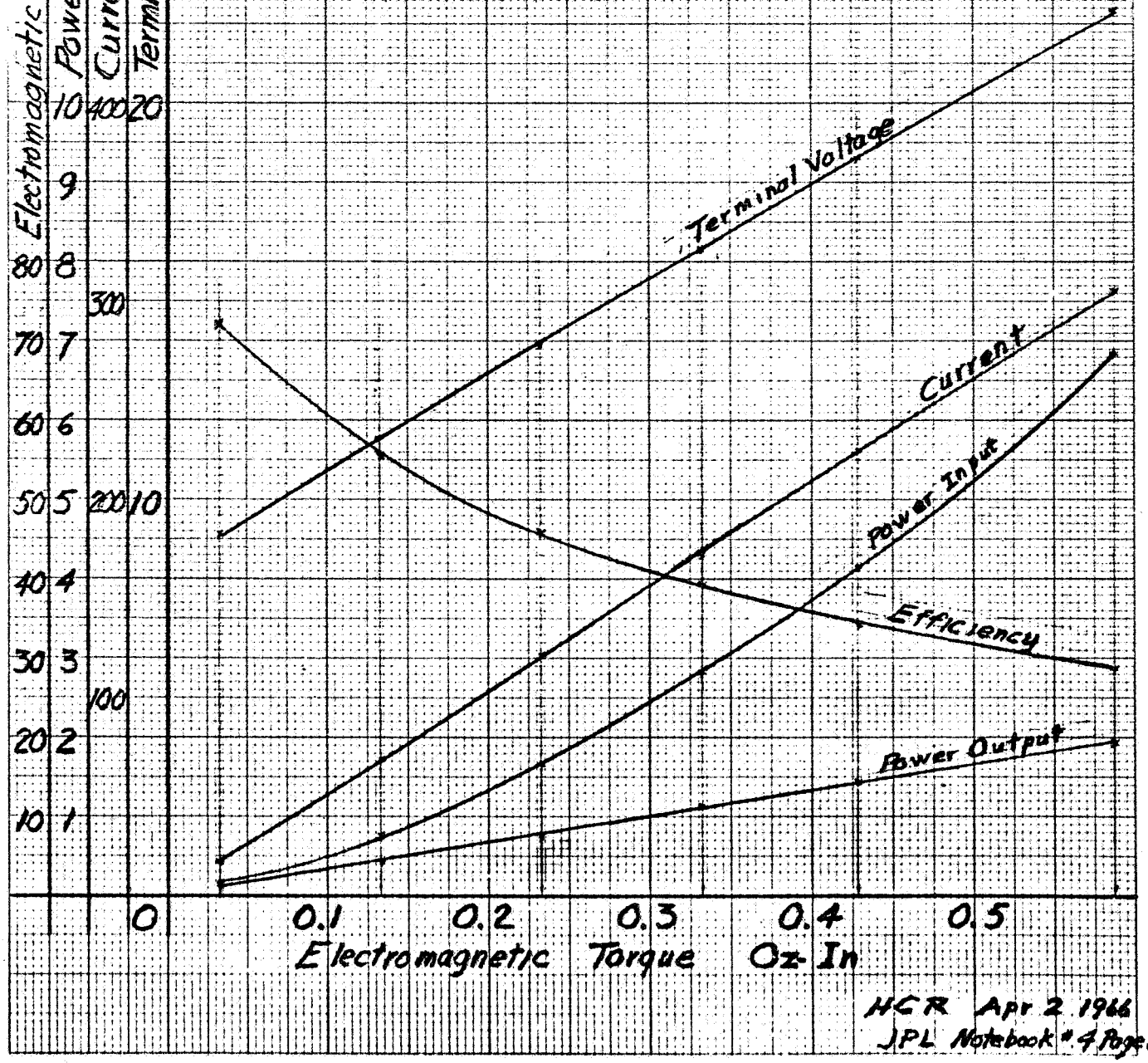


HCR Apr 2 1966
JPL Notebook #4 Page 15

# PERFORMANCE CHARACTERISTICS BRUSHLESS DC MOTOR
## DESIGN NO. 1
## JET PROPULSION LABORATORIES
## CONTRACT #951463

**Speed 4500 rpm**

**Herbert C. Roters Associates, Inc.** **April 6, 1966**

**DATA:**

Case - 3/4" Dia x 1.294" long
Rotor - 5/16" Dia x 0.300" long, Alnico IX
Winding - 121 t/c #40 HF - 11 teeth, 0.037" wide
Resistance between terminals - 71.0Ω
Air Gap 0.020" radial

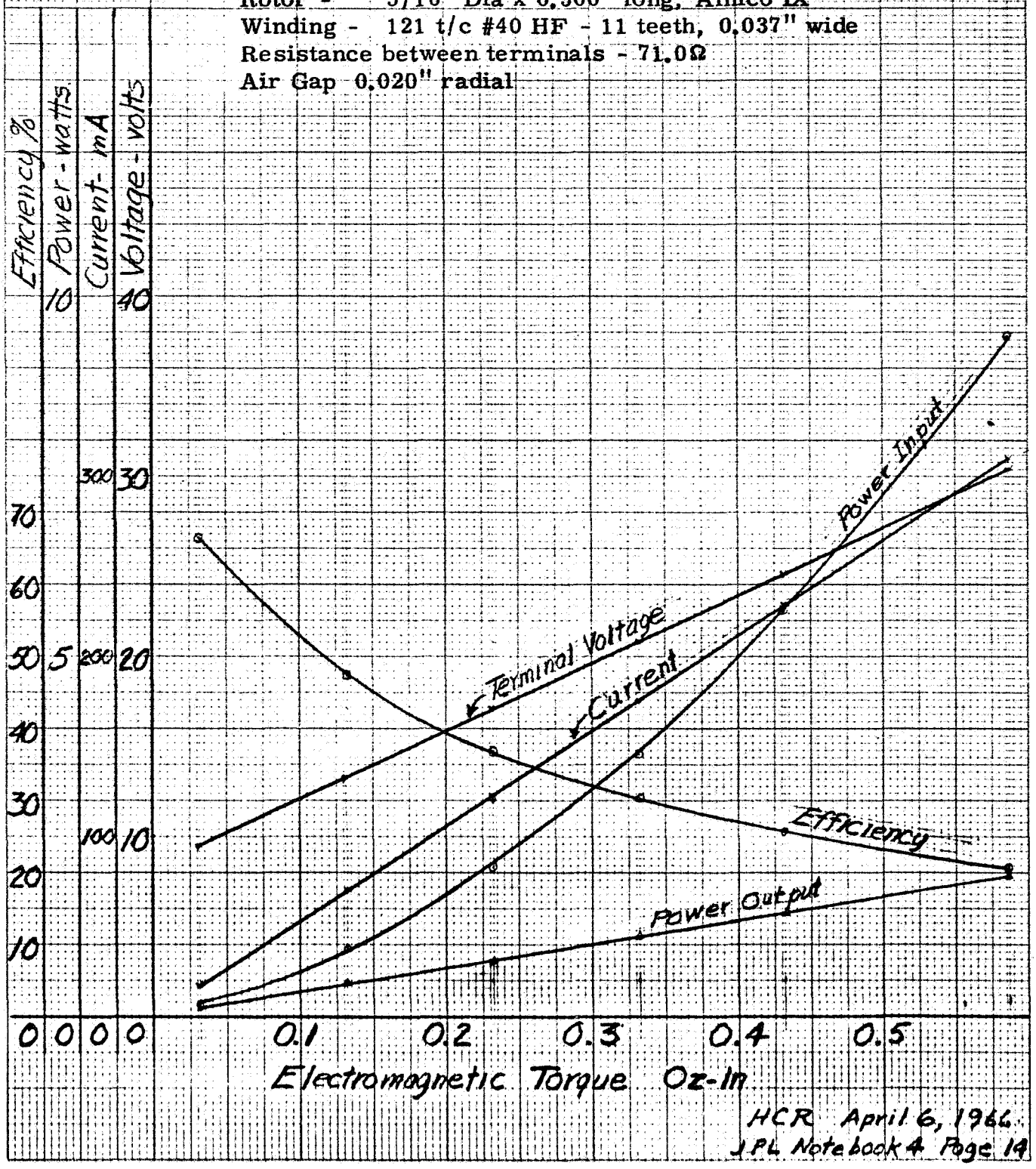


HCR April 6, 1966.
JPL Notebook 4 Page 14

# PERFORMANCE CHARACTERISTICS BRUSHLESS DC MOTOR.

DESIGN NO. 3 CALCULATED

JET PROPULSION LABORATORY

CONTRACT #951463

Speed 4500 rpm

Herbert C. Roters Associates, Inc. May 9, 1966

**DATA:**

Case - 3/4" Dia x 1-5/16" long

Rotor - 5/16" Dia x 0.372" long, Alnico IX

Winding - 12 coils of 82 t/c #38 HF, full pitch, 2 coil sides per slot

Resistance between terminals - 36.0 Ω

Air Gap - 0.015" radial

Note: Performance shown does not include power requirement for obtaining commutating signal and transistor drive. Torques shown do not include the equivalent iron loss drag torque of 0.0109 oz-in. This torque will require a current of 6.5 mA.

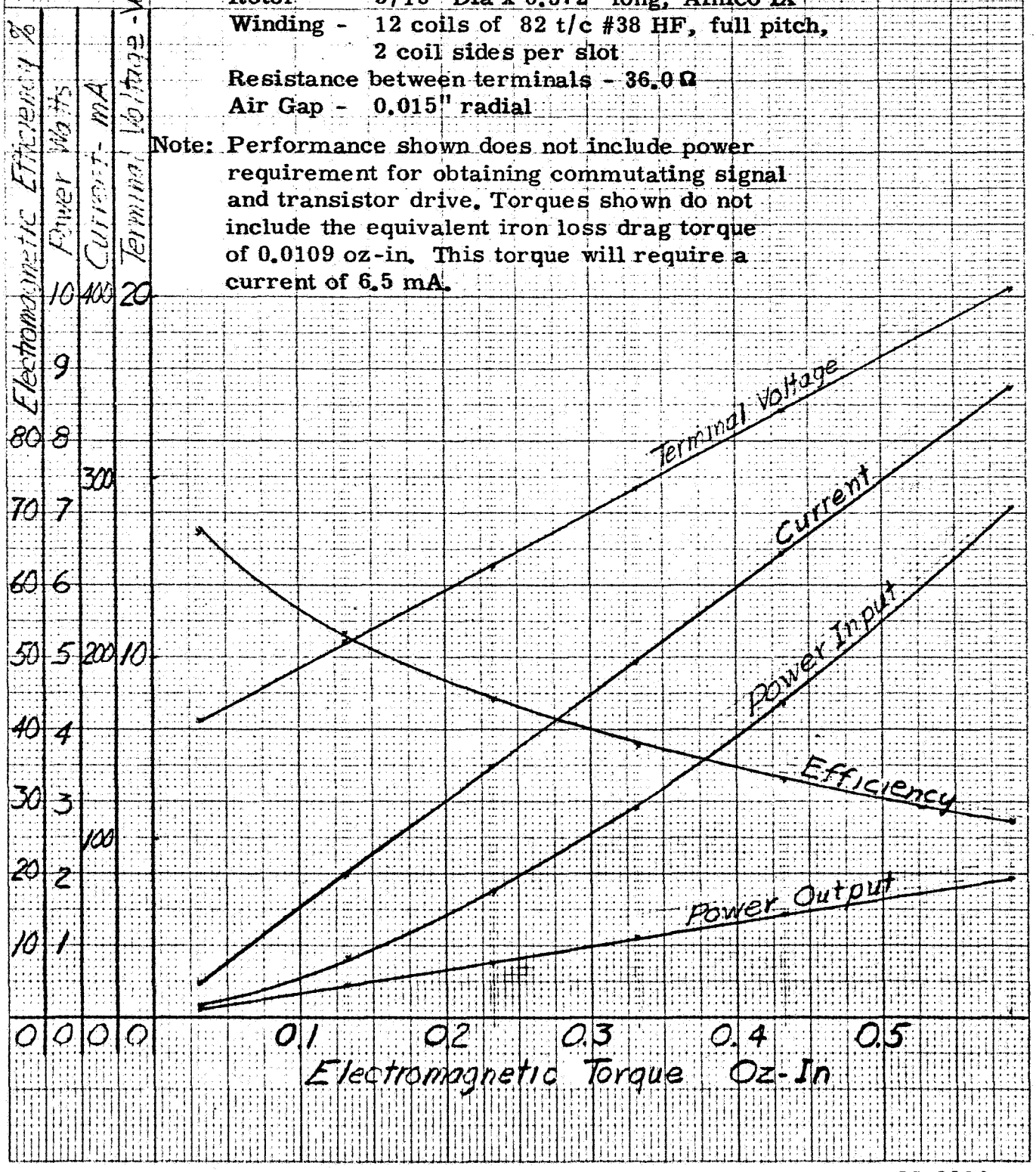

# VARIATION OF VOLTAGE OUTPUT FROM ONE-SHOT MULTIVIBRATORS OF SPEED CONTROL CIRCUIT A-2761B VERSUS SIGNAL FREQUENCY

JET PROPULSION LABORATORY #951463

Herbert C. Roters Associates, Inc. April 1967

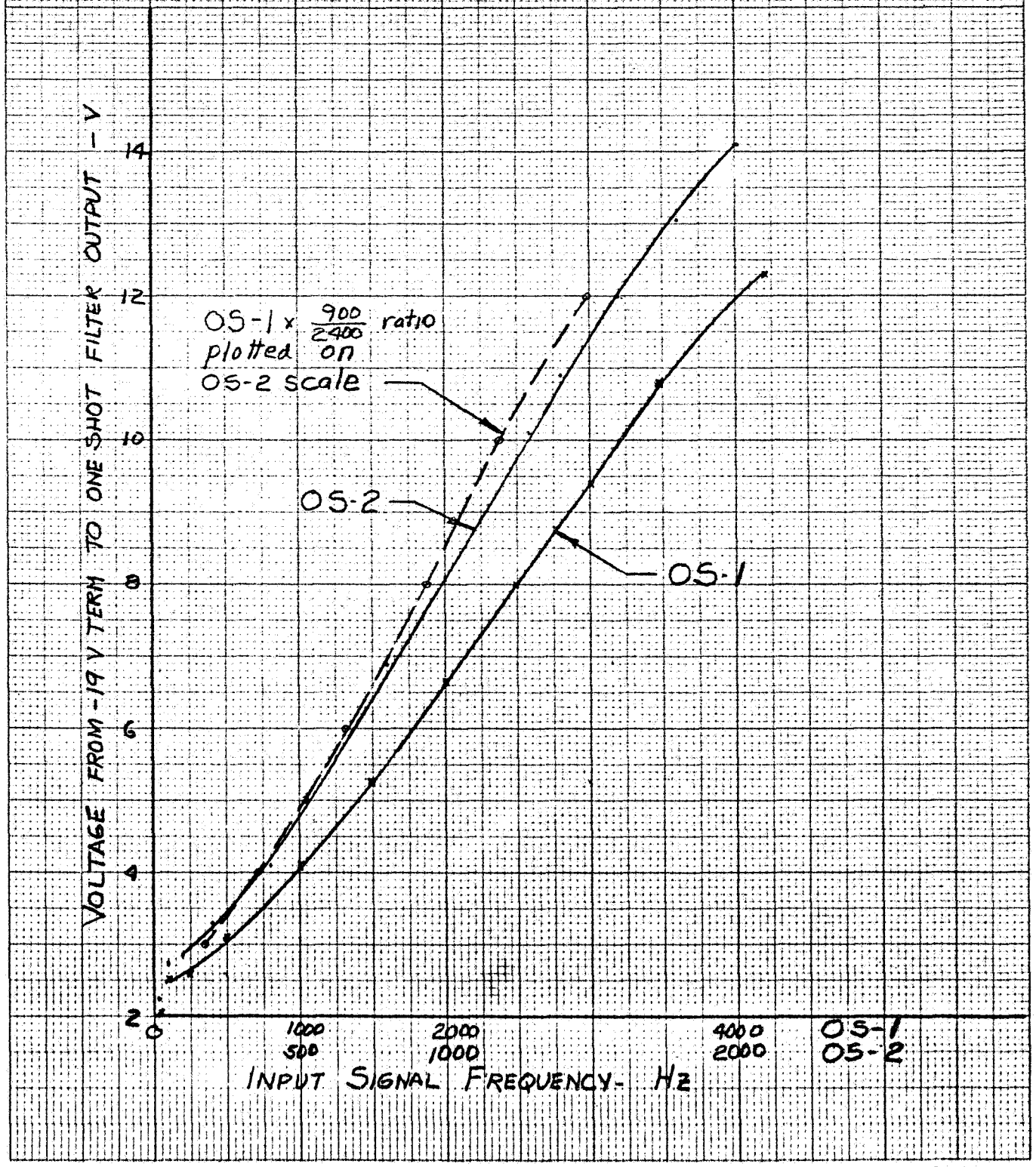

# MOTOR CHARACTERISTICS
## UNIT 159 DC BRUSHLESS MOTOR
## AND LOGIC CONTROLLED COMMUTATION POWER SUPPLY

Jet Propulsion Laboratory - P. O. #951463
17 volts on Motor Stator

Herbert C. Roters Associates, Inc. July 1967

Case: 3/4" Dia x 1-5/16" long

Winding: 12 coils 82 t/c #38 HF, full pitch, 2 coil sides/slot
Ring connected, 12 external terminal wires
Resistance across diameter of ring 36.0Ω

Rotor: 5/16" Dia x 0.572" long, Alnico IX, two-pole

Air Gap: 0.015" Radial (Magnetic) 0.005" Radial (Mechanical)

Powers shown are exclusive of:

| | | | |
|---|---|---|---|
| Oscillator Input | 15 V | 2.9 mA | 43.5 mW |
| Logic Input | 5 V | 290 mA | 1450 mW |

Note: Core Loss, Windage, and Bearing Friction Torques unknown at this time. These unknown torques are included in the motor losses.

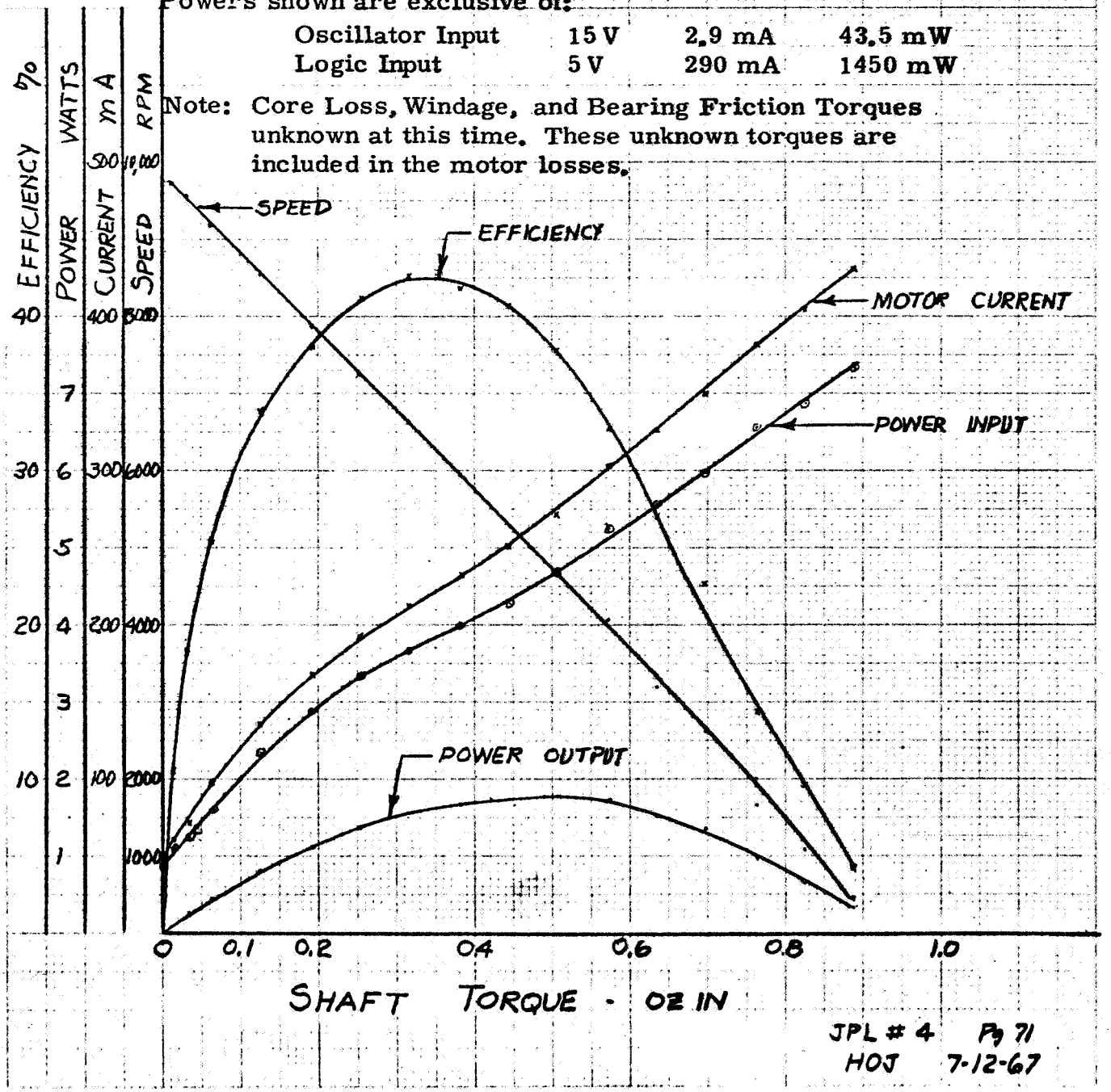


JPL # 4 Pg 71
HOJ 7-12-67

# MOTOR CHARACTERISTICS
## UNIT 159 DC BRUSHLESS MOTOR
## AND LOGIC CONTROLLED COMMUTATION POWER SUPPLY

Jet Propulsion Laboratory - P.O. #951463
23 volts on Motor Stator

Herbert C. Roters Associates, Inc. July 1967

Case: 3/4" Dia x 1-5/16" long
Winding: 12 coils 82 t/c #38 HF, full pitch, 2 coil sides/slot.
Ring connected, 12 external terminal wires
Resistance across diameter of ring 36.0Ω
Rotor: 5/16" Dia x 0.572" long, Alnico IX, two-pole
Air Gap: 0.015" Radial (Magnetic) 0.005" Radial (Mechanical)
Powers shown are exclusive of:

| | | | |
|---|---|---|---|
| Oscillator Input | 15 V | 2.9 mA | 43.5 mW |
| Logic Input | 5 V | 290 mA | 1450 mW |

Note: Core Loss, Windage, and Bearing Friction Torques unknown at this time. These unknown torques are included in the motor losses.

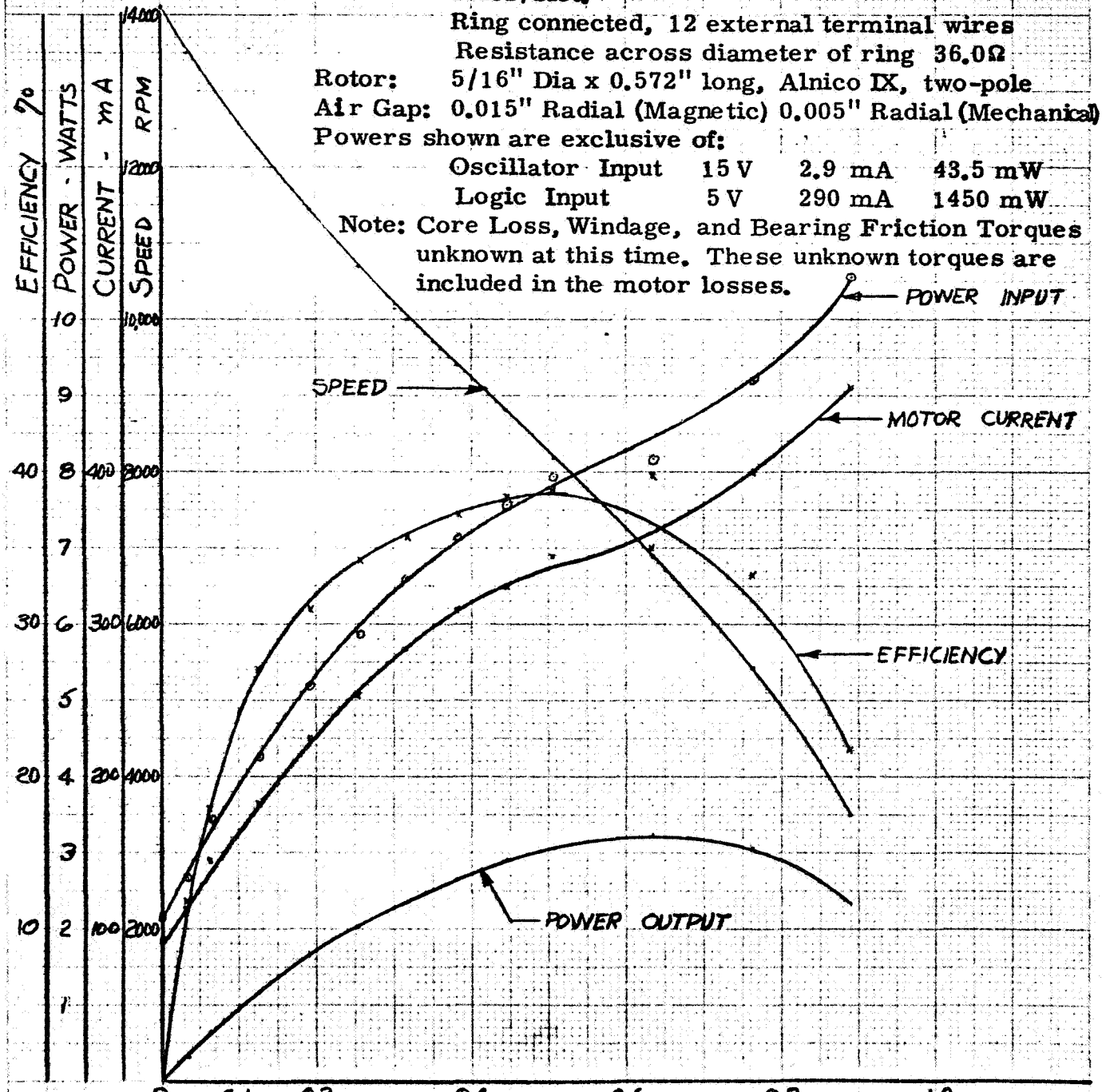


JPL-#4 Pg 71
HOJ 7-12-67

# MOTOR CHARACTERISTICS
## UNIT 159 DC BRUSHLESS MOTOR
## AND LOGIC CONTROLLED COMMUTATION POWER SUPPLY

Jet Propulsion Laboratory - P.O. #951463

10 volts on Motor Stator Power Supply

Herbert C. Roters Associates, Inc. Jan. 1968

Case: 3/4" Dia x 1-5/16" long

Winding: 12 coils 82 t/c #38 HF, full pitch, 2 coil sides/slot.
Ring connected, 12 external terminal wires
Resistance across diameter of ring 36.0Ω

Rotor: 5/16" Dia x 0.572" long, Alnico IX, two-pole

Air Gap: 0.015" Radial (Magnetic) 0.005" Radial (Mechanical)

| | | | | |
|---|---|---|---|---|
| Sensor Oscillator Input: | 15 V | 3.5 mA | 52 mW | not included |
| Logic Input: | 5 V | 290 mA | 1450 mW | not included |

Room Ambient Temperature

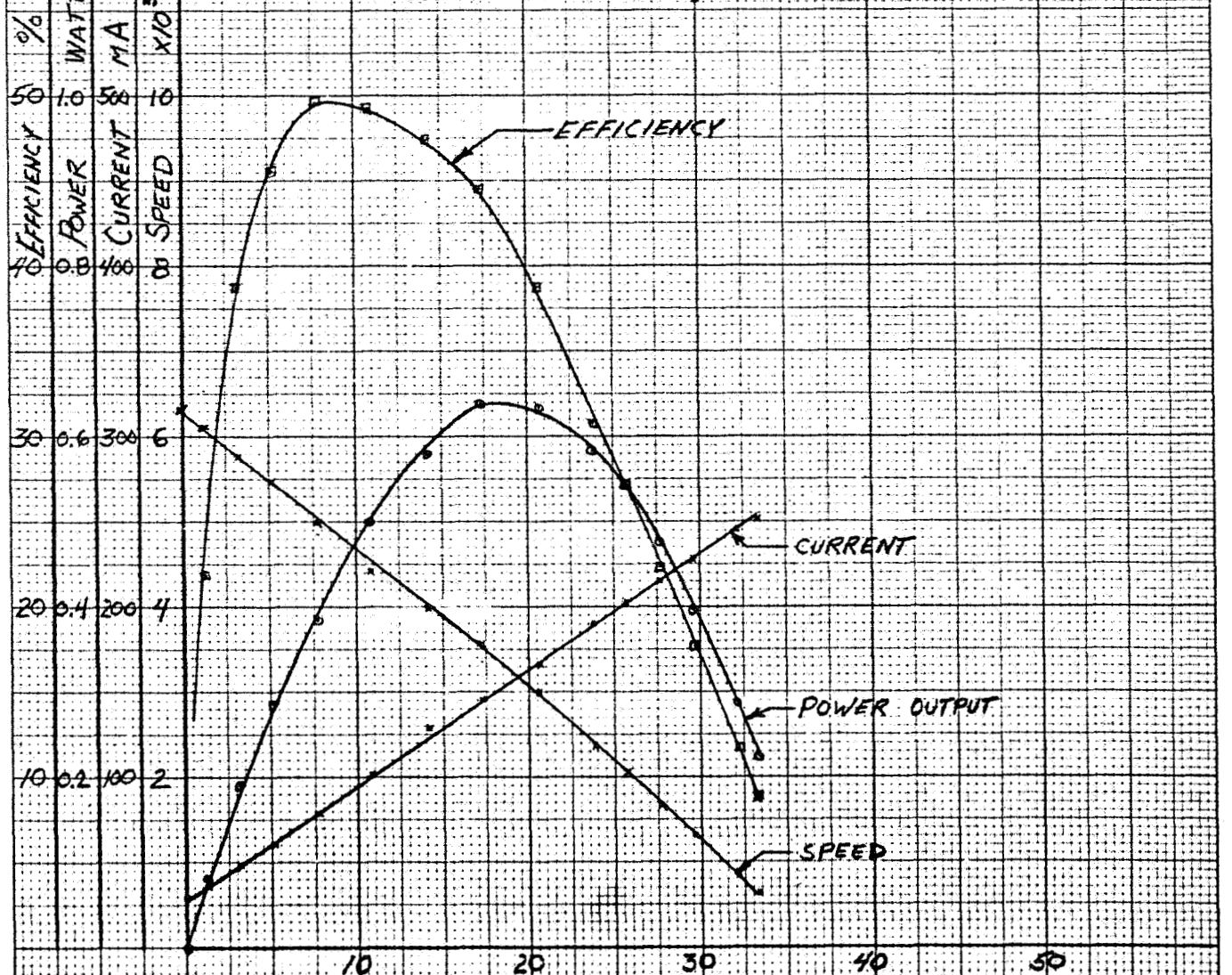


JPL #951463 Book #4 P 75
TTL 1/9/68

# MOTOR CHARACTERISTICS
## UNIT 159 DC BRUSHLESS MOTOR
## AND LOGIC CONTROLLED COMMUTATION POWER SUPPLY

Jet Propulsion Laboratory - P. O. #951463

25 volts on Motor Stator Power Supply

Herbert C. Roters Associates, Inc. Jan. 1968

Case: 3/4" Dia x 1-5/16" long

Winding: 12 coils 82 t/c #38 HF, full pitch, 2 coil sides/slot.
Ring connected, 12 external terminal wires
Resistance across diameter of ring 36.0Ω

Rotor: 5/16" Dia x 0.572" long, Alnico IX, two-pole

Air Gap: 0.015"Radial (Magnetic) 0.005" Radial (Mechanical)

| | | | | |
|---|---|---|---|---|
| Sensor Oscillator Input: | 15 V | 3.5 mA | 52 mW | not |
| Logic Input: | 5 V | 290 mA | 1450 mW | included |

Room Ambient Temperature

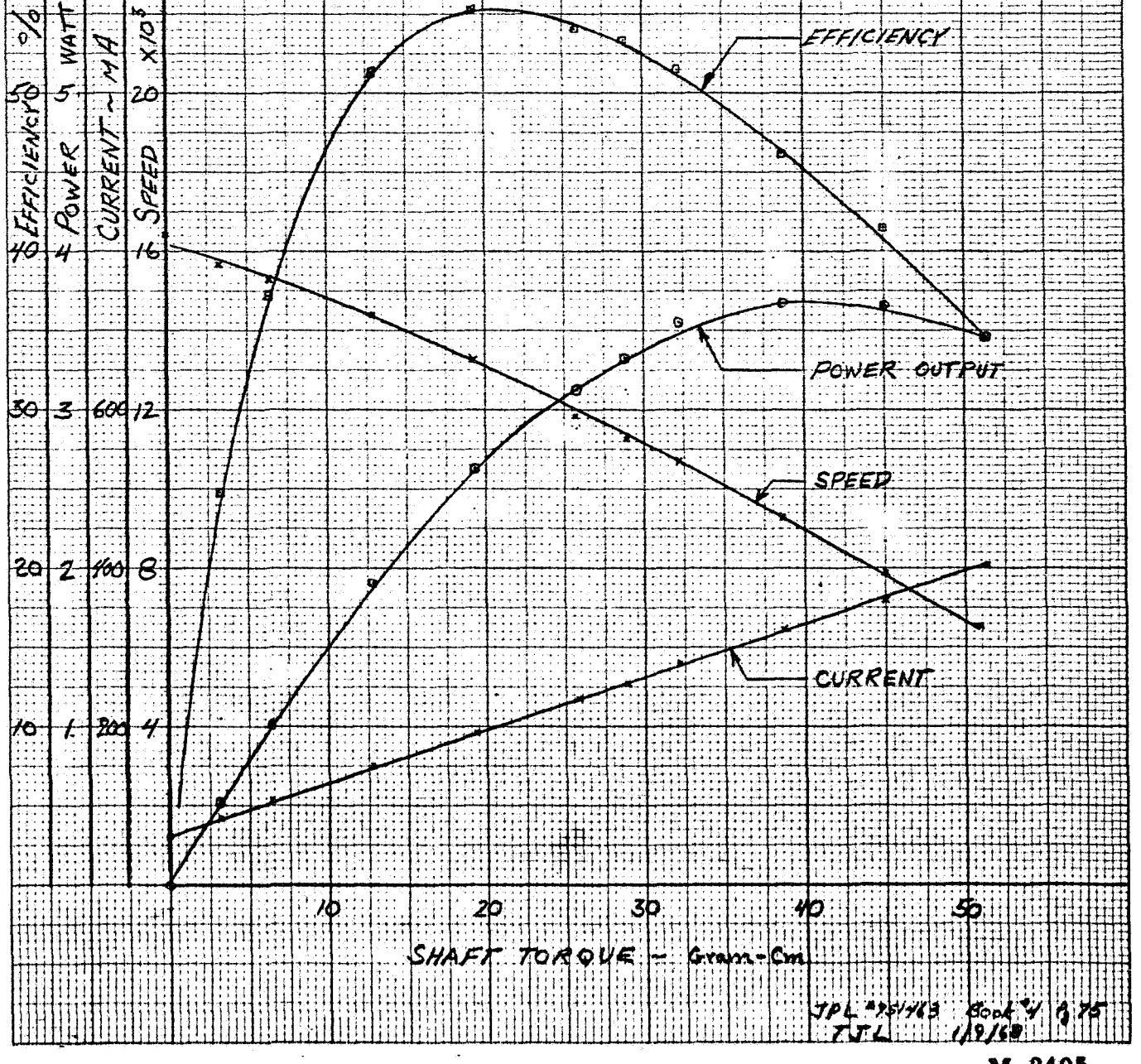


JPL #951463 Book 4 p 75
TJL 1/19/68

# NO LOAD MOTOR CHARACTERISTICS
## UNIT 159 DC BRUSHLESS MOTOR
## AND LOGIC CONTROLLED COMMUTATION POWER SUPPLY

Jet Propulsion Laboratory - P.O. #951463

Herbert C. Roters Associates, Inc. Jan. 1968

Case: 3/4" Dia x 1-5/16" long

Winding: 12 coils 82 t/c #38 HF, full pitch, 2 coil sides/slot.
Ring connected, 12 external terminal wires
Resistance across diameter of ring 36.0Ω

Rotor: 5/16" Dia x 0.572" long, Alnico IX, two-pole

Air Gap: 0.015" Radial (Magnetic) 0.005" Radial (Mechanical)

Sensor Oscillator Input: 15 V 3.5 mA 52 mW } not included
Logic Power: 5 V 290 mA 1450 mW }

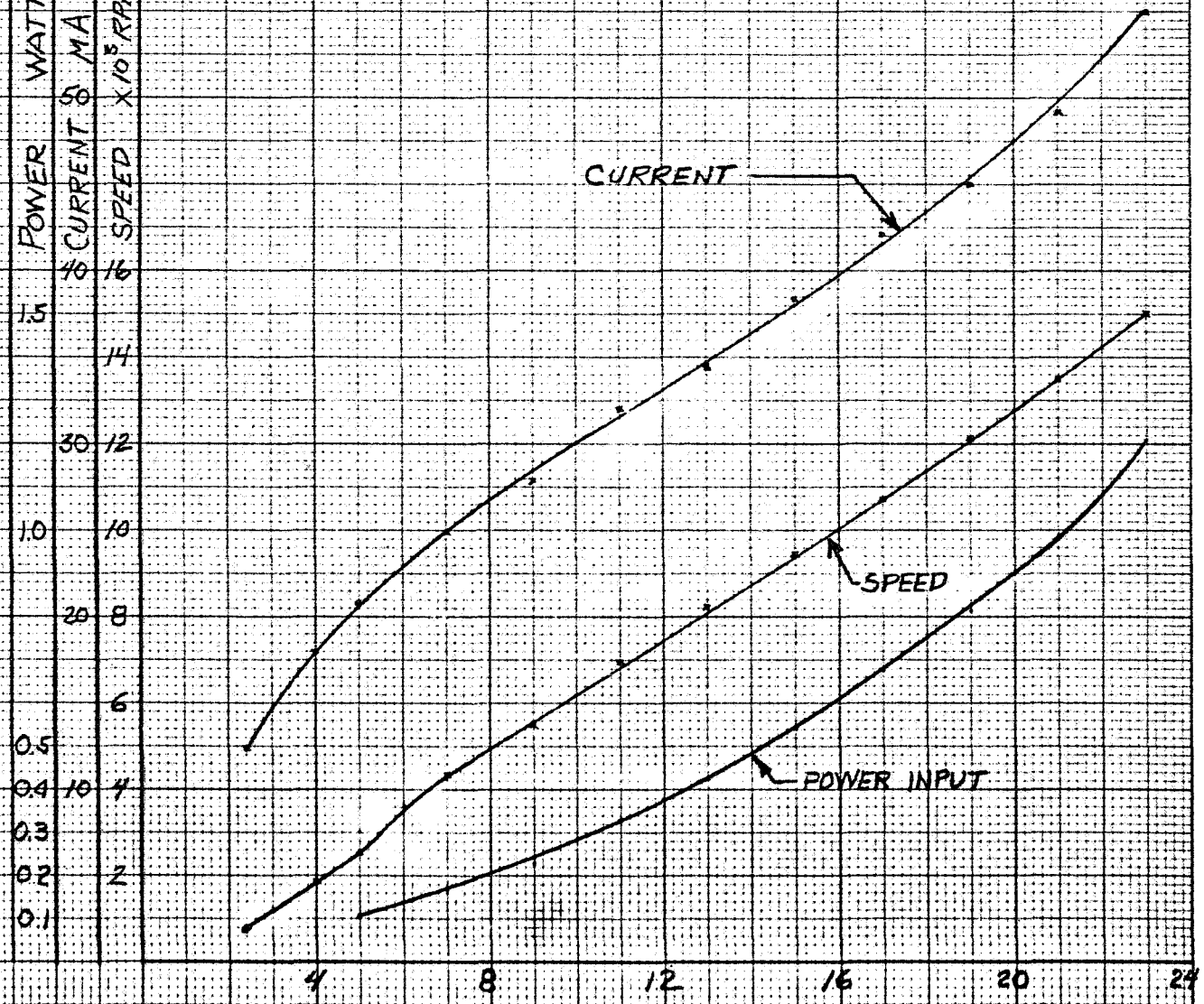


JPL #951643 Book #4 P 13
TJT 1/9/68

# MOTOR CHARACTERISTICS FOR 10 GRAM-CM TORQUE UNIT 159 DC BRUSHLESS MOTOR AND LOGIC CONTROLLED COMMUTATION POWER SUPPLY

Jet Propulsion Laboratory - P.O. #951463

Herbert C. Roters Associates, Inc. Jan. 1968

Case: 3/4" Dia x 1-5/16" long

Winding: 12 coils 82 t/c #38 HF, full pitch, 2 coil sides/slot.
Ring connected, 12 external terminal wires
Resistance across diameter of ring 36.0Ω

Rotor: 5/16" Dia x 0.572" long, Alnico IX, two-pole

Air Gap: 0.015" Radial (Magnetic) 0.005" Radial (Mechanical)

Sensor Oscillator Input: 15 V 3.5 mA 52 mW
Logic Power: 5 V 290 mA 1450 mW
} not included

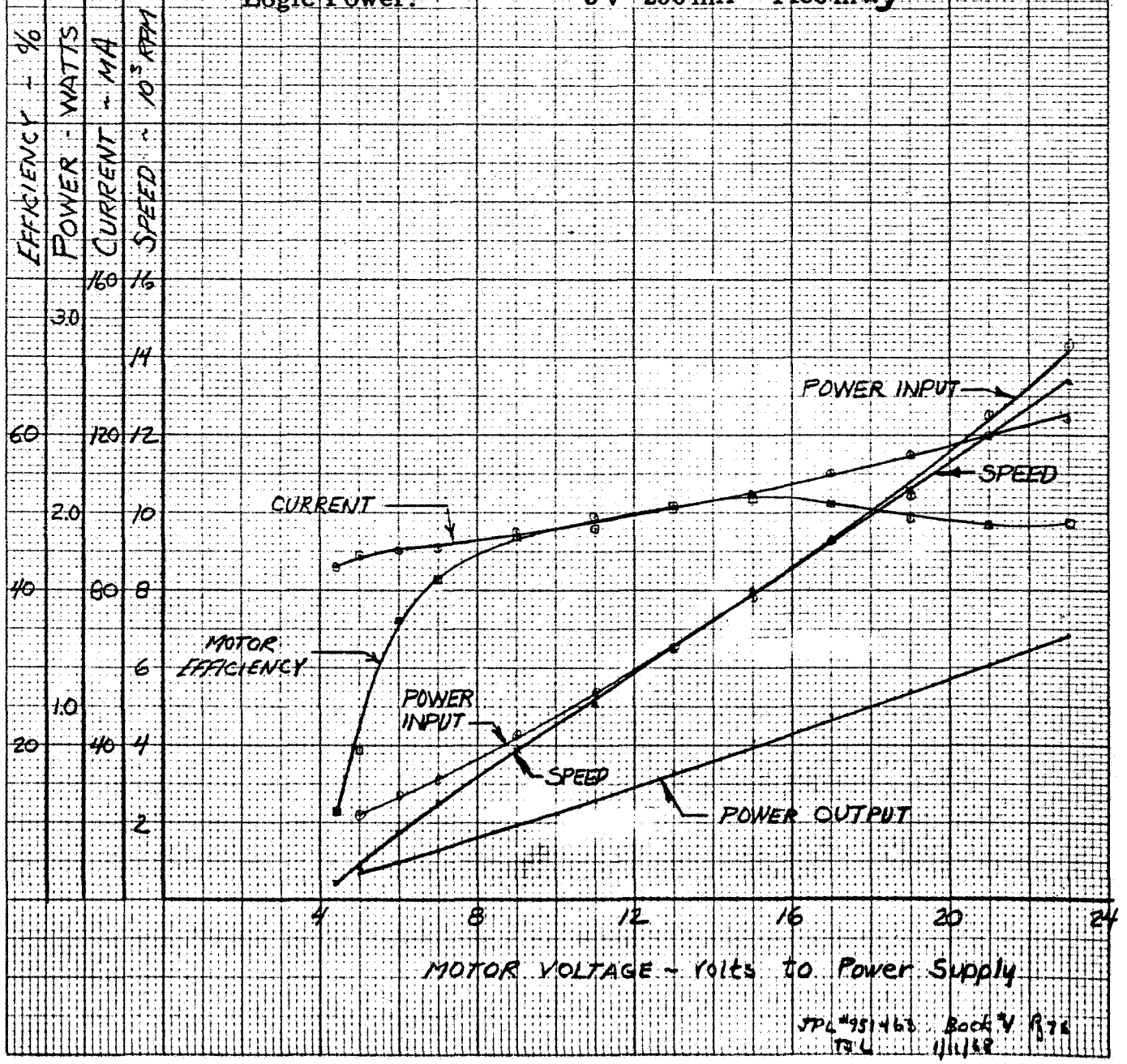


JPL #951463 Book V R76 TEL 1/11/68

# MOTOR CHARACTERISTICS FOR 19.9 GRAM-CM TORQUE UNIT 159 DC BRUSHLESS MOTOR AND LOGIC CONTROLLED COMMUTATION POWER SUPPLY

Jet Propulsion Laboratory - P.O. #951463

Herbert C. Roters Associates, Inc. Jan. 1968

Case: 3/4" Dia x 1-5/16" long

Winding: 12 coils 82 t/c #38 HF, full pitch, 2 coil sides/slot.
Ring connected, 12 external terminal wires
Resistance across diameter of ring 36.0Ω

Rotor: 5/16" Dia x 0.572" long, Alnico IX, two-pole

Air Gap: 0.015" Radial (Magnetic) 0.005" Radial (Mechanical)

| | | | | |
|---|---|---|---|---|
| Sensor Oscillator Input: | 15 V | 3.5 mA | 52 mW | not included |
| Logic Power: | 5 V | 290 mA | 1450 mW | not included |

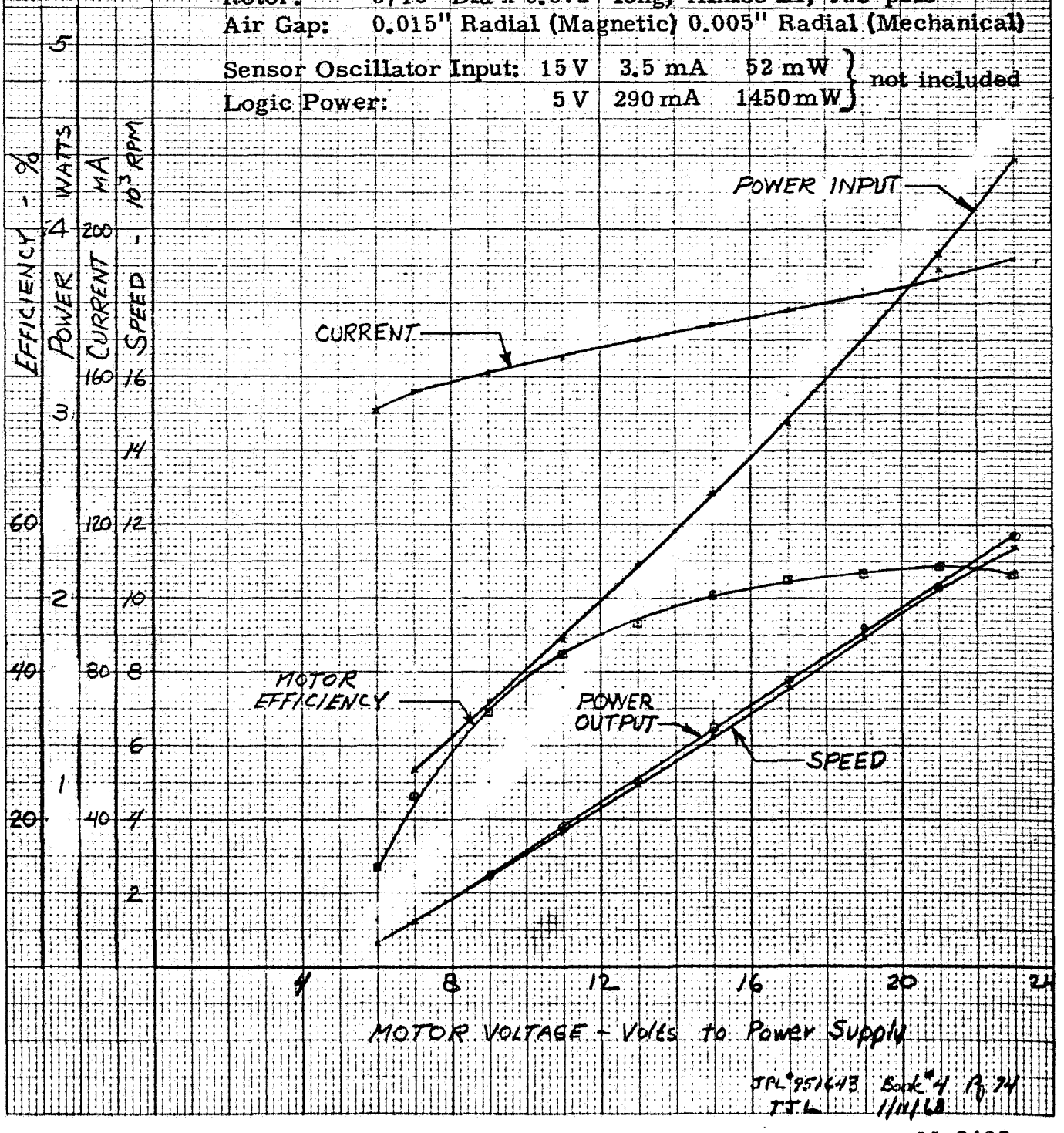


JPL 951643 Book 4 P. 24
ITL 1/11/68

# MOTOR CHARACTERISTICS
## UNIT 159 DC BRUSHLESS MOTOR
## AND LOGIC CONTROLLED COMMUTATION POWER SUPPLY

Jet Propulsion Laboratory - P.O. #951463
25 Volts on Motor Stator Power Supply
+10°C Ambient Temperature (Motor only)

Herbert C. Roters Associates, Inc. Feb. 1968

Case: 3/4" Dia x 1-5/16" long
Winding: 12 coils 82 t/c #38 HF, full pitch, 2 coil sides/slot.
Ring connected, 12 external terminal wires
Resistance across diameter of ring 36.0Ω
Rotor: 5/16" Dia x 0.572" long, Alnico IX, two-pole
Air Gap: 0.015" Radial (Magnetic) 0.005" Radial (Mechanical)
Sensor Oscillator Input: 18.6 V, 4.7 mA, 87.4 mW } not included
Logic Power Input: 5 V, 253 mA, 1265 mW }

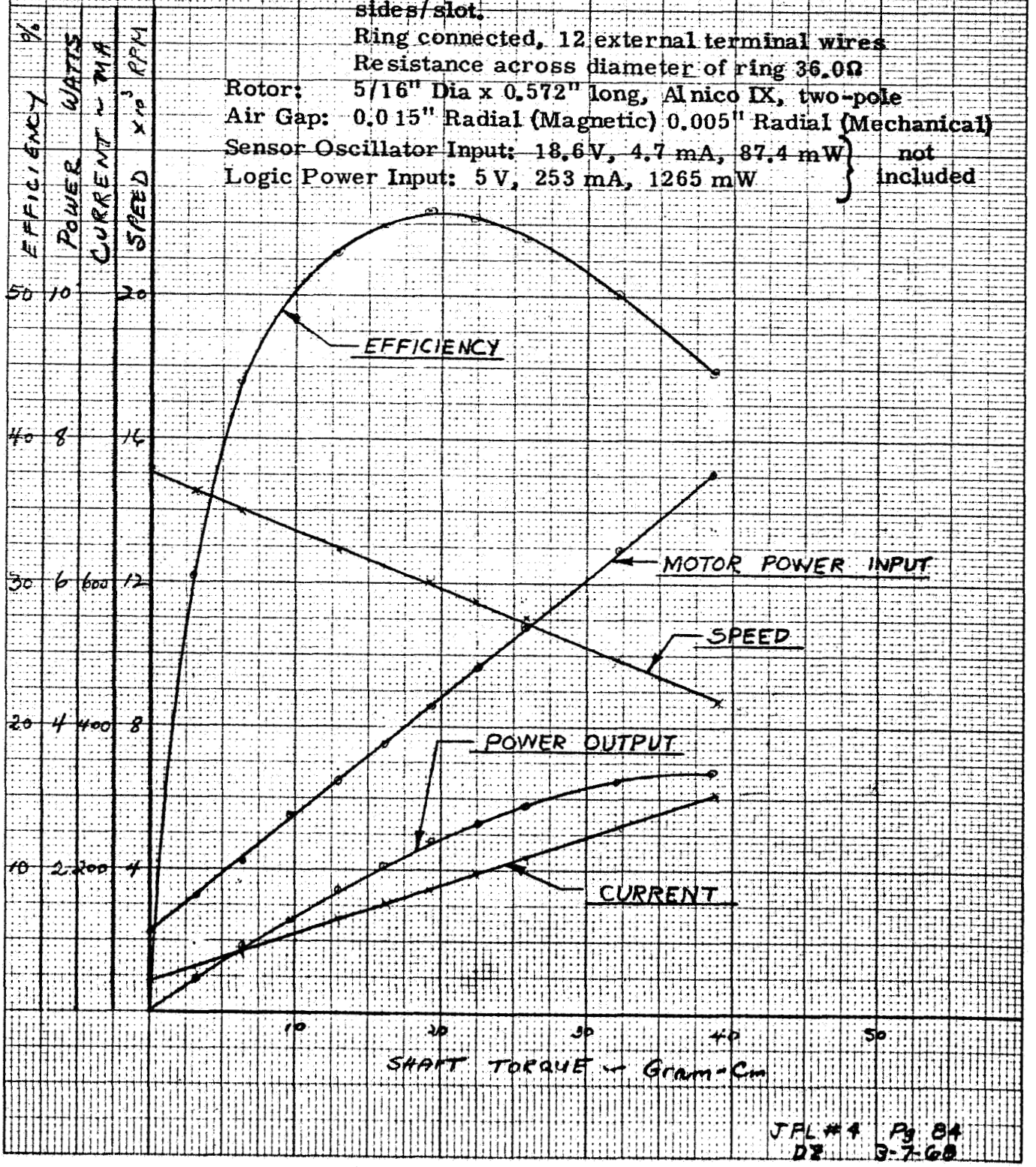


JPL #4 Pg 84
DE 3-7-68

# MOTOR CHARACTERISTICS
## UNIT 159 DC BRUSHLESS MOTOR
## AND LOGIC CONTROLLED COMMUTATION POWER SUPPLY

Jet Propulsion Laboratory - P. O. #951463

25 Volts on Motor Stator Power Supply

+75°C Ambient Temperature (Motor only)

Herbert C. Roters Associates, Inc. Feb. 1968

Case: 3/4" Dia x 1-5/16" long

Winding: 12 coils 82 t/c #38 HF, full pitch, 2 coil sides/slot.
Ring connected, 12 external terminal wires
Resistance across diameter of ring 36.0Ω

Rotor: 5/16" Dia x 0.572" long, Alnico IX, two-pole

Air Gap: 0.015" Radial (Magnetic) 0.005" Radial (Mechanical)

Sensor Oscillator Input: 20.3 V, 4.8 mA, 97.4 mW
Logic Power Input: 5 V, 265 mA, 1325 mW
} not included

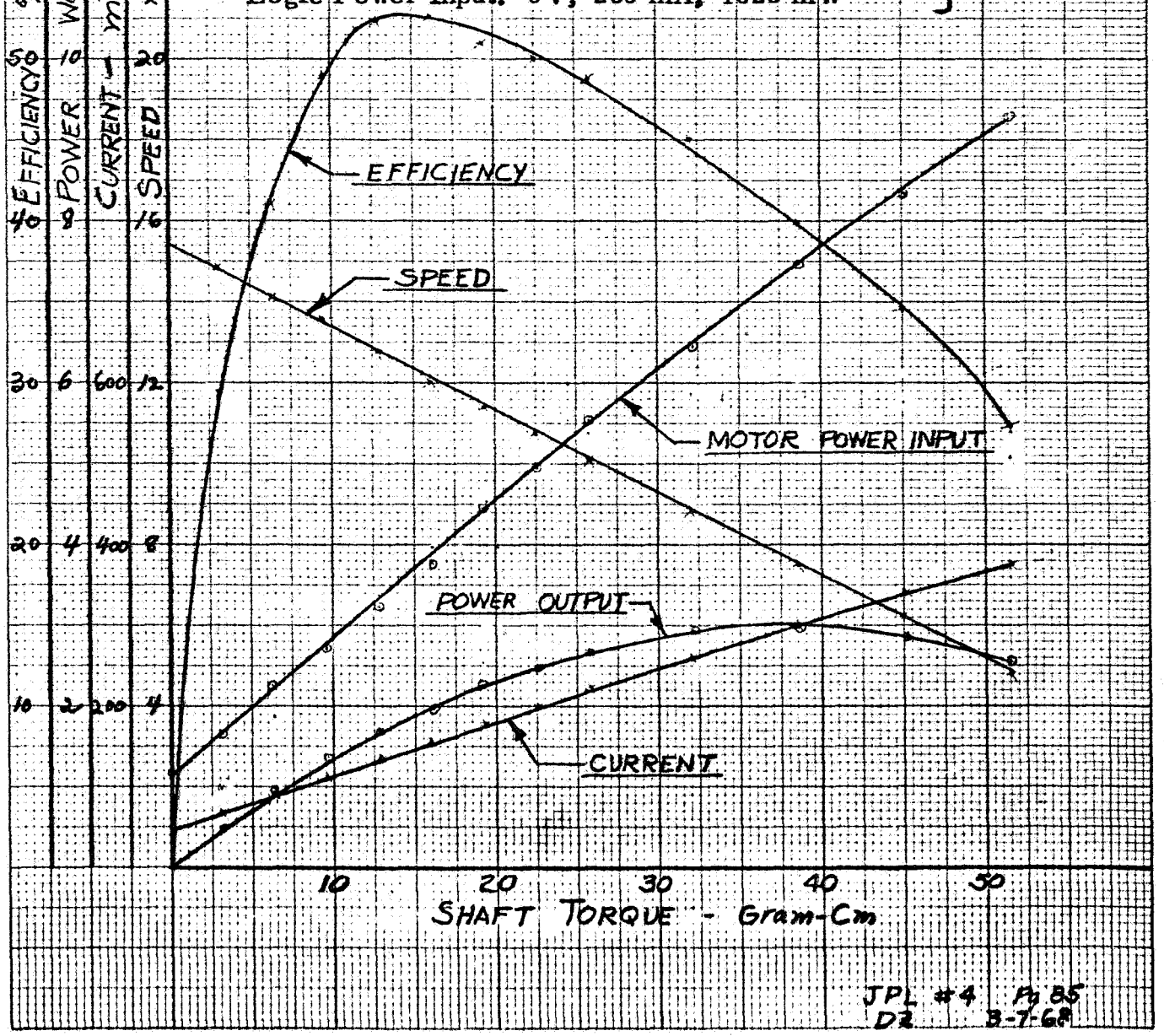


JPL #4 Pg 85
D2 3-7-68

# MOTOR CHARACTERISTICS
## UNIT 159 DC BRUSHLESS MOTOR
## AND LOGIC CONTROLLED COMMUTATION POWER SUPPLY

J et Propulsion Laboratory - P.O. #951463
25 Volts on Motor Stator Power Supply
Room Ambient Temperature
Tested after -10°C and +75°C tests were done
Herbert C. Roters Associates, Inc. Feb. 1968

Case: 3/4" Dia x 1-5/16" long
Winding: 12 coils 82 t/c #38HF, full pitch, 2 coil sides/slot.
Ring connected, 12 external terminal wires
Resistance across diameter of ring 36.0Ω
Rotor: 5/16" Dia x 0.572" long, Alnico IX, two-pole
Air Gap: 0.015" Radial (Magnetic) 0.005" Radial (Mechanical)

Sensor Oscillator Input: 19.2 V, 4.5 mA, 86.4 mW } not included
Logic Power Input: 5 V, 254 mA, 1270 mW }

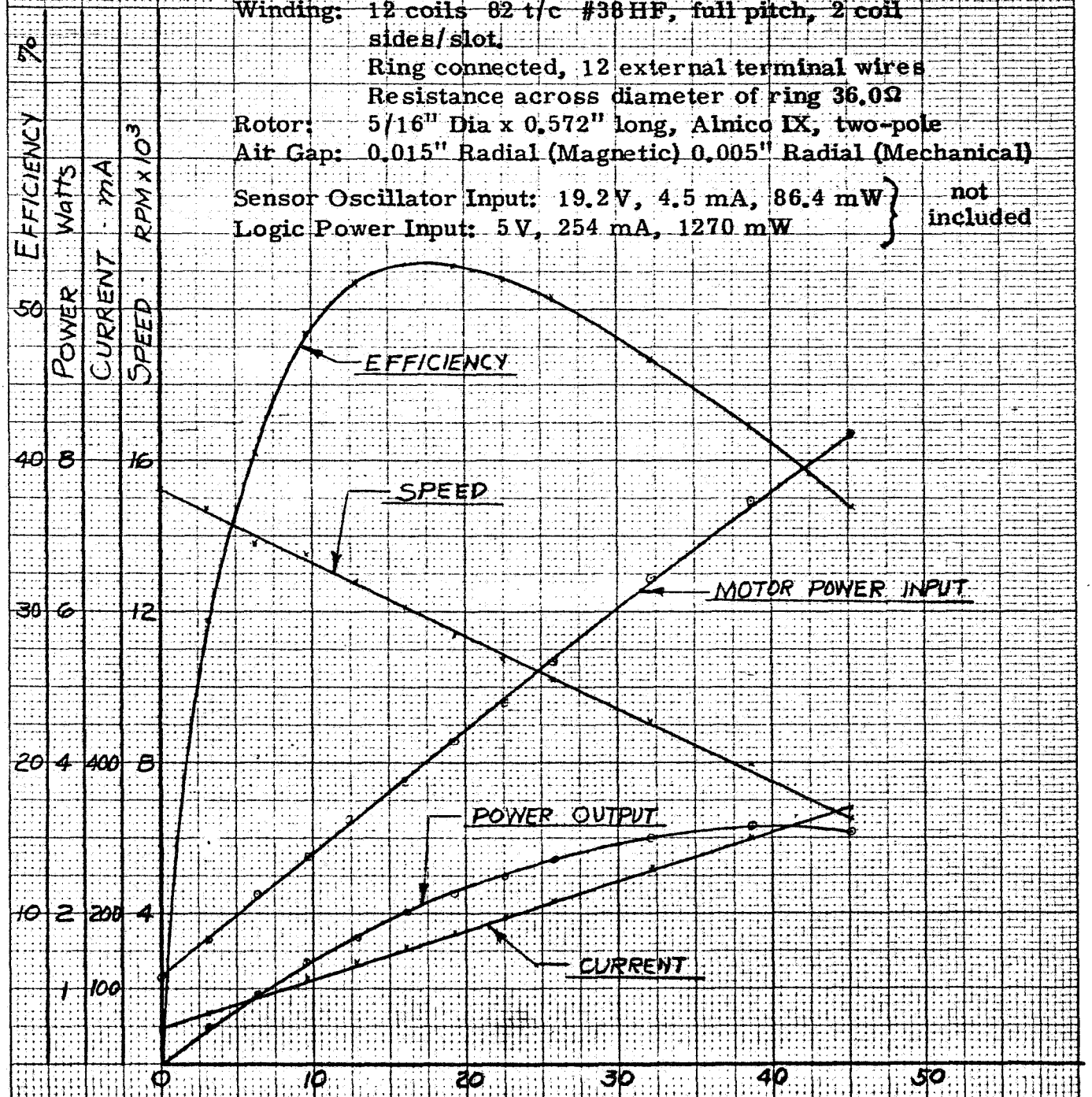


JPL #9 Pg 86
HDT 3-7-68

# COMPARISON OF DESIGN AND TEST PERFORMANCE
## BRUSHLESS DC MOTOR DESIGN NO. 3
## JET PROPULSION LABORATORY
## CONTRACT #951463

Speed 4500 rpm

Herbert C. Roters Associates, Inc. September 1968

**DATA:**

Case - 3/4" Dia x 1-5/16" long
Rotor - 5/16" Dia x 0.372" long, Alnico IX
Winding - 12 coils of 82 t/c #38 HF, full pitch, 2 coil sides per slot
Resistance between terminals - 36.0Ω
Air Gap - 0.015" radial

Note: Performance shown does not include iron losses estimated as requiring 6.5 mA of current. Windage and friction torques of approximately 0.038 oz-in included in electromagnetic torques

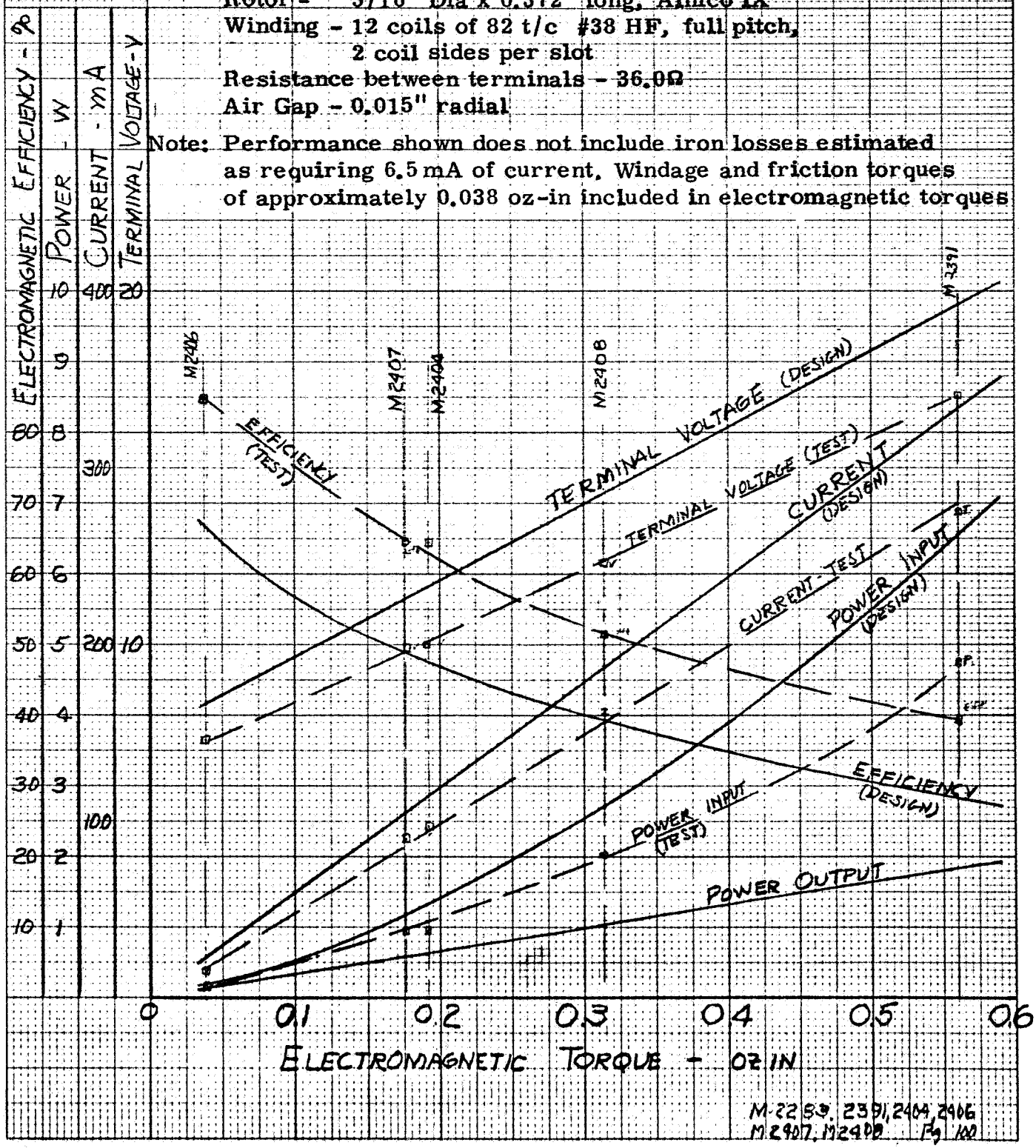


M-2283, 2391, 2404, 2406
M2407, M2408 Pg 100

# MOTOR CHARACTERISTICS
## UNIT 159 DC BRUSHLESS MOTOR
## AND LOGIC CONTROLLED COMMUTATION POWER SUPPLY

Jet Propulsion Laboratory - P. O. #951463

25 Volts on Motor Stator Power Supply

Room Ambient Temperature

Tested after environmental tests were made

(Compare M-2416 before environmental tests)

Herbert C. Roters Associates, Inc. September 1968

Case: 3/4" Dia x 1-5/16" long

Winding: 12 coils 82 t/c #38 HF, full pitch, 2 coil sides/slot.
Ring connected, 12 external terminal wires
Resistance across diameter of ring 36.0Ω

Rotor: 5/16" Dia x 0.572" long, Alnico IX, two-pole

Air Gap: 0.015" Radial (Magnetic) 0.005" Radial (Mechanical)

Sensor Oscillator Input: 21.3 V, 5.08 mA, 108 mW } not included
Logic Power Input: 5.0 V, 262 mA, 1310 mW }

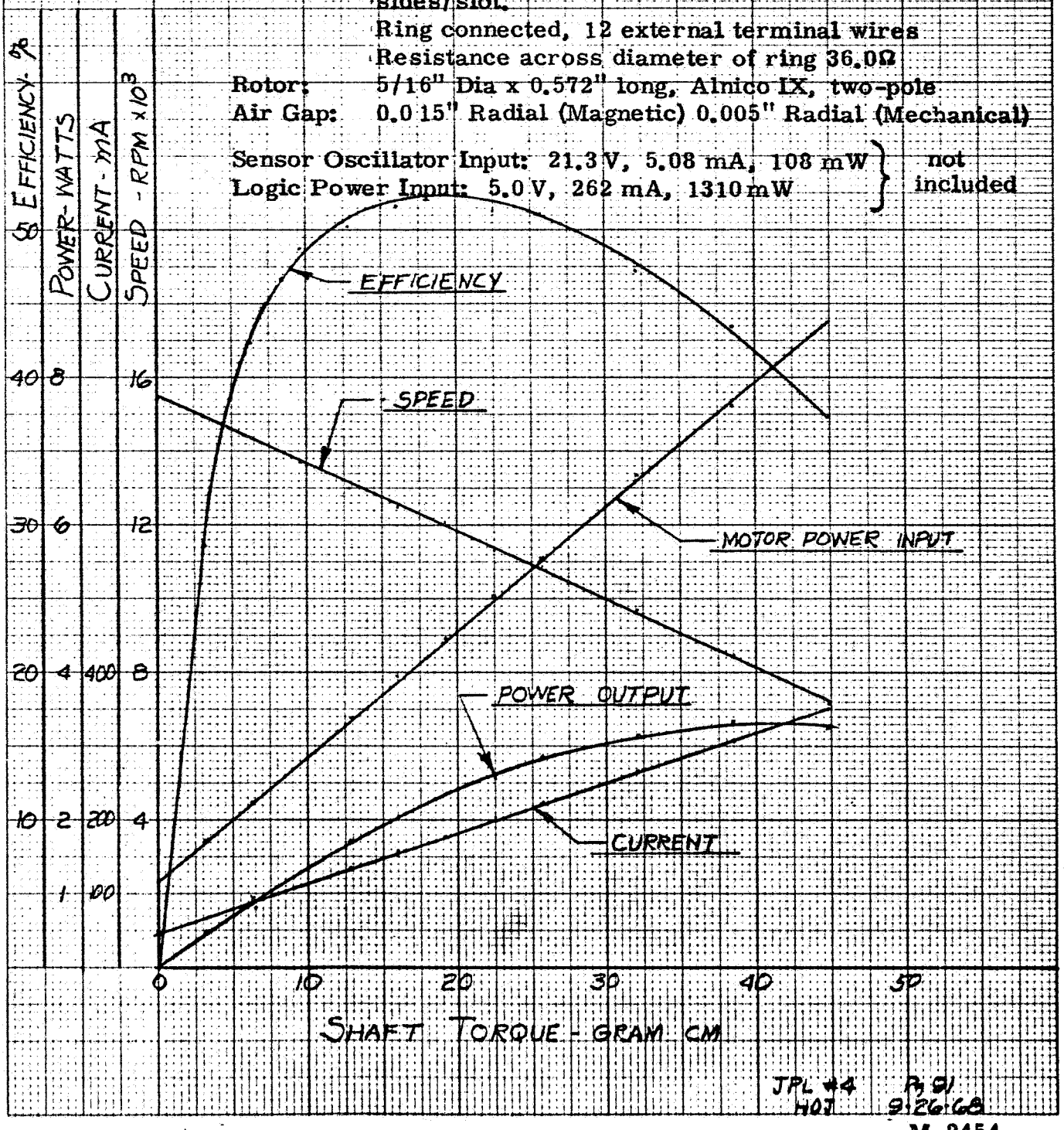


JPL #4 R 91
HOJ 9-26-68

# MOTOR CHARACTERISTICS
## UNIT 159 DC BRUSHLESS MOTOR
## AND LOGIC CONTROLLED COMMUTATION POWER SUPPLY

**Jet Propulsion Laboratory - P. O. #951463**

25 Volts on Motor Stator Power Supply
Room Ambient Temperature
Tested after environmental tests were made,
and motor disassembled for examination.

Herbert C. Roters Associates, Inc. September 1968

Case: 3/4" Dia x 1-5/16" long
Winding: 12 coils 82 t/c #38 HF, full pitch, 2 coil sides/slot.
Ring connected, 12 external terminal wires
Resistance across diameter of ring 36.0Ω
Rotor: 5/16" Dia x 0.572" long, Alnico IX, two-pole
Air Gap: 0.015" Radial (Magnetic) 0.005" Radial (Mechanical)
Sensor Oscillator Input: 20.8 V, 5.8 mA, 120 mW } not included
Logic Power Input: 5V, 287 mA, 1430 mW }

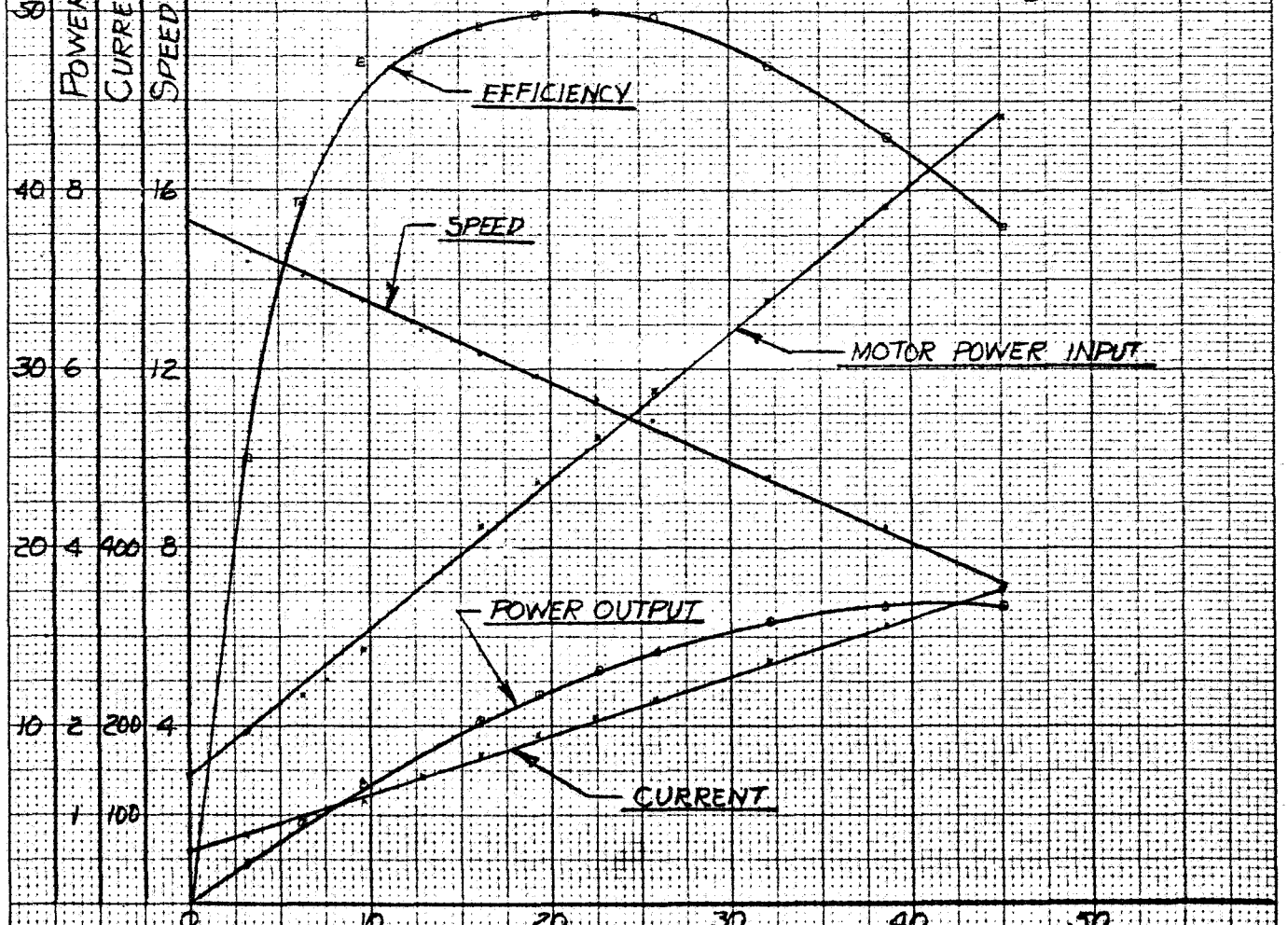


JPL #4 B 92
HOJ 9-24-68

M-2455

PHOTOGRAPH OF UNIT #159 S/N 1
BRUSHLESS DC MOTOR, SHIELDED
CABLE AND CONNECTOR

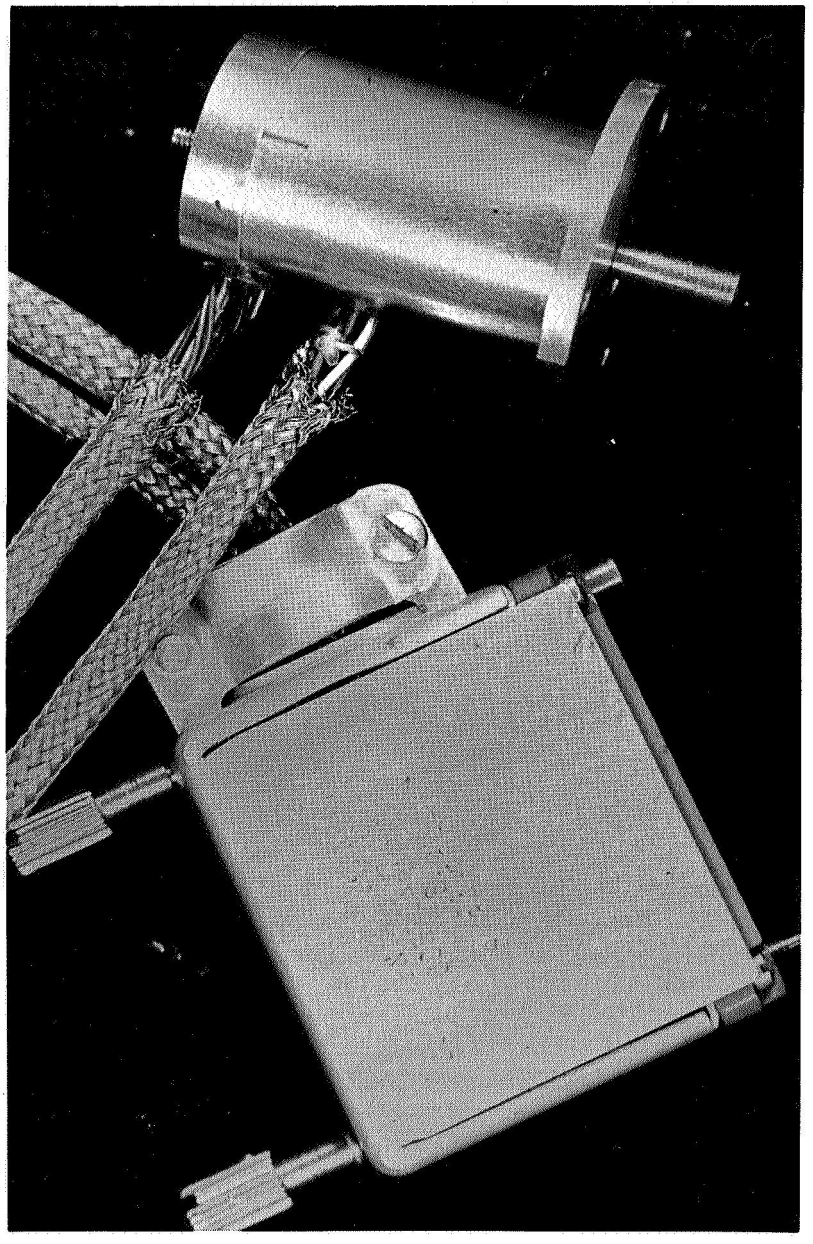

1/32" scale divisions

BRUSHLESS DC MOTOR INCLUDING ELECTRONICS
DC BRUSHLESS MOTOR UNIT #159 S/N 1
EXPERIMENTAL COMMUTATION CIRCUIT (TOP),
INTERCONNECTING SHIELDED CABLE AND
CONNECTORS, AND OSCILLATOR.

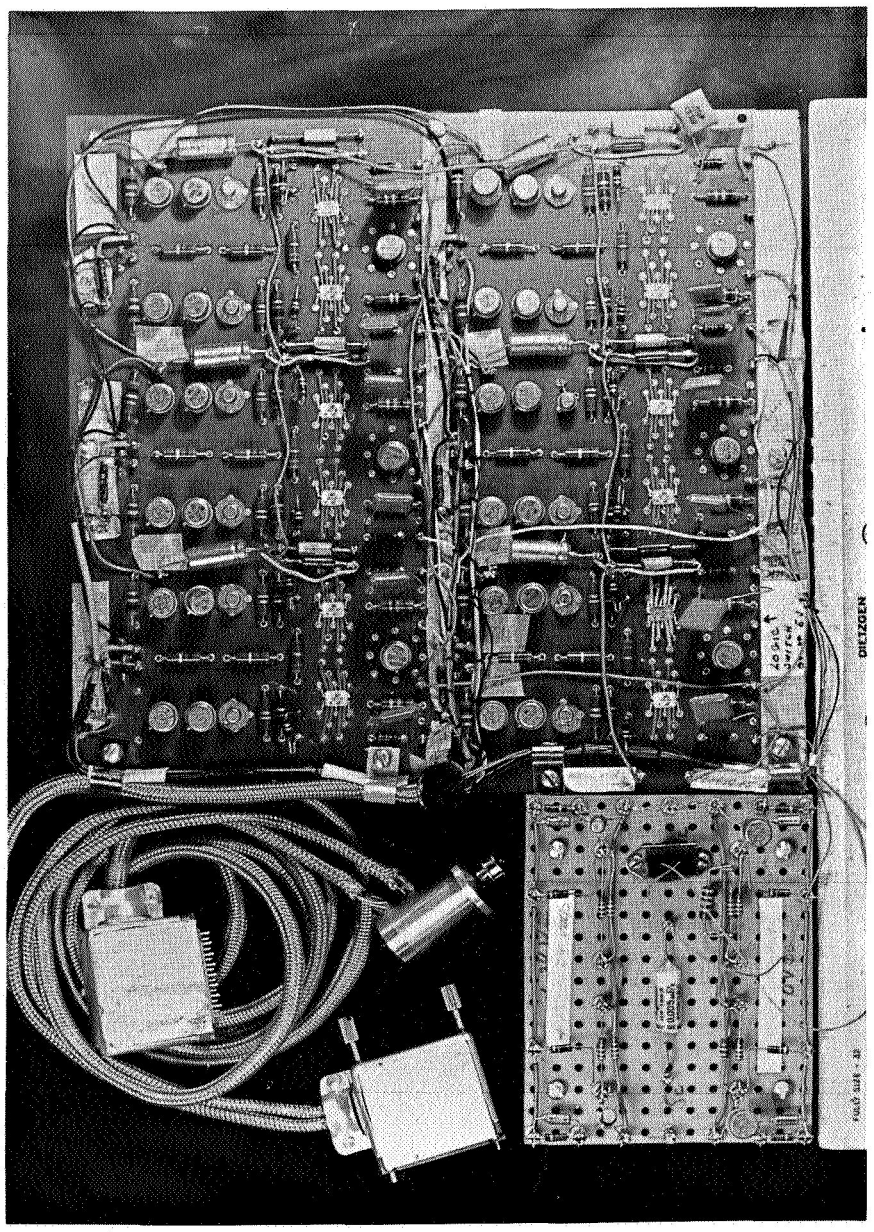

EXPERIMENTAL COMMUTATION CIRCUIT (BOTTOM)
FOR DC BRUSHLESS MOTOR

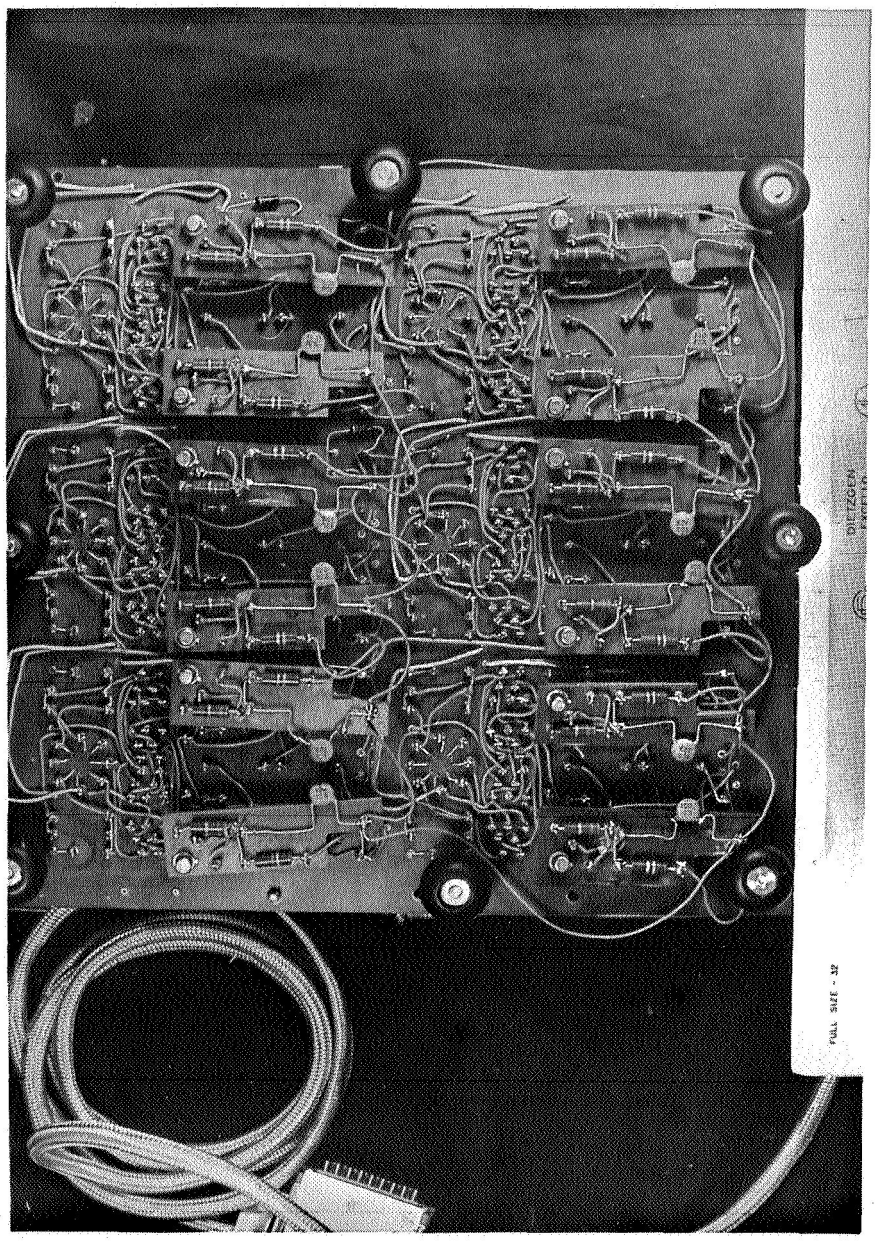

UNIVERSAL REPORT NO. _____

ORIGINATORS REPORT NO. 6D108-4

REVISION _____

# REPORT OF TEST
# ON

BRUSHLESS D.C. MOTOR
UNIT 159, PROTOTYPE

TEST PERFORMED BY Ogden Technology Laboratories, Inc.

TEST AUTHORIZED BY HERBERT C.ROTERS ASSOCIATES, INC.

CONTRACT NUMBER _____

PURCHASE ORDER NUMBER 1940

OTL JOB NUMBER 7667

| | Date | Signature | |
|---|---|---|---|
| Test Initiated | 4/11/68 | | |
| Test Completed | 4/18/68 | | |
| Report Written By | 5/7/68 | H. Golinger | H. Golinger |
| Technician | | | |
| Test Engineer | 5/7/68 | H. Golinger | H.Golinger |
| Supervisor Chief Engr. | 5/7/68 | A. Helfand | A.Helfand |
| Supervisor | | | |
| Quality Assurance | 5/7/68 | B Kalman | B.Kalman |
| Government Repr. (if applicable) | | | |
| Final Release | | | |
| | | | |

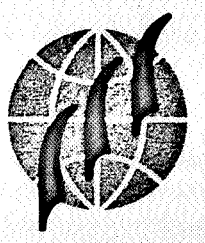

TABLE OF CONTENTS PAGE

## Notices

When Government drawings, specifications or other data are used for any purpose other than in connection with a definitely related Government procurement operation, the United States Government thereby incurs no responsibility nor any obligation whatsoever; and the fact that the Government may have in any way formulated, furnished, or supplied the said drawings, specifications, or other data, is not to be regarded by implication or otherwise as in any manner licensing the holder or any other person or corporation of conveying any rights or permission to manufacture, use, or sell any patented invention that may in any way be related thereto.

## ADMINISTRATIVE DATA

| | |
|---|---|
| TEST REPORT: | 6D108-4 |
| TEST CONDUCTED: | Environmental Tests |
| MANUFACTURER: | Herbert C. Roters Associates<br>45 North Mall<br>Plainview, N.Y. 11803 |
| MANUFACTURER'S TYPE OR MODEL NO.: | Brushless D.C.Motor<br>Unit 159, Prototype |
| DRAWING, SPECIFICATION OR EXHIBIT: | Jet Propulsion Laboratory Spec.No.30250B, dated 15 March 1963<br>Para.s 4.3.1, Amend.2, 4.3.2, 4.3.3.3, Amend.1 & 2 |
| QUANTITY OF ITEMS TESTED: | One (1) unit |
| SECURITY CLASSIFICATION OF ITEMS: | Unclassified |
| DATE TEST COMPLETED: | 18 April 1968 |
| TEST CONDUCTED BY: | Ogden Technology Laboratories,Inc. |
| DISPOSITION OF SPECIMENS: | Returned to Roters Associates |
| DATE OF TEST REPORT: | 7 May 1968 |
| MANUFACTURER'S PURCHASE ORDER NO.: | 1940 |

ABSTRACT: Refer to Test Results, Para. 4.0.

## FACTUAL DATA

### 1.0 TEST EQUIPMENT

1.1 Centrifuge
Genisco Co.
Model: 50159 S/N C-30
Calibration: Annually
Last Calibration: 5/22/67

1.2 Vibration Exciter
M. B. Electronics
Model: C50
Calibration: None required

1.3 Power Amplifier
M. B. Electronics
Model: 4150
Calibration: None required

1.4 Accelerometer
Columbia Research Labs.
Model: 902 S/N 136
Calibration: 6 months
Last Calibration: 1/9/68

1.5 Automatic Vibration Exciter Controller
Bruel & Kjaer
Model: 1019
Calibration: Before each use

1.6 Tracking Filter
Spectral Dynamics Corp.
Model: SD-101A
Calibration: Before each use

1.7 Signal Amplifier
Unholtz-Dickie Corp.
Model: 607-RMG-3A
Calibration: Before each use

1.8 Tape Transport
Minneapolis-Honeywell Co.
Model: LAR-7400
Calibration: Before each use

1.9 Automatic Random Equalization Console
M. B. Electronics
Model: T388 80/25
Calibration: Before each use

1.10 Low Frequency Vibration Exciter
Ogden Technology Laboratories,Inc.
Calibration: None required

1.11 Controller
Data Trak
Model: FGE5110
Calibration: Before each use

1.12 Low Frequency Function Generator
Hewlett-Packard Corp.
Model: 202A
Calibration: 6 months
Last Calibration: 12/9/67

All instrumentation and equipment calibration is conducted in accordance with Specification MIL-Q-9858A as further defined in MIL-C-45662A "Calibration System Requirements" and is traceable to the National Bureau of Standards.

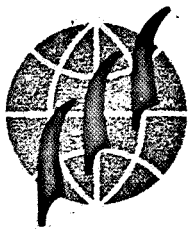

## 2.0 TEST SEQUENCE

2.1 Electromagnetic Interference Test

2.2 Vibration Test

2.3 Shock Test

2.4 Acceleration Test

## 3.0 TEST PROCEDURE

### 3.1 Electromagnetic Interference Test

The test was performed in accordance with Report No. 6D108-4A (included herein as Appendix A)

### 3.2 Vibration Test

The D.C. Brushless Motor, Unit No. 159, Prototype, hereinafter referred to as the test sample, was attached firmly and securely to the vibration exciter. The test sample was then subjected to the vibration test along an axis parallel to the vehicle axis of thrust and in two other orthogonal directions, which were also perpendicular to the axis of thrust. The test sample was subjected to two test procedures - Test Procedure I Low frequency test and Procedure III complex wave vibration test.

#### 3.2.1 Low Frequency Vibration Test

The test sample was subjected to sinusoidal vibration at frequencies between 1 cps to 15 cps for three minutes at an amplitude of $\pm$ 1.5 inches displacement from one (1) to 4.4 cps, and 2.1 g RMS (at 3.0 g peak) from 4.4 to 15 cps.

Sweep time from 1 to 15 cps was 1.5 minutes and was performed twice.

3.2.2 Complex Wave Vibration Test

The test sample was subjected to the vibration tests specified and the test executed by means of a magnetic recording tape. The test consisted of a taped programmed sequence of band limited Gaussian noise and combined noise and sinusoidal vibration. The total time in each orthogonal direction was thirteen (13) minutes and 36 seconds. The test sample was operating during this test.

The test(programmed) was as follows:

(a) White Gaussian Noise: 0.2 $g^2$/cps from 300 to 1000 cps, with a 6 db per octave roll-off from 1000 to 2000 cps, a 3 db per octave roll-off from 300 cps to 20 cps, and a 24 db per octave roll-off below 30 and above 2000 cps for three minutes.

(b) White Gaussian Noise: 5.0 g (RMS), band limited between 15 and 2000 cps plus a 2.0 g (RMS) sinusoidal superimposed on the noise between 15 and 40 cps.

(c) White Gaussian Noise: 5.0 g RMS, band limited between 15 and 2000 cps plus a 9.0 g RMS sinusoidal superimposed on the noise between 40 and 2000 cps. The sinusoidal sweep was from 15 to 2000 and back to 15 cps in 10 minutes at a rate increasing directly with frequency.

3.3 Shock Test

The test sample was subjected to five (5) terminal peak sawtooth shock pulses of 200 g magnitude and 0.7 $\pm$ 0.2 millisecond rise time applied in each of the three (3) orthogonal directions. The test was performed utilizing the electrodynamic shock synthesis technique. The test sample was operating during this test.

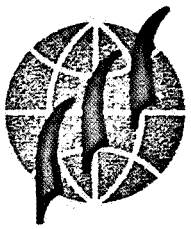

## 3.4 Static Acceleration

The test sample was subjected to a static acceleration of ± 14 g in three orthogonal directions, one direction parallel to the axis of thrust, for five minutes each. ( The test sample was not operated during acceleration.)

## 4.0 TEST RESULTS

### 4.1 Electromagnetic Interference Test

a. See Appendix A - EMI Test Report.

### 4.2 Vibration Test

#### 4.2.1 Low Frequency Vibration Test

a. There was no visible evidence of damage to the test sample.

b. Electrical operation of the test sample was performed by Roters representative and was reported operating correctly after the test.

#### 4.2.2 Complex Wave Vibration Test

a. There was no visible evidence of damage to the test sample.

b. Electrical operation of the test sample was performed by Roters representative and was reported operating correctly after the test.

c. See Appendix B - Equalization Curve

d. See Appendix C - Photographs

4.3 Shock Test

a. There was no visible evidence of damage to the test sample.

b. Electrical operation of the test sample was performed by Roters representative, and was reported operating correctly after the test.

c. See Appendix C - Photographs

4.4 Static Acceleration

a. There was no visible evidence of damage to the test sample.

b. Electrical operation of the test sample was performed by Roters representative and was reported operating correctly after the test.

c. See Appendix C - Photographs

5.0 RECOMMENDATIONS

None. Test results contained herein are submitted for your evaluation.

# APPENDIX A

## Electromagnetic Interference Test

*UNIVERSAL REPORT NO.* _____

*ORIGINATORS REPORT NO.* 6D108-4 A

*REVISION* _____

# REPORT OF TEST ON

*TEST PERFORMED BY* Ogden Technology Laboratories, Inc.

*TEST AUTHORIZED BY* Roters Associates

*CONTRACT NUMBER* _____

PURCHASE ORDER NUMBER 1940

OTL JOB NUMBER 7667

| | Date | Signature | |
|---|---|---|---|
| Test Initiated | 4/9/68 | | |
| Test Completed | 4/9/68 | | |
| Report Written By | 4/18/68 | D McParland | D. McParland |
| Technician | | D McParland | D. McParland |
| Test Engineer | | | |
| Supervisor | | | |
| Supervisor | | | |
| Quality Assurance | | | |
| Government Repr. (if applicable) | | | |
| Final Release | | | |
| | | | |

## Notices

When Government drawings, specifications or other data are used for any purpose other than in connection with a definitely related Government procurement operation, the United States Government thereby incurs no responsibility nor any obligation whatsoever; and the fact that the Government may have in any way formulated, furnished, or supplied the said drawings, specifications, or other data, is not to be regarded by implication or otherwise as in any manner licensing the holder or any other person or corporation of conveying any rights or permission to manufacture, use, or sell any patented invention that may in any way be related thereto.

# ADMINISTRATIVE DATA

| | |
|---|---|
| TEST REPORT: | 6D108-4A |
| TEST CONDUCTED: | Radio Frequency Interference Control |
| MANUFACTURER: | Roters Associates |
| MANUFACTURER'S TYPE OR MODEL NO.: | Brushless DC Motor<br>Unit 159 - Prototype |
| DRAWING, SPECIFICATION OR EXHIBIT: | Jet Propulsion Laboratory Specification 30236A dated 20 October 1961, Para. 4.4.2 and 4.4.4.2 |
| QUANTITY OF ITEMS TESTED: | One |
| SECURITY CLASSIFICATION OF ITEMS: | Unclassified |
| DATE TEST COMPLETED: | April 9, 1968 |
| TEST CONDUCTED BY: | Ogden Technology Laboratories, Inc. |
| DISPOSITION OF SPECIMENS: | |
| DATE OF TEST REPORT: | April 18, 1968 |
| MANUFACTURER'S PURCHASE ORDER NO.: | 1940 |
| ABSTRACT: | See Test Results |

## Section 1.0 Test Equipment

### 1.1 Noise and Field Intensity Meters & Pickup Devices

A. NF-105, Serial Number 3440
Frequency 0.15 to 1,000 MHz
CAL: 2/7/68
CAL DUE: 5/7/68

B. 41 Inch Rod Antenna (VA-105)

C. Dipole Antennas DM-105-T1, T2, T3

D. NF-112, Serial Number 129
Frequency 1 to 10 GHz
CAL: 4/5/68
CAL DUE: 7/5/68

E. AT-112 Pyramidal Antenna

### 1.2 Signal Sources

A. General Radio Type 1330-A, Serial Number 2282
Frequency: 10 kHz to 50 MHz
CAL: 2/1/68
CAL DUE: 5/1/68

B. General Radio Type 1215B, Serial Number 308
Frequency: 50 to 250 MHz
CAL: 2/1/68
CAL DUE: 5/1/68

C. General Radio Type 1209C, Serial Number 7278
Frequency: 250 to 960 MHz
CAL: 3/18/68
CAL DUE: 6/18/68

D. Narda Signal Source 451, Serial Number 13-109
Frequency: 750 to 2750 MHz
CAL: 2/1/68
CAL DUE: 5/1/68

E. Polarad Signal Source 1206, Serial Number 1-7
Frequency: 2.0 to 4.0 GHz
CAL: 3/1/68
CAL DUE: 6/1/68

F. FXR Test Oscillator Model C772A, Serial Number 388
FRequency: 4.0 to 8.0 GHz
CAL: 3/1/68
CAL DUE: 6/1/68

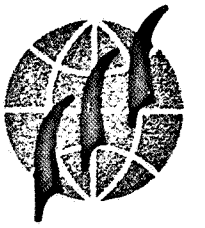

G. FXR Test Oscillator Model X772A, Serial Number 382
Frequency: 7.0 to 11.0 GHz
CAL: 3/1/68
CAL DUE: 6/1/68

H. Tektronix Oscilloscope
Type 535, Serial Number 10217
CAL: 12/26/67
CAL DUE: 6/26/68

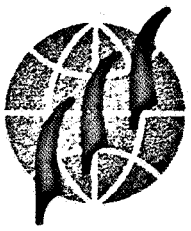

## 2.0 Test Sequence

### 2.1 Radio Frequency Interference Control

#### 2.1.1 Radiated Interference (0.15 to 10,000 MHz)

#### 2.1.2 Radio Frequency Radiated Susceptibility (0.10 to 10,000 MHz)

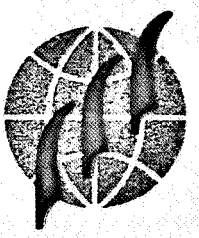

## 3.0 Test Procedure

### 3.1 Radio Frequency Interference Control

#### 3.1.1 Radiated Interference (0.15 to 10,000 MHz)

The DC Brushless Motor, Unit 159, Prototype, hereinafter referred to as the test sample, was set up on the ground plane of the shielded enclosure. The test sample was connected to +5 VDC and -19 VDC through a circuit board by means of a multiconductor cable.

The speed of the test sample was regulated by a control unit and was operated in its normal operating condition. The test sample was insulated from the ground plane by a non-conductive pad.

The power supplies, circuit board, and the control unit were shielded by aluminum foil to insure that the interference observed was not emanating from them and that they would not be affected by the susceptibility signals radiated at the test sample.

Broadband radiated interference was measured from 0.15 to 400 MHz and all frequencies from 0.15 to 10,000 MHz were scanned for narrowband interference.

#### 3.1.2 Radio Frequency Radiated Susceptibility (0.10 to 10,000 MHz)

The test sample was subjected to an R-F field in accordance with Para. 4.4.4.2 of JPL Specification 30236A. The antennas listed below were positioned one foot from the test sample in the frequency range of 0.10 to 1,000 MHz and at three feet distance in the frequency range of 1 to 10 GHz. The signal was modulated 30% with 400 Hz.

| Frequency | Microvolts | Antenna |
|---|---|---|
| 0.10 to 25 MHz | 100,000 | 41 inch rod |
| 25 to 35 MHz | 100,000 | 35 MHz Dipole |
| 35 to 1,000 MHz | 100,000 | Tuned Dipole |
| 1,000 to 10,000 MHz | 100,000 | AT-112 Antenna |

The voltages specified are those which exist when the generator is terminated in its characteristic impedance.

The test was conducted with the same setup described in Para. 3.1.1 of this report. The output of the test sample was monitored for any change by means of an oscilloscope. Any change in indication, malfunction or degradation of performance would be considered an exhibition of susceptibility.

## 4.0 Test Results

### 4.1 Radio Frequency Interference Control

#### 4.1.1 Radiated Interference (0.15 to 10,000 MHz)

Interference exceeding the limits shown in Figure 8 of JPL Spec. No. 30236A was observed at 0.15, 0.20, 0.30, 0.40, 0.60, 0.80, 1.0, and 2.5 MHz. This is shown on Data Sheet 2, Appendix A, and Figure 1, Appendix B.

Interference exceeding the limits shown in Figure 8 of JPL Spec. No. 30236A was observed at 77 and 110 MHz. This is shown on Data Sheet 3, Appendix A, and Figure 1, Appendix B.

No other interference exceeding the limits mentioned above was observed. This is shown on Data Sheets 2, 3, and 4 of Appendix A.

#### 4.1.2 Radio Frequency Radiated Susceptibility (0.10 to 10,000 MHz)

No change in indication, malfunction or degradation of performance was observed. This is shown on Data Sheet 5 of Appendix A.

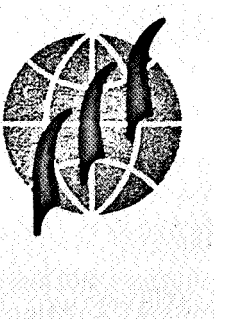

# APPENDIX A

## Data Sheets Including Sketch of Test Set Up and Observed Data

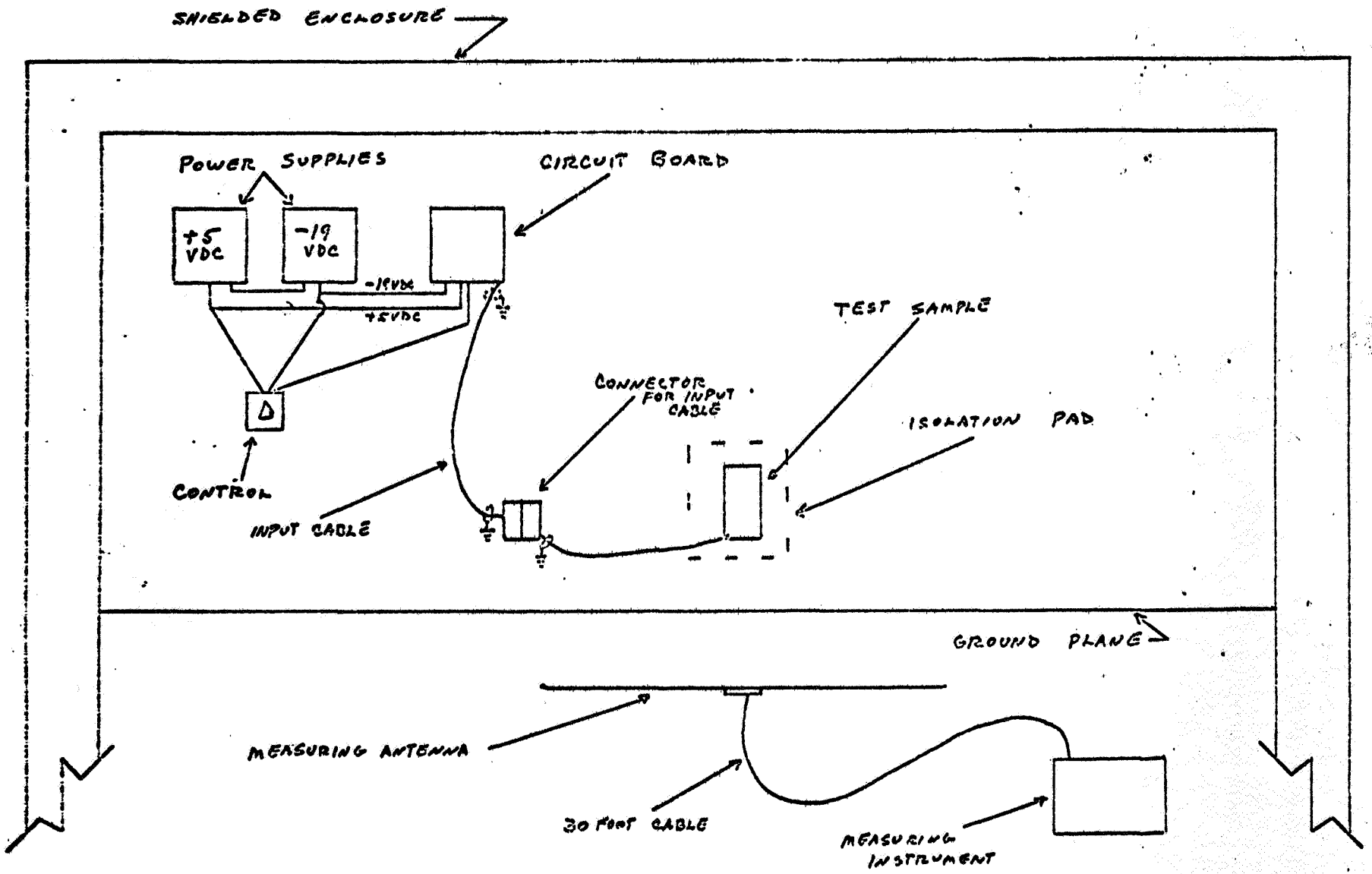


TEST SETUP FOR ROTORS ASSOCIATES, BRUSHLESS DC MOTOR, UNIT 159, PROTOTYPE AT OGDEN TECHNOLOGY LABORATORIES, INC, DEER PARK, NEW YORK

BY _____ DATE _____
CHKD. BY _____ DATE _____
SUBJECT TEST SETUP
DATA SHEET
SHEET NO. 1 OF 5
JOB NO. 7667

# RADIO FREQUENCY INTERFERENCE TEST

SHEET NO. 2 OF 5
JOB NO. 7667
DATE APRIL 9, 1968

## DATA SHEET

RADIATED INTERFERENCE

TEST EQUIPMENT: 0.15 TO 25 MHZ
MODEL: NF-105
SERIAL: 3440
PICKUP: 41" ROD ANTENNA (VA-105)

INPUT: 24 VDC
+45 VDC
-19 VDC

TEST SAMPLE: UNIT 159 — BRUSHLESS DC MOTOR — PROTOTYPE

| FREQ MHZ | CORR FACTOR | METER READ DBMHZ | CORR DBMHZ | LIMIT DBMHZ | |
|---|---|---|---|---|---|
| 0.15 | 37 | 45 | 82 | 77 | |
| 0.20 | 37 | 44 | 81 | 75 | |
| 030 | 37 | 43 | 80 | 73 | |
| 0.40 | 30 | 51 | 81 | 71 | |
| 0.60 | 31 | 45 | 76 | 70 | |
| 0.80 | 33 | 43 | 76 | 70 | |
| 1.0 | 30 | 49 | 79 | 69 | |
| 1.5 | 29 | 28 | 57 | 69 | |
| 2.0 | 27 | 30 | 57 | 69 | |
| 2.5 | 26 | 45 | 71 | 68 | |
| 3.5 | 23 | 39 | 62 | 68 | |
| 5.0 | 24 | 28 | 52 | 68 | ALL FREQUENCIES SCANNED. NO "CW" OR PULSED "CW" TYPE OF INTERFERENCE (NARROW BAND) WAS OBSERVED. |
| 6.0 | 19 | 30 | 49 | 67 | |
| 9.0 | 19 | 32 | 51 | 67 | |
| 12.0 | 20 | 47 | 67 | 67 | |
| 15 | 17 | 40 | 57 | 66 | |
| 20 | 15 | 29 | 44 | 66 | |
| 25 | 15 | 28 | 43 | 66 | |

TESTED BY David DeLand

Ogden Technology Laboratories, Inc.
Deer Park, N. Y.

# RADIO FREQUENCY INTERFERENCE TEST

## DATA SHEET

SHEET NO. 3 OF 5
JOB NO. 7667
DATE APRIL 9, 1968

RADIATED INTERFERENCE

TEST EQUIPMENT: 25 TO 1000 MHZ
MODEL: NF-105
SERIAL: 3440
PICKUP: RESONANT DIPOLE ANTENNA

INPUT: 24 VDC
+5 VDC
-19 VDC

TEST SAMPLE: BRUSHLESS DC MOTOR
UNIT 159
PROTOTYPE

| FREQ MHZ | CORR FACTOR | METER READ DB/MHZ | CORR DB/MHZ | LIMIT DB/MHZ |
|---|---|---|---|---|
| 30 | 8 | 37 | 45 | 48 |
| 40 | 8 | 27 | 35 | 50 |
| 60 | 9 | 30 | 39 | 52 |
| 77 | 9 | 45 | 54 | 53 |
| 110 | 9 | 47 | 56 | 53 |
| 150 | 9 | 39 | 48 | 54 |
| 180 | 9 | 41 | 50 | 55 |
| 200 | 10 | 31 | 41 | 55 |
| 300 | 10 | 24 | 34 | 57 |
| 400 | 11 | 22 | 33 | 58 |
| 400 ↕ 1,000 | | SCANNED FOR "C.W." NO "CW" OR PULSED "CW" OBSERVED | | |

ALL FREQUENCIES SCANNED. NO "CW" OR PULSED "CW" TYPE OF INTERFERENCE (NARROWBAND) WAS OBSERVED.

TESTED BY Daniel Mc Farland

Ogden Technology Laboratories, Inc.
Deer Park, N. Y.

# RADIO FREQUENCY INTERFERENCE TEST

## DATA SHEET

SHEET NO. 4 OF 5
JOB NO. 7669
DATE: APRIL 9, 1968

RADIATED INTERFERENCE

| | |
|---|---|
| TEST EQUIPMENT: | 1 TO 10 GHZ |
| MODEL: | NF-112 |
| SERIAL: | 129 |
| PICKUP: | AT-112 ANTENNA |

TEST SAMPLE: BRUSHLESS DC MOTOR
UNIT 159 PROTOTYPE

| FREQ GHZ | |
|---|---|
| 1.0 ↕ 10.0 | ALL FREQUENCIES SCANNED. NO "CW" OR PULSED "CW" TYPE OF INTERFERENCE (NARROW BAND) WAS OBSERVED. |

TESTED BY Daniel McFarland

Ogden Technology Laboratories, Inc.
Deer Park, N.Y.

# RADIO FREQUENCY INTERFERENCE TEST

## DATA SHEET

SHEET NO. 5 OF 5
JOB NO. 7667
DATE APRIL 9, 1968

RADIATED SUSCEPTIBILITY

TEST EQUIPMENT: 0.15 TO 10,000 MHZ
MODEL:
SERIAL:

TEST SAMPLE: BRUSHLESS DC MOTOR
UNIT 159 PROTOTYPE

| FREQ MHZ | |
|---|---|
| 0.15 ↕ 10,000 | ALL FREQUENCIES SCANNED. NO CHANGE IN INDICATION, MALFUNCTION, OR DEGRADATION OF PERFORMANCE WAS OBSERVED WHEN THE TEST SAMPLE WAS IMMERSED IN AN R-F FIELD AS SPECIFIED IN PARAGRAPH 4.4.4.2 OF JPL SPEC. NO. 30236 A. |

TESTED BY Daniel McFarland

Ogden Technology Laboratories, Inc.
Deer Park, N.Y.

APPENDIX B

Graphical Presentation Including Interference

Observed and Specification limits

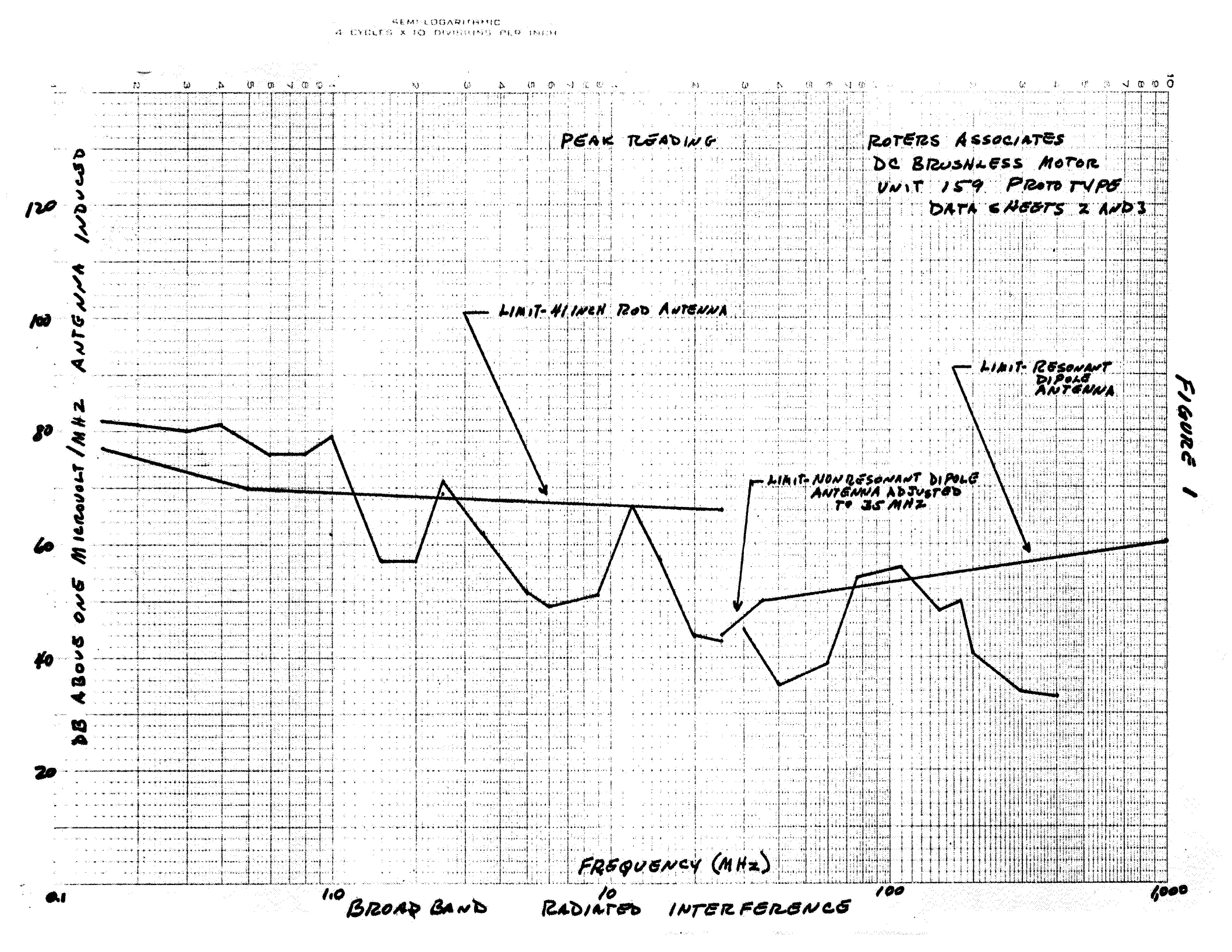
SEMI LOGARITHMIC
4 CYCLES X 10 DIVISIONS PER INCH
PEAK READING
ROTERS ASSOCIATES
DC BRUSHLESS MOTOR
UNIT 159 PROTOTYPE
DATA SHEETS 2 AND 3
LIMIT- 41 INCH ROD ANTENNA
LIMIT- RESONANT DIPOLE ANTENNA
LIMIT- NONRESONANT DIPOLE ANTENNA ADJUSTED TO 35 MHZ
DB ABOVE ONE MICROVOLT/MHZ ANTENNA INDUCED
120
100
80
60
40
20
FREQUENCY (MHZ)
0.1
1.0
10
100
1,000
BROAD BAND RADIATED INTERFERENCE

FIGURE 1

# APPENDIX B

## Random Vibration
## Equalization Spectrum

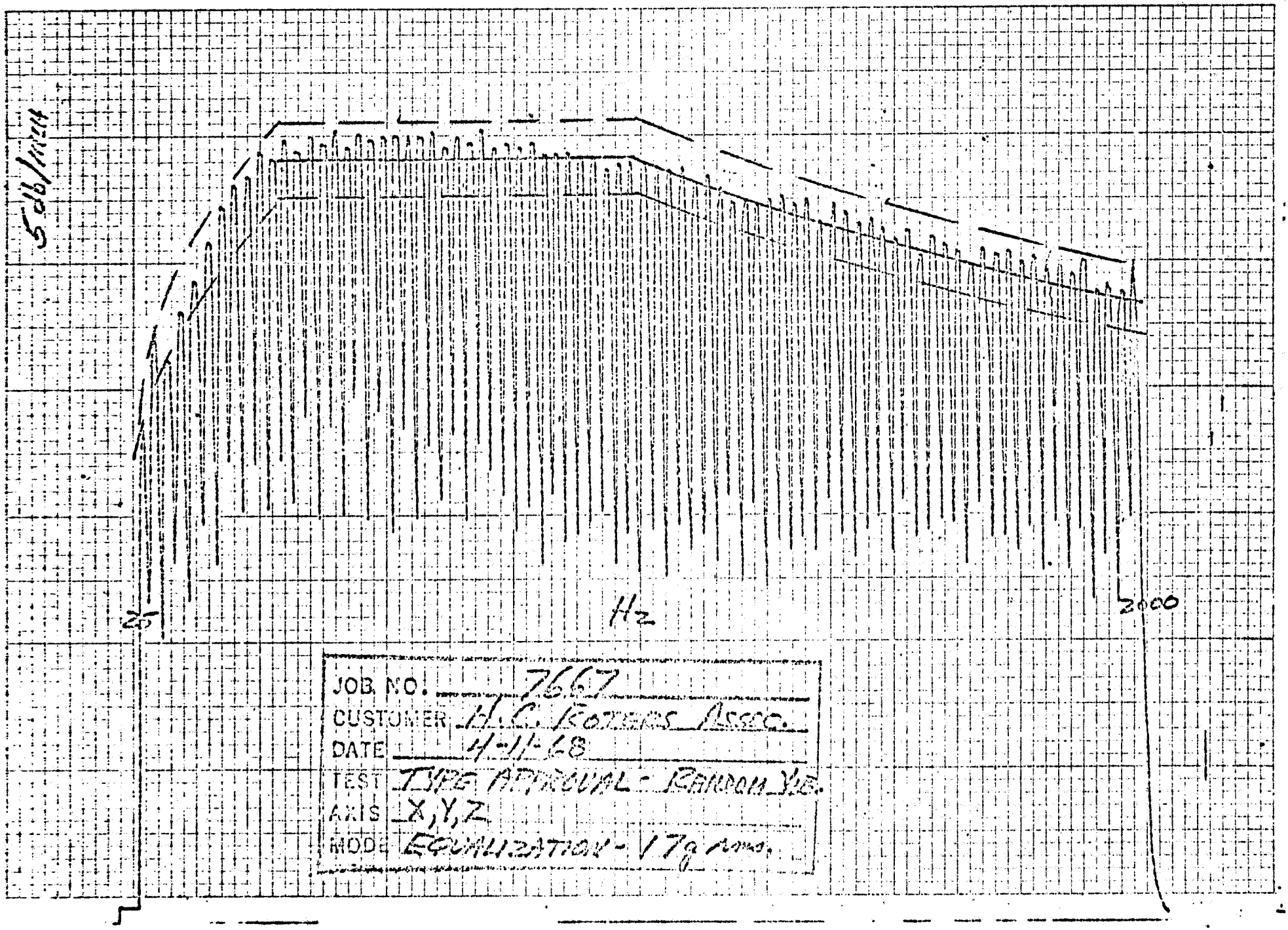

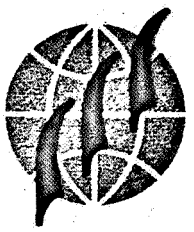

# APPENDIX C

## Photographs

Z Axis

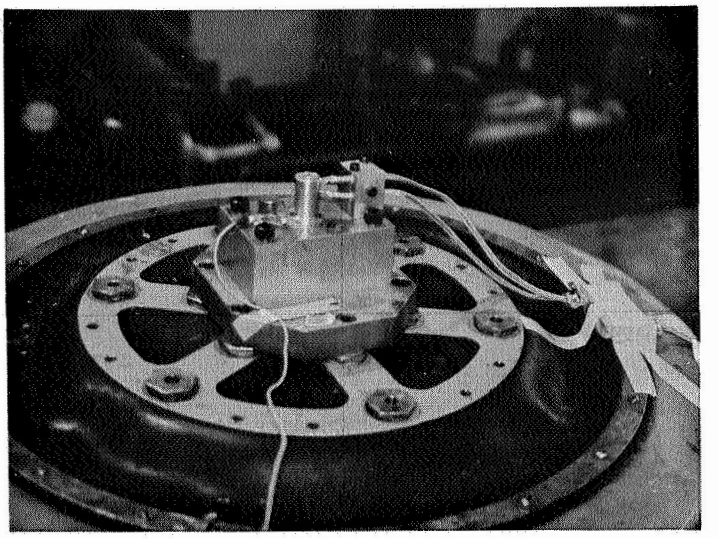

X Axis

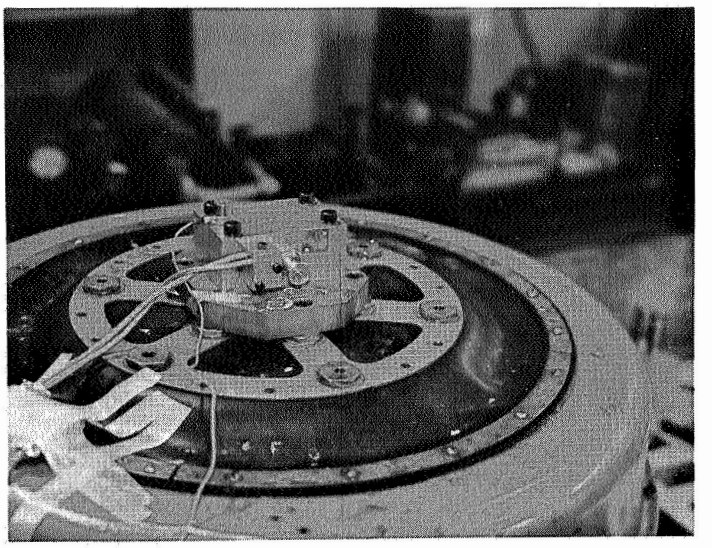

Y Axis

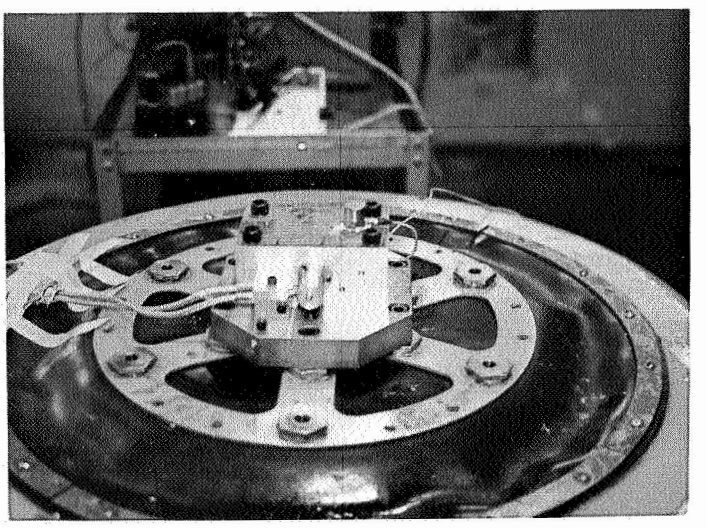

SHOCK PULSE PHOTOGRAPHS

X Axis

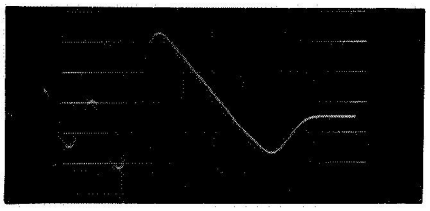

Calibration

Vertical: 50 g/cm

Horiz: 0.2 ms/cm

Y Axis

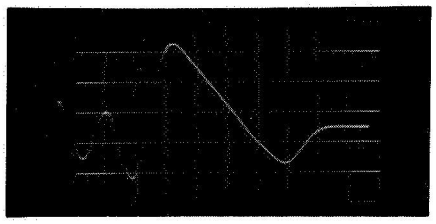

Z Axis

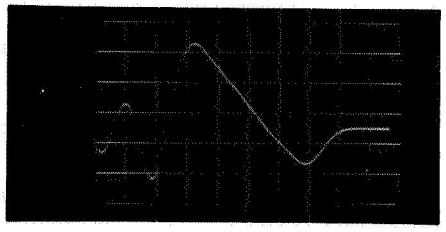

# ACCELERATION TESTING

X Axis

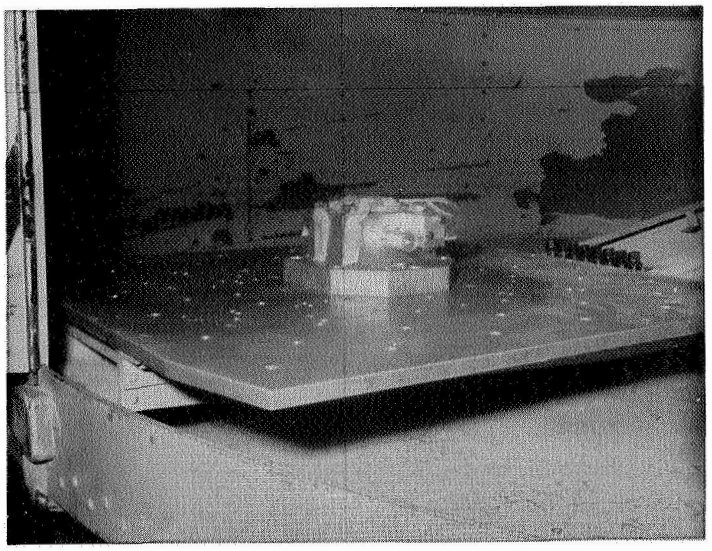

Y Axis

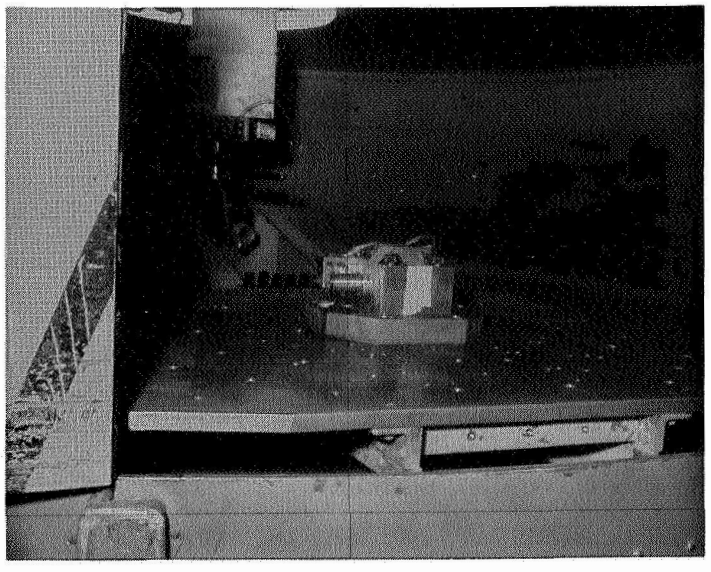

Z Axis